THE DRYING OF LUMBER IN A FLUIDIZED BED OF INERT SOLIDS

by

MAJA VELJKOVIC

B.A.Sc., University of Belgrade, 1972

A THESIS SUBMITTED IN PARTIAL FULFILMENT OF THE REQUIREMENTS FOR THE DEGREE OF MASTER OF APPLIED SCIENCE

in the Department of CHEMICAL ENGINEERING

We accept this thesis as conforming to the required standard

THE UNIVERSITY OF BRITISH COLUMBIA

January 1976

In presenting this thesis in partial fulfilment of the requirements for an advanced degree at the University of British Columbia, I agree that the Library shall make it freely available for reference and study. I further agree that permission for extensive copying of this thesis for scholarly purposes may be granted by the Head of my Department or by his representatives. It is understood that copying or publication of this thesis for financial gain shall not be allowed without my written permission.

Department of Chemical Engineering

The University of British Columbia
2075 Wesbrook Place
Vancouver, Canada
V6T 1W5

Date March 23, 1976

ABSTRACT

The use of fluidized beds of hot inert solids for drying wood is a relatively new concept. Recent investigations on fluidized bed drying of thin veneer (1,2) have shown that more rapid drying can be achieved by this method than by conventional means.

In the present work, blocks of Western Hemlock wood, 2 in. x 4 in. x 1 ft. containing 70% to 100% moisture (dry-basis) were dried in a fluidized bed of -20 +30 mesh sand at four levels of bed temperature (175, 190, 204, and 217°F) and three air velocities. The drying time required to reach 15% moisture content (M.C.) was 14-15 hrs. for lumber dried at 204°F as against two or more days generally taken in Kiln drying. The quality of the wood dried at bed temperatures of 204°F and below was not adversely affected. Bed temperature had a strong inverse effect on drying time, while the fluidizing air flow rate had little effect.

The diffusion equation was employed to describe the movement of moisture during the falling-rate period of drying and the heat conduction equation to describe the unsteady-state movement of heat inside the drying block of wood. Mathematically, drying was treated both as a one and a two-dimensional problem. The resulting equations were solved on a digital computer to predict the average moisture content

and the average temperature of the drying block of wood, each as a function of time. The distribution of moisture content within the drying block was also computed. The calculated results showed a good agreement with experimental data. The economics of fluidized bed drying were estimated and compared with the cost of Kiln drying. The results showed that the capital cost of the fluidized bed system is considerably lower while the operating cost is similar to that for kiln drying.

TABLE OF CONTENTS

LIST OF TABLES

LIST OF FIGURES

ACKNOWLEDGEMENTS

The author would like to express her appreciation to her research advisor Dr. K.B. Mathur for his advice and encouragement in this work. The author is also grateful to Drs. A. Meisen and N. Epstein for their help with the theoretical aspects of the work and to Drs. P. Watkinson and R.M.R. Branion for useful discussions.

Also acknowledged is the work done by the staff of the workshop of the Chemical Engineering Department.

The author is indebted to Dr. J. Wilson and other members of the Faculty of the U.B.C. Department of Forestry.

Special thanks are due to Dr. V. Mathur of MacMillan Bloedel Research Ltd. for supplying and testing wood samples, and for many helpful discussions.

Finally, the author would like to acknowledge the advice and encouragement by her student colleagues, and specially for the assistance with computer programming given by B. Bowen and with the apparatus by S. Tam.

CHAPTER 1

INTRODUCTION

The aim of this investigation was to assess the feasibility of drying lumber in a bed of inert solids fluidized with hot air. It is known that heat can be transferred rapidly and evenly from a fluidized bed to an object immersed in the bed. One of the remarkable features of the fluidized bed is its temperature uniformity in both radial and axial directions with effective thermal conductivity of up to one hundred times that of silver, (3, p. 265). The high rate of bed-to-object heat transfer is due to the bubble-induced vigorous mixing of the solid phase which also causes practically isothermal conditions in the bed (4).

Ziegler et al. (5), who studied simultaneous heat and mass transfer from the surface of a wet sphere in a gas stream and a gas fluidized bed, found that the presence of solid particles in the fluidized state increased the rate of mass transfer several times and of heat transfer 10 to 20 times.

In drying experiments Loos (1) found that the drying time required to dry 1/10" green loblolly pine veneer from 107.3% M.C. down to 5% M.C. in a fluidized bed of sand at 400°F was 1 3/4 minutes. The highest drying rates obtained in this study were three times faster for a fluidized bed

of sand than those for jet dryers run at the same temperatures. Similar results have been reported by Babailov (2) who found that the drying time required to dry 0.06" thick peeled veneer from 80% M.C. to 6% M.C. in a fluidized bed of metallurgical slag at 293°F was 1 minute.

Fluidized bed drying appears to have several advantages over convective drying with hot air, which can be summarized as follows.

1. A uniform and closely controllable temperature throughout the bed.
2. Shorter drying time than in other types of dryers, owing to the high rates of heat and mass transfer between the bed and an object immersed in it.
3. The capital cost is expected to be lower than for other types of dryers since with the high drying rates attainable, the dryer would be relatively small. Heavy buildings and foundations would therefore not be needed for housing the dryer.
4. The operation and maintenance of the dryer is relatively simple, as it is of simple construction with no moving parts. The operation can be automated without difficulty.

Preliminary experiments done by Tam on drying of 2" x 4" pieces of W. Hemlock in a fluidized bed of sand showed the drying to be much faster than in the absence of the sand bed (42).

The work reported in this thesis covers further experiments on drying of samples of Western Hemlock immersed in a fluidized bed

of -20 + 30 mesh sand, formulation of a theoretical model to describe the simultaneous heat and mass transfer processes involved and finally an economic assessment of fluidized bed drying versus kiln drying of lumber.

The work has been carried out in consultation with MacMillan Bloedel Research Ltd.

CHAPTER 2

BACKGROUND AND PREVIOUS WORK

2.1 Drying Mechanism for Wood

1. Definition of drying

Drying is defined as the removal of a relatively small amount of liquid moisture from a wet solid by evaporation. In the evaporation process heat has to be supplied to the material so that simultaneous transfer of heat and mass occur. The evaporating moisture is usually carried away by means of an external drying medium circulated over the drying solid. Often this medium consists of dry air, which may be heated to act as the heat transfer medium.

2. Moisture movement in drying

Water occurs in wood as free water in cell cavities and as adsorbed or bound water which is held within the structure of cell walls. Free water present in cell cavities above the fiber-saturation point (F.S.P. - the moisture content at which the cell walls are saturated with water but there is no free water in cell cavities) does not affect the properties of wood other than weight. The bound-water, however, does affect wood properties, it is more difficult to remove and requires additional energy for its removal

(bonding energy). According to Stamm (cited in ref. 35), there are three ways in which adsorbed water may be held within cell walls: (1) as water of constitution that cannot be removed from wood without causing chemical change in the nature of cell walls, (2) as surface-bound water, and (3) as capillary-condensed water in the transient cell-wall capillaries. The removal of water present in the last two forms does not cause any chemical change in the wood.

Above the fiber saturation point, the cell walls are saturated with water and no unbalanced force exists which would tend to cause diffusion from regions of high concentration to those of low concentration. However, the cell cavities contain varying amounts of water, and that water moves by capillary action. Below the fiber-saturation point, water occurs in wood as liquid in cell walls and as water vapor in cell cavities, and moves by diffusion due to differences in moisture content and vapor pressure respectively.

Moisture can move within softwood by various mechanisms. According to Brown (6, p. 26) there are five main paths of travel (see Fig. 1),

1. through the cavities of tracheids
2. through the pits
3. through the wood ray cells
4. through the intercellular spaces, i.e., between the tracheids which do not actually rest against each other and
5. through the transitory cell-wall passages, which

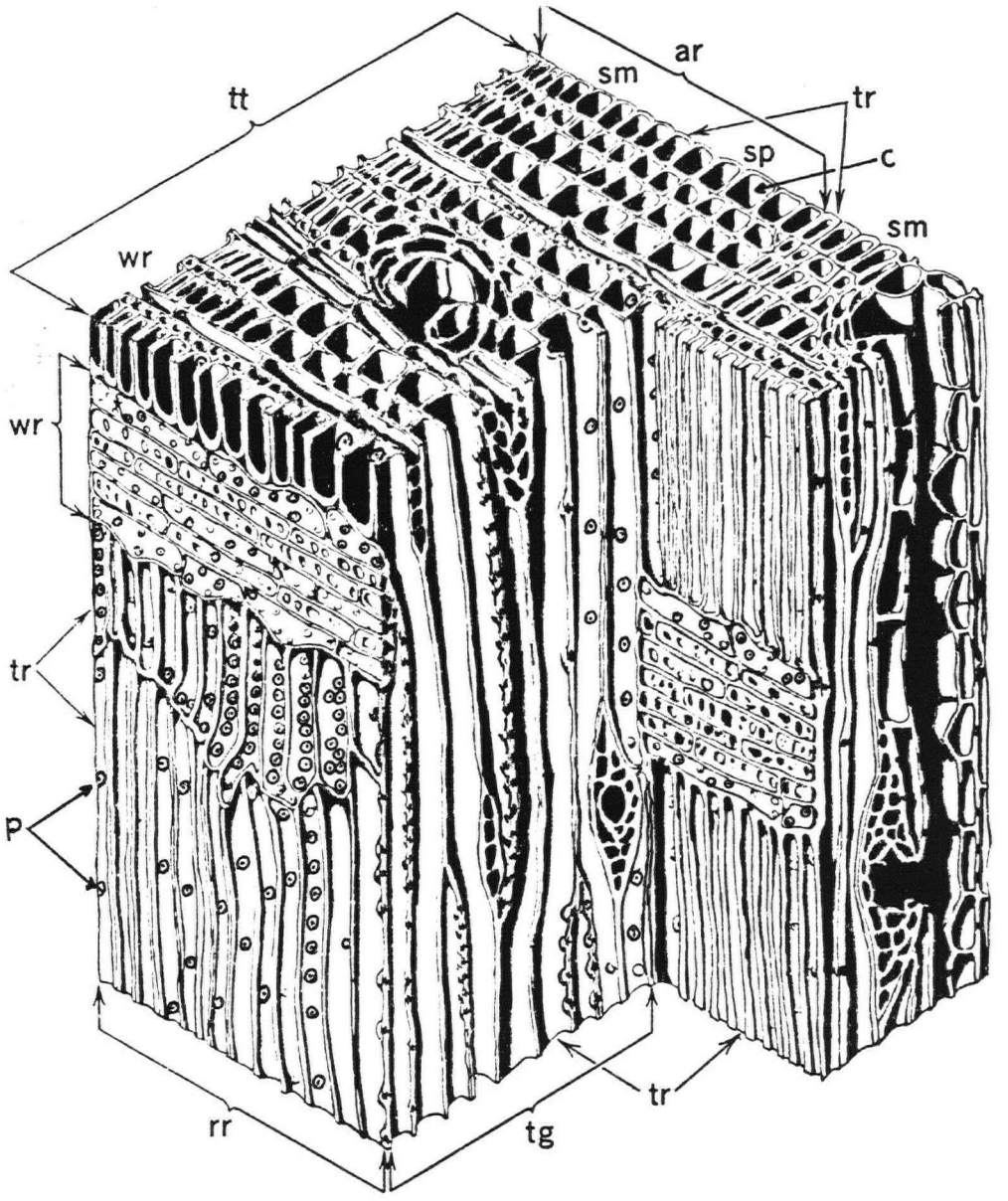

Fig.1. Magnified three-dimensional sketch of a softwood

tt: end-grain surface; tg: tangential surface; rr: radial surface;

tr: tracheid; wr: wood ray; p: pits; c: cell cavity; sp: springwood;

sm: summerwood; ar: annular ring

exist within the cell wall only when liquid separates the submicroscopic components of the wall, and which disappear when the liquid is removed.

The available space for moisture movement is said to be from 25 to 85% of the total volume of wood (6), the available space for wood of high specific gravity (bone-dry wt. of wood*/wt. of an equal volume of water) being less. Of the total movement area, the ray cells represent only 2%, and the intercellular spaces even less (6, p. 26). Hence, the main areas available for movement of moisture (in any form) are: cell cavities, pits, and the transitory cell wall passages.

3. Periods of drying

There are two periods of drying in which the pattern of drying rate is radically different: the "constant-rate period" and the "falling-rate period". From data obtained during drying of solids, a curve of moisture content (dry basis) as a function of time (Fig. 2) may be plotted. The variation of drying rate with moisture content can be better seen if the M.C. versus time curve is graphically or numerically differentiated and plotted as $dm/d\theta$ vs. m, (see Fig. 3) where m percentage moisture content, dry-basis, is given by the following equation:

---

* Bone-dry weight or oven-dry weight is defined as the weight obtained on drying wood to constant weight in an oven at 212°F.

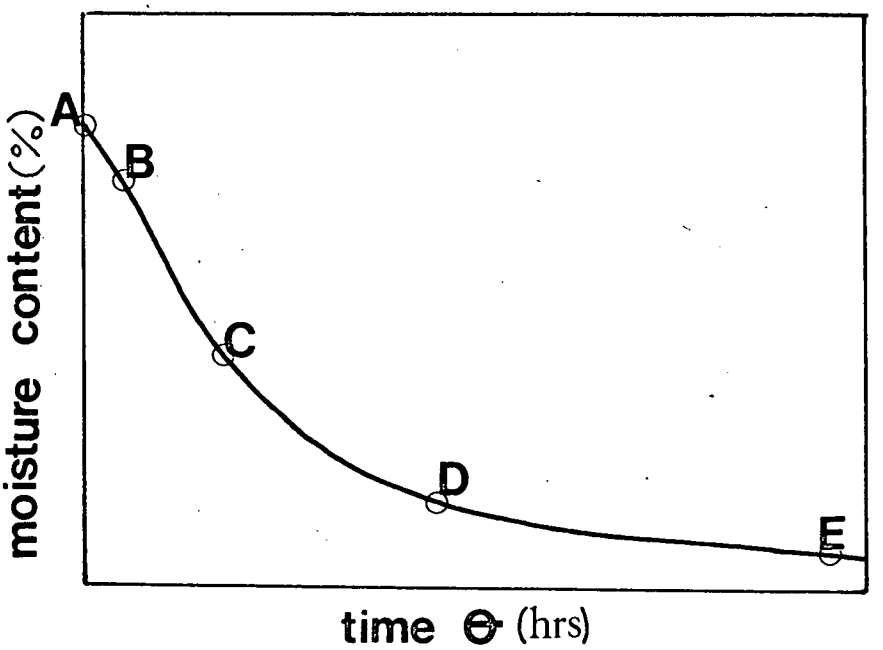

Fig.2 MOISTURE CONTENT vs. TIME

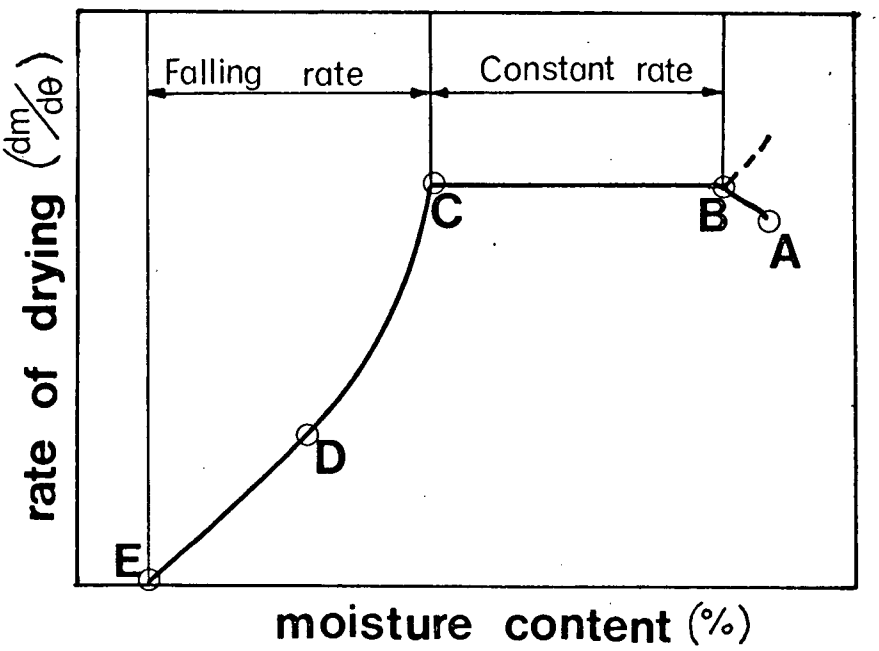

Fig.3 DRYING RATE vs. MOISTURE CONTENT

$$m = \frac{\text{(Original weight)} - \text{(bone-dry weight)}}{\text{(bone-dry weight)}} \times 100 \qquad A$$

The constant-rate period on each curve is represented by section BC, and the falling-rate period by CE which begins when the moisture content reaches the critical value (point C). The section CD is usually called the first falling rate period during which the solid surface is no longer fully covered with moisture. As more and more of the surface becomes dry, the drying rate decreases. The portion DE is the second falling-rate period during which the solid surface is assumed to be completely dry.

4. Constant-rate period

In the first drying period (constant-rate) the rate of drying depends entirely on external parameters such as the velocity, flow pattern, temperature and humidity of the drying air. During this period, the resistance to internal transfer of moisture to the surface is small compared to the external resistance to removal of moisture from the surface. Hence, the evaporation rate of liquid at the solid surface controls the drying rate. If the external conditions are kept constant, then the drying rate in this period is constant. During this period, the solid has a continuous film of liquid over the entire drying surface. It is also known that if all the heat for evaporation of water is supplied in the drying air (convective drying), the temperature of the solid will equilibrate at or close to the wet-

bulb temperature of air. The equilibrium between heat transfer to the solid surface and mass transfer from the saturated surface of the solid, which exists during this period of drying, can be expressed as follows (7),

$$\left(\frac{dm}{d\theta}\right)_c = \frac{h\Delta T}{\rho_{so}\ell\Lambda} = \frac{k_g \Delta P}{\rho_{so}\ell} \qquad 1$$

assuming no change in solid volume during drying,

where $\Delta T = T_g - T_{sc}$ (°F)

T_g = gas dry-bulb temp. (°F)

T_{sc} = surface temp. during evaporation (°F)

$\Delta P = P_{sc} - P_g$ (atm.)

P_g = partial pressure of water in the gas (atm.)

P_{sc} = vapor pressure of water at T_{sc} (atm.)

h = heat transfer coefficient (BTU/ft.^{2} hr. °F)

Λ = latent heat of vaporization (BTU/lbm.)

k_g = mass transfer coefficient (lbm./ft.^{2} hr. atm.)

ρ_{so} = solid density (lbm./ft.^{3}) of dry wood

ℓ = half thickness of solid (ft.)

A = surface area (ft.^{2})

$\left(\frac{dm}{d\theta}\right)_c$ = drying rate during the constant-rate period $\left(\frac{\text{lbm. water}}{\text{lbm. bone-dry wood}}, \text{hrs.}\right)$

After the critical M.C. is reached the falling rate period of drying begins.

5. Falling-rate period

Since there is no longer any free moisture on the solid surface, an additional resistance to moisture transfer arises, inside the material being dried. The drying rate therefore decreases and becomes governed by the rate of moisture movement within the solid. The internal mass transfer rate depends on the internal physical nature of the solid and its moisture content. In addition, the solid surface is no longer at the wet bulb temperatures, so that it becomes necessary to take into account both temperature and moisture content distributions within the body.

Most of the various theoretical models which have been proposed for interpretation of moisture distribution and rate of moisture movement inside porous solids fall into the following categories:

A. Diffusion theory

B. Capillary theory

and the most recent one

C. Moving boundary theory.

A. Diffusion theory

This theory, which assumes that liquid moisture moves through the solid body as a result of concentration driving force, was first proposed by Sherwood (9) and Newman (10).

They used Fick's second law of diffusion, which has a mathematical form analogous to Darcy's law and Fourier's heat-conduction law to describe the rate of moisture movement inside the drying solid.

Fick's second law of diffusion is written as follows:

$$\frac{dm}{d\theta} = D \frac{d^2m}{dy^2} \qquad 2$$

where y is the thickness of the solid in the direction of diffusion and D is the diffusion coefficient. Sherwood (9) and Newman (10) found a complex solution for this equation for the drying of a slab in the falling-rate period. The assumptions used in deriving this equation were:

1. Surface has a constant moisture content.
2. Evaporation takes place at the surface.
3. The diffusion coefficient D is constant.

For these conditions the solution of the diffusion equation for a slab given by Newman (10) is as follows:

$$X = \frac{8}{\pi^2}\left[e^{-\frac{D\theta\pi^2}{4\ell^2}} + \frac{1}{9} e^{-\frac{9D\theta\pi^2}{4\ell^2}} + \frac{1}{25} e^{-\frac{25D\theta\pi^2}{4\ell^2}} + \ldots\right] \qquad 3$$

where D = diffusion coefficient

ℓ = half-thickness

θ = time

X = the fractional amount of moisture unremoved

$$X = \frac{m - m_\infty}{m_c - m_\infty}$$

D varies with moisture content as well as with temperature but over small ranges of moisture content and temperature, the assumption of constancy of D is a good approximation, and is often used.

For long drying times, Eq. (3) simplifies to a limiting form of the diffusion equation as follows:

$$X = \frac{8}{\pi^2} e^{-D\theta\pi^2/4\ell^2} \qquad 3.1$$

Eq. (3.1) may be differentiated to give the drying rate as

$$\frac{dm}{d\theta} = -\frac{\pi^2 D}{4\ell^2} (m - m_\infty) \qquad 3.2$$

where $\frac{dm}{d\theta}$ drying rate, lb./(hr.)(lb. dry solid).

m, m_c, m_∞ average moisture content (dry basis) at any time θ, at the start of the falling-rate period, and at the surface, respectively, lb./lb.

The diffusion model has been widely accepted for drying of porous solids. Ceaglske and Hougen (12) believed that the diffusion equation was applicable to the drying of a solid having a fine uniform fibrous structure, such as wood, because the capillary tension, which causes the flow of liquid varies directly with the degree of saturation of the solid. They

suggested that the movement of water in fibrous materials such as textiles, wood, paper and starch takes place by diffusion rather than by gravity, capillarity or external pressure.

On the other hand, it is evident that there is a difference between the bound water diffusion during drying of wood and the Fickian diffusion described by the diffusion model (11). In the former only very small temperature dependent portion of water molecules migrate at any times (i.e., water molecules bounded to their sorption sites migrate to new sites when they receive energy in excess of the bonding energy) whereas in the latter all water molecules migrate at all times. This leads to the conclusion that strictly speaking Fick's second law does not necessarily hold true for bound water diffusion. Nevertheless, the diffusion equation has been found to give reasonable agreement with experimental data and can be used within the limits imposed by the assumptions listed earlier in this section.

B. Capillary theory

The capillary flow theory (7,8,13,14,15,16) assumes that liquid moisture in a porous solid moves through a very large number of capillaries extending in all directions by liquid-solid molecular attraction. It postulates that during the constant-rate period, there is a water film on the solid surface since the capillaries are full. As water evaporates from the surface, some unsaturated surface portions

appear and water starts to flow from the large capillaries into the smaller capillaries and to the surface. In this way, some capillaries are drained out and more dry surface appears. As a result of the reduced mass transfer area at the surface, the rate of drying decreases. For thick solids with long capillaries, an internal flow resistance is also postulated. The main assumptions involved in this model are:

1. liquid moisture moves only by capillary motion
2. evaporation takes place only at the surface
3. surface temperature equals wet-bulb temperature at the critical point, and increases up to the dry bulb temperature as the equilibrium M.C. is reached
4. effect of mass transfer on heat transfer is negligible.

The falling-rate, as suggested by Perry (ref. 7; see Fig. 3) can be expressed with fair accuracy over the required range of moisture contents by an equation similar to Eq. (3.2); thus

$$\frac{dm}{d\theta} = \left(\frac{dm}{d\theta}\right)_{\text{falling-rate}} = K_1(m-m_\infty) \qquad 4$$

where K_1 is related to the drying rate over the constant-rate period as follows:

$$K_1 = -\frac{(dm/d\theta)_c}{(m_c-m_\infty)} \qquad 5$$

Substituting $(dm/d\theta)_c$ from Eq. (1) into Eq: (5), and putting K_1 into Eq. (4) gives:

$$\frac{dm}{d\theta} = - \frac{h(T_g - T_{sc})(m - m_\infty)}{\rho_s \Lambda \ell \ (m_c - m_\infty)} \qquad 6$$

This theory of moisture movement could only be applicable for liquid water (free and capillary condensed) moving continuously in capillaries through fiber cavities, pit chambers, pit membranes and other voids by mass flow. However, a part of the bound water in wood is surface bound water and its movement through cell walls cannot be negligible.

This view is supported by experimental data which, in general, show a non-linear relationship between drying rate and moisture content (e.g., Fig. 20) rather than the linear relationship assumed in writing Eq. (4).

C. Moving boundary model

This is the most recent model for interpretation of moisture distribution inside a porous solid during drying, widely accepted in the eastern world (14, 17, 18). The solid is considered to have a wet zone and a dry zone. Evaporation takes place at the interface between the wet and dry zones which moves inwards during drying. According to this model, the interface and the dry zone offer the main resistance to the flow of moisture, the resistance of the wet zone being negligible in comparison. Moisture movement in the

wet zone is considered to be by capillary motion and in the dry zone by vapor diffusion. More detailed discussion of this model is given in Section 2.2.

D. Other models

It is important to add that over 30 years ago Lȳkov (cited in ref. 13) found that moisture can move through a wet material due to temperature gradient (known as thermo-diffusional effect). This effect according to Lȳkov was the result of thermodynamic coupling of the heat and mass transfer processes.

Valchar (19) suggested that liquid moisture movement may be effected by changes in concentration of vapor moisture, as a result of coupling of heat and mass transfer processes.

There have been a few attempts to generalize the problem, for example by Krischer and his school (20) (cited in ref. 13). They wrote the differential mass and heat equations, assuming that moisture may move by two mechanisms: capillarity characterized by a "moisture conductivity coefficient" and diffusion characterized by a "moisture diffusivity coefficient". The two mechanisms may act in series, in parallel, or in series and parallel combinations. The two coefficients are functions of the nature of the solid, its moisture content and temperature, so that Krischer's analysis leads to differential equations with variable coefficients. Hence, a complicated calculation procedure is involved in

determining the rate of internal moisture transfer.

On the basis of Krischer's hypothesis, Lȳkov et al. (27) (cited in ref. 13) modified their original concept and applied the methods of thermodynamics of irreversible processes to the internal heat and mass transfer processes in drying. According to them, moisture transfer occurs due to a moisture transfer driving force (which takes in all possible mechanisms of moisture transfer) characterized by a moisture diffusivity coefficient, and due to a temperature gradient, which is characterized by a thermo-gradient coefficient. Values of both the coefficients are dependent on moisture content and temperature, as well as on the nature of solid. It should be noted that in this approach the Lȳkov "moisture diffusivity" attempts to include both of Krischer's coefficients in one parameter by using a generalized driving force instead of two separate driving forces (diffusional and capillary).

Although the concept of moisture movement occurring simultaneously by one or more mechanisms is very realistic, the mathematics involved becomes very complex and therefore such models have not been applied in practice.

2.2 Fluidized Bed Drying

1. Drying of wood

The use of fluidized beds of inert particles to dry wood is a relatively new concept. Loos (1) dried green pine veneer

in fluidized beds of sand and Ceraspheres (hollow ceramic spheres -10 +30 mesh), using two veneer thicknesses (1/10 inch and 3/16 inch), three bed temperatures (250, 325, and 400°F) and two air velocities (30 and 60 cfm). The shortest drying time to reach 5% M.C., starting from 107.3% M.C. was found to be 1 3/4 minutes for the thicker veneer. The maximum drying rates obtained were three times faster with sand beds and two times faster with Cerasphere beds than those for a jet drier at the same temperature. Increasing the bed temperature had the greatest effect on drying rate. Air flow rate had an effect on drying rate only at low bed temperatures and with the slower drying rate medium (Ceraspheres), but had negligible effect at higher temperatures and with sand beds.

Babailov and Petri (2) have recently reported similar work on drying of peeled veneer of thicknesses 1.9 mm, 1.45 mm, 1.1 mm inch and 0.65 mm, in a fluidized bed of metallurgical slag (particle size, 0.515 - 1.125 mm), from 80% M.C. to 6% M.C. at several temperatures and air velocities. They found that the drying time for 1.45 mm thick veneer decreased by a factor of 6.5 as the bed temperature increased from 105 to 280°C; however, for bed temperature increase from 260°C to 280°C, the drying time decreased very little.

They also found that the velocity of gas did not play an important role in veneer drying. Babilov and Petri reported the following linear relationship between drying time (τ) and the thickness of veneer (S_1):

$$\tau = k_1 S_1 - b_1 \qquad 7$$

where coefficients k_1 and b_1 are bed temperature (τ) dependent

$$k_1 = 1.98 \times 10^7 \times t^{-2.63} + 7.78 \qquad 8$$

$$b_1 = 11.9 \times 10^7 \times t^{-3.29} + 1.41 \qquad 9$$

where S_1 is in millimeters, t in degrees centigrade and τ is in seconds.

From a comparison between fluidized bed dryers and other types of dryers (convective dryer, contact dryer and rotary dryer), Babailov and Petri showed that drying time in the fluidized bed is much shorter.

A mathematical model for calculating the rate of veneer or wood drying in a fluidized bed has been presented by Wen and Loos (22). The symbols used in this model and their physical relationship to the drying veneer are shown in Fig. (4).

Fig. 4 FLUIDIZED BED DRYING MODEL OF WEN AND LOOS

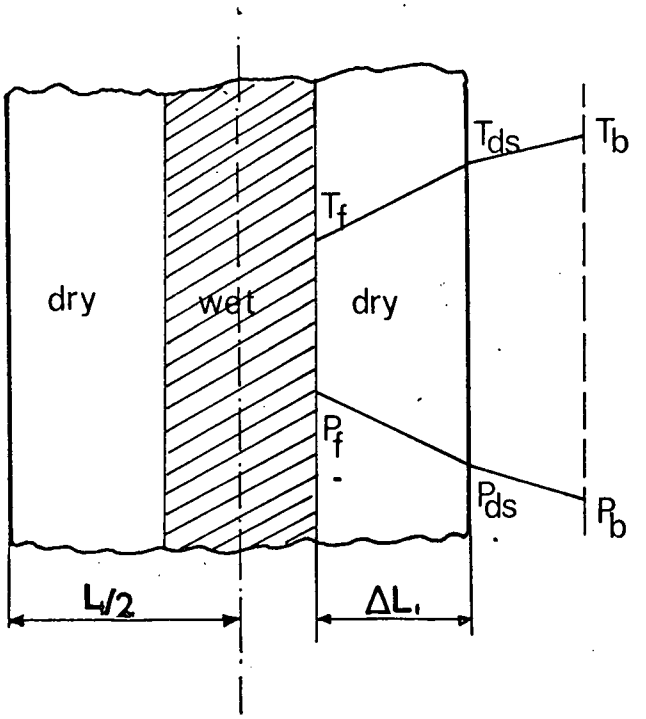

T_b = bed temperature (°F)

T_{ds} = surface temperature of dry layer (°F)

T_f = temperature of interface between wet and dry layers (°F)

P_b = vapor pressure of water in bed (atm.)

P_{ds} = vapor pressure of water at T_{ds} (atm.)

P_f = vapor pressure of water at interface (atm.)

L_1 = thickness of wood (feet)

ΔL_1 = thickness of dry layer (feet).

From heat transfer equation

$$q = h(T_b - T_{ds}) = \frac{k_{s1}}{\Delta L_1}(T_{ds} - T_f) \qquad 10$$

and mass transfer equation

$$N_w = k_{g1}(P_{ds} - P_b) = \frac{D_e}{RT_a} \cdot \frac{P_f - P_{ds}}{\Delta L_1} \qquad 11$$

they derived

$$(1-X) = \frac{8D_e M_w}{L_1^2 RT_a \rho_w}(P_f - P_b)\left(\frac{\theta}{1-X}\right) - \frac{4}{L_1}\frac{D_e}{k_{g1}} \cdot \frac{1}{RT_a} \qquad 12$$

and

$$(1-X) = \frac{8k_{s1}}{L_1^2 \rho_w \Lambda}(T_b - T_f)\left(\frac{\theta}{1-X}\right) - \frac{4}{L_1}\frac{k_{s1}}{h} \qquad 13$$

where q = flux of heat transfer, BTU/(ft.^{2})(hr.)

T_a = average temperature in the wood, °F

h = heat transfer coefficient across gas film, BTU/(hr.)(ft.^{2})(°F)

k_{s1} = effective thermal conductivity of wood, BTU/(hr.)(ft.)(°F)

k_{g1} = mass transfer coefficient across gas film, lb. moles/(hr.)(ft.^{2})(atm.)

D_e = effective diffusivity of water vapor through dry wood layer, ft.^{2}/hr.

R = gas constant, (atm.)(ft.^{3})/(lb. moles)(°F)

X = fraction of water remaining in wood

Λ = latent heat of vaporization of water, BTU/lb.

M_w = molecular wt. of water, lbs.

ρ_w = initial wt. of water per unit vol. of wood, lbm./ft.^{3}

θ = time, hrs.

Plots of $1-X$ vs. $\frac{\theta}{1-X}$ using experimental data at a bed temperature of 250°F gave straight lines and were used to calculate k_{s1}, D_e, h, and k_{g1}, assuming T_f in Eq. (13) to be the boiling point of water (212°F) and P_f in Eq. (12) to be one atmosphere. However, at bed temperatures of 300°F and above, the plots did not give straight lines, and the data showed the rate of drying above 250°F to be a weaker function of bed temperature than indicated by Eq. (12). The assumption that the temperature at the interface between the dry and wet layers is the boiling temperature of water is an arbitrary one and apparently becomes invalid at high bed temperatures. It would also not apply at bed temperatures lower than 212°F. A more reasonable assumption for T_f would appear to be the wet bulb temperature. However, plots of $1-X$ vs. $\theta/1-X$ using experimental data obtained in this work did not give straight lines. The model described above is therefore considered to be of limited validity.

2. Heat transfer between a fluidized bed and a submerged object

Heat transfer between a fluidized bed and a surface in contact with it is much more rapid than in single-phase gas flow, or in a fixed bed. Bed-to-object heat transfer coefficients in gas fluidized beds have been found to be 20 to 40 times those for gases alone (5, 3). Possible explanations for good heat transfer in fluidized beds have been summarized by Ziegler et al. (5) as follows:

1. The increase in heat transfer is a consequence of the scrubbing action of particles against the transfer surface. This action disturbs the gas film, decreases its resistance to the flow of heat and so increases heat transfer coefficient (23, 24, 25).
2. Fluidized particles move in pockets from the core of the bed to the heat transfer surface, absorbing or giving up heat by unsteady state conduction and returning to the core of the bed (27, 28). The gas serves as a stirring agent and also as a heat transfer medium between the particles and the surface. The presence of the fluidized particles causes the heat capacity of the pockets to be high thereby giving faster heat transfer than with a gas alone.

Several equations for calculating heat transfer coefficients proposed by different investigators, are given in the book by Kunii and Levenspiel (3, p. 268).

CHAPTER 3

THEORETICAL ANALYSIS OF DRYING IN FALLING-RATE PERIOD

3.1 Definition of the Problem

The problem is to formulate a mathematical model for drying in the falling-rate period which can be used to predict distribution of moisture and temperature inside the wood during drying with a finite external resistance to heat and mass transfer. The model will be restricted to the drying of a uniformly wet slab of wood with heat and mass transfer occurring in one dimension and in two dimensions.

3.2 Selection of a Model

The various models for moisture transfer inside wet bodies discussed in the previous sections were examined, and the liquid diffusion model was selected for the following reasons:

1. The capillary theory of moisture movement is applicable only to that fraction of water which moves through capillaries by mass flow (free and capillary condensed water) but not to surface bound moisture whose movement by molecular diffusion cannot be negligible, especially at low moisture contents.
2. The moving boundary model assumes that the tempera-

ture at the interface between the dry and wet zones is the boiling temperature of water. This is an arbitrary assumption and apparently becomes invalid at bed temperatures higher than, as well as lower than, 212°F. A more reasonable assumption for the interface temperature would appear to be the wet bulb temperature, but plots of (1-X) vs. $\theta/(1-X)$ using the experimental data obtained in this work did not give the expected straight line. This model is therefore considered to be of limited validity. Besides, the concept of having a completely dry zone and a wet zone does not seem to be realistic.

3. The diffusion model on the other hand offers a more reasonable mechanism for the movement of bound water during drying, and is amenable to mathematical analysis. It has, therefore, received acceptance in the literature (7).

Sherwood (9) and Newman (10) have thoroughly investigated the problem of diffusion in porous solids when the mass transfer coefficient through the gas film is infinite (i.e., zero surface resistance to mass transfer). In the analysis presented here, their solutions are extended to include the more general boundary condition where the surface mass transfer coefficient is finite. In addition, the theory developed is capable of yielding the distribution of moisture within the solid as a function of time, while Newman's diffusion model provides only average values of moisture content of

wood during drying.

3.3 Assumptions

1. The effective diffusivity D and thermal diffusivity α are assumed to remain constant during the course of a drying run.
2. Liquid evaporates only from the surface.
3. The surrounding air is dry ($m_b \simeq 0$).
4. The so called "radiation" boundary condition exists (30). This boundary condition describes the situation where the flux of heat or mass across the surface is proportional to the temperature or partial pressure gradients between the surface and the surrounding medium (i.e., finite surface resistance to heat and mass transfer).

3.4 Theoretical Analysis

In the following analysis, the drying of a block of wood is treated as a two-dimensional problem, assuming that temperature and moisture gradients in the x-direction (along the grain) (see Fig. 5) can be neglected.

This assumption is valid for drying of a long piece of lumber (2"x4"x12"), and was satisfied in the experimental work by insulating the two ends of the block for both heat and mass transfer.

Note that y direction is a radial direction (across the growth zones) and z is a tangential direction (parallel

Fig. 5 **GEOMETRY OF BLOCK**

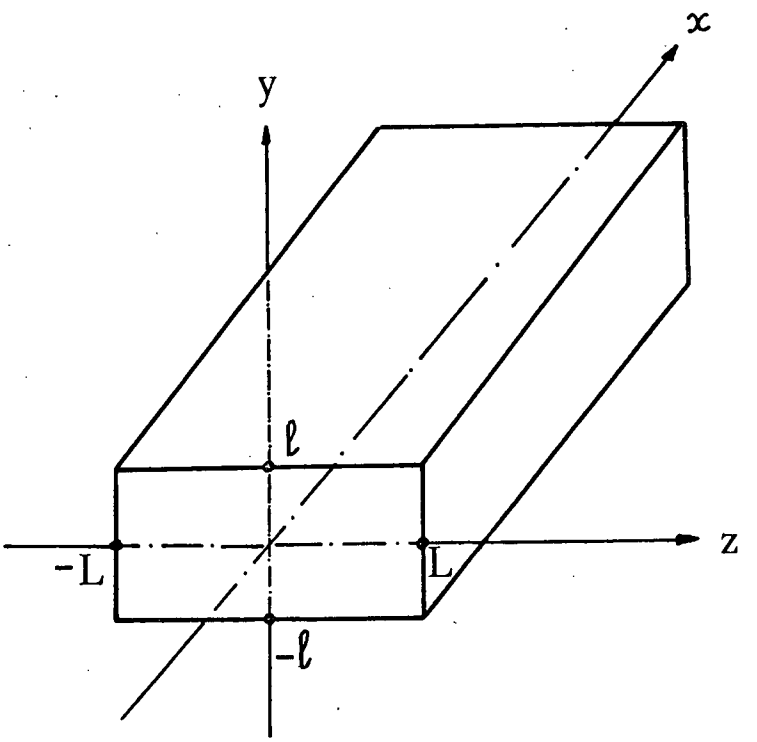

to the growth zones).

When a block of wet wood is subjected to convective thermal drying, two processes occur simultaneously.

1. Transfer of heat to the surface by convection and then into the interior of the block by conduction.
2. Transfer of mass as liquid from the interior to the surface by diffusion and as vapor from the surface to the surroundings by convection.

1. Heat transfer

An elementary heat balance inside the block gives:

$$\frac{\partial \overline{T}}{\partial \theta} = \alpha\{\frac{\partial^2 \overline{T}}{\partial y^2} + \frac{\partial^2 \overline{T}}{\partial z^2}\} \qquad 1$$

where

$$\alpha = \frac{k_s}{C_{ps}\rho_{so}} \quad \text{(subscript s refers to solid properties)} \qquad 2$$

$$\overline{T} = \frac{(T_b - T)}{(T_b - T_0)}, \quad \text{dimensionless temperature} \qquad 3$$

k_s = thermal conductivity (BTU/ft.hr.°F), assumed constant

C_{ps} = specific heat (BTU/lbm.°F)

ρ_{so} = density (lbm./ft.^{3}) of dry wood

T = temperature at any point inside block (°F)

T_b = temperature of fluidized bed (°F)

T_0 = initial temperature of block (°F) at the beginning of the falling-rate period, assumed constant throughout the block

θ = time (hours)

α = thermal diffusivity (ft.^{2}/hr.), (average value over the drying period).

Equation (1) must satisfy the following initial and boundary conditions.

Initial condition

$$\theta = 0, \quad \text{for all } y,z: \quad T = T_0 \quad \text{or} \quad \overline{T} = 1 \qquad 4$$

Final condition

$$\theta \to \infty, \quad \text{for all } y,z: \quad T \to T_b \quad \text{or} \quad \overline{T} \to 0 \qquad 5$$

Boundary conditions

$$\theta > 0, \quad y = \ell, \quad -L < Z < L:$$

$$k_s \frac{\partial T}{\partial y} - \Lambda D \rho_{so} \frac{\partial m}{\partial y} = h(T_b - T) \qquad 6$$

where Λ = latent heat of vaporization of water (BTU/lbm.)

m = mass of water/mass of dry wood (lbm./lbm.)

h = external heat transfer coefficient (BTU/ft.^{2}hr.°F)

D = diffusivity of water in wood (average value over the drying period) (ft.^{2}/hr.).

Let

$$M = \frac{(m - m_\infty)}{(m_0 - m_\infty)} \qquad 7$$

where m_0 (assumed constant throughout the block) and m_∞ are the moisture contents of the wood at $\theta = 0$, (at the beginning of the falling-rate period) and $\theta \to \infty$, respectively. Substitution from Eqs. (3) and (7) into Eq. (6) gives

$$- k_s(T_b - T_0) \frac{\partial \overline{T}}{\partial y} - \Lambda D \rho_{so}(m_0 - m_\infty) \frac{\partial M}{\partial y} = h(T_b - T_0)\overline{T} \qquad 8$$

or

$$- \frac{\partial \bar{T}}{\partial y} - \frac{\Lambda D \rho_{so}(m_0 - m_\infty)}{k_s(\bar{T}_b - T_0)} \frac{\partial M}{\partial y} = \left(\frac{h}{k_s}\right)\bar{T} \qquad 9$$

Putting

$$\frac{\Lambda D \rho_{so}(m_0 - m_\infty)}{\{k_s(\bar{T}_b - T_0)\}} = a \qquad 10$$

and

$$\frac{h}{k_s} = b \qquad 11$$

in Eq. (9), gives

$$- \frac{\partial \bar{T}}{\partial y} - a \frac{\partial M}{\partial y} = b\bar{T} \qquad 12$$

The boundary conditions for the other three surfaces can be found in a similar manner. Thus for $\theta > 0$, $y = -\ell$, and $-L < Z < L$

$$+ \frac{\partial \bar{T}}{\partial y} + a \frac{\partial M}{\partial y} = b\bar{T} \qquad 13$$

For $\theta > 0$, $z = L$, and $-\ell < y < \ell$,

$$- \frac{\partial \bar{T}}{\partial z} - a \frac{\partial M}{\partial z} = b\bar{T} \qquad 14$$

For $\theta > 0$, $z = -L$, and $-\ell < y < \ell$,

$$+ \frac{\partial \overline{T}}{\partial z} + a \frac{\partial M}{\partial z} = b\overline{T} \qquad 15$$

2. Mass transfer

A simple material balance on an element inside the block gives

$$\frac{\partial M}{\partial \theta} = D\{\frac{\partial^2 M}{\partial y^2} + \frac{\partial^2 M}{\partial z^2}\} \qquad 16$$

The initial, final, and boundary conditions are:

$$\theta = 0, \quad \text{for all } y,z: \quad M = 1 \qquad 17$$

$$(\theta \to \infty, \quad \text{for all } y,z: \quad M \to 0) \qquad 18$$

For $\theta > 0$, $y = \ell$, $-L < Z < L$

$$- D\rho_{so}\frac{\partial m}{\partial y} = k_g(P_s - P_b) \qquad 19$$

where k_g = external mass transfer coefficient (lbm./ft.^{2} hr.atm.)

P_s = partial pressure of water vapor at the surface (atm.)

P_b = partial pressure of water vapor in the bed (atm.)

If we assume that the water vapor concentration in the surrounding is zero, i.e., $P_b = 0$, and the partial pressure of water vapor at the surface is given by

$$P_s = P_{vp} \cdot S^{-1} \cdot m_s \qquad 20$$

where P_{vp} is the vapor pressure at the surface, and S is the slope of the desorption isotherm curve for Western Hemlock (Fig. 6) representing the relationship between moisture content (%) and relative humidity (%), the boundary condition (i.e., Eq. (19)) becomes:

$$- D\rho_{so}(m_0 - m_\infty) \frac{\partial M}{\partial y} = k_g P_{vp} S^{-1} \{(m_0 - m_\infty)M + m_\infty\} \qquad 21$$

However, since $m_\infty \simeq 0$, Eq. (21) becomes

$$- \frac{\partial M}{\partial y} = \frac{k_g P_{vp} S^{-1}}{D\rho_{so}} \cdot M \qquad 22$$

Letting

$$\frac{k_g P_{vp} S^{-1}}{D\rho_{so}} = C \qquad 23$$

Eq. (22) becomes

$$- \frac{\partial M}{\partial y} = CM \qquad 24$$

Fig.6 **ADSORPTION AND DESORPTION ISOTHERMS AT 30°C**

for western hemlock (ref.30)

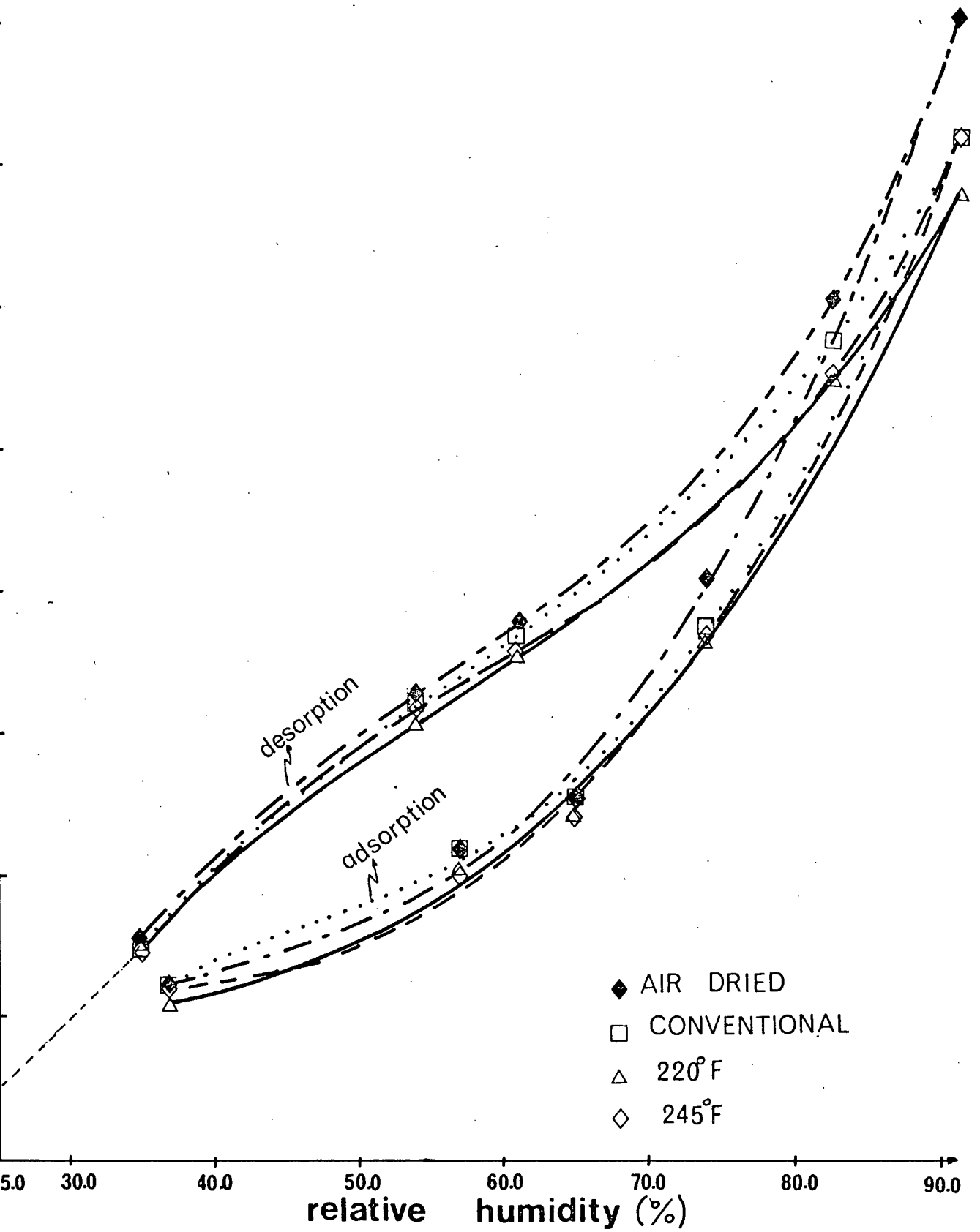

In a similar way, for $\theta > 0$, $y = -\ell$, $-L < Z < L$

$$+ \frac{\partial M}{\partial y} = CM \qquad 25$$

for $\theta > 0$, $z = L$, $-\ell < y < \ell$

$$- \frac{\partial M}{\partial z} = CM \qquad 26$$

for $\theta > 0$, $z = -L$, $-\ell < y < \ell$

$$+ \frac{\partial M}{\partial z} = CM \qquad 27$$

3.5 Solution of the Mass and Heat Transfer Equations

The mass transfer boundary conditions represented by Eq.'s (24), (25), (26) and (27) are independent of temperature, hence it is appropriate to solve the mass transfer equations first. The equations are linear and can therefore be solved by separation of variables (39, p. 363).

1. Mass transfer

Let us assume that the solution of Eq. (16) is of the form:

$$M = \psi_1(\theta)\psi_2(y)\psi_3(z) \qquad 28$$

i.e., the independent variables can be separated, ψ_1, ψ_2, ψ_3

being functions of θ, y, z, respectively. Substituting (16) into (28) and rearranging gives:

$$\frac{\psi_1'}{\psi_1} = D\{\frac{\psi_2''}{\psi_2} + \frac{\psi_3''}{\psi_3}\} \qquad 29$$

The left hand side (LHS) is only a function of θ whereas the right hand side (RHS) is a function of y and z. This condition can only be met if

$$\frac{\psi_1'}{\psi_1} = D\{\frac{\psi_2''}{\psi_2} + \frac{\psi_3''}{\psi_3}\} = \text{constant} \qquad 30$$

Let the constant be denoted by $-D\lambda^2$ so that:

$$\frac{\psi_1'}{\psi_1} = - D\lambda^2 \qquad 31$$

and

$$\frac{\psi_2''}{\psi_2} + \frac{\psi_3''}{\psi_3} = - \lambda^2 \qquad 32$$

The solution of Eq. (31) is

$$\psi_1 = e^{-D\lambda^2\theta} \qquad 33$$

omitting the constant of integration multiplying the RHS of Eq. (33).

From Eq. (32) we have

$$\frac{\psi_2''}{\psi_2} = -\frac{\psi_3''}{\psi_3} - \lambda^2 \qquad 34$$

Once again the LHS and RHS of Eq. (34) are functions of different independent variables so that

$$\frac{\psi_2''}{\psi_2} = -\beta^2 \qquad 35$$

and

$$-\frac{\psi_3''}{\psi_3} - \lambda^2 = -\beta^2 \qquad 36$$

The general solution of Eq. (35) is

$$\psi_2 = A'\sin(\beta y) + B'\cos(\beta y) \qquad 37$$

where A' and B' are constants of integration.

If we rewrite Eq. (36) is

$$\psi_3'' + (\lambda^2-\beta^2)\psi_3 = 0 \qquad 38$$

and put

$$\Omega^2 = \lambda^2 - \beta^2 \qquad 38.1$$

then, the general solution of Eq. (38) is:

$$\psi_3 = A''\sin(\Omega z) + B''\cos(\Omega z) \qquad 39$$

where A" and B" are constants of integration.

From symmetry

$$y = 0 \quad \partial M/\partial y = 0 \quad \partial\psi_2/\partial y = 0 \quad \therefore \quad A' = 0$$

$$z = 0 \quad \partial M/\partial z = 0 \quad \partial\psi_3/\partial z = 0 \quad \therefore \quad A'' = 0 \qquad 40$$

Hence, Eqs. (37) and (39) become

$$\psi_2 = B'\cos(\beta y) \qquad 41$$

$$\psi_3 = B''\cos(\Omega z) \qquad 42$$

Eq. (28) therefore becomes

$$M = Be^{-D\lambda^2\theta}\cos(\beta y)\cos(\Omega z) \qquad 43$$

where B = constant of integration = B'·B"

D = diffusivity

β, Ω, and λ are eigen values.

To find the constant β, substitute Eq. (43) into Eq. (24)

$$+ Be^{-D\lambda^2\theta}\beta \sin(\beta\ell)\cos(\Omega z) = CBe^{-D\lambda^2\theta}\cos(\beta\ell)\cos(\Omega z) \quad 44$$

or

$$\beta \tan(\beta\ell) = C \quad 45$$

This equation has an infinite number of solutions for β. Let us denote them by β_n, where n is an integer. Hence Eq. (45) can be written as:

$$\beta_n \tan(\beta_n\ell) = C \quad 45.1$$

Note that substitution from Eq. (43) into Eq. (25) leads also to Eq. (45). By a similar method we find

$$\Omega \tan(\Omega L) = C \quad 46$$

with Ω_m as solutions where m is an integer or

$$\Omega_m \tan(\Omega_m L) = C \qquad 46.1$$

Eqs. (45.1) and (46.1) can be solved numerically for β_n and Ω_m, which are eigen values as defined by equations (45.1) and (46.1), respectively. It follows from Eq. (38.1) that

$$\lambda_n^2 = \beta_n^2 + \Omega_m^2 \qquad 47$$

We therefore have as a particular solution of Eq. (16)

$$M = B_m e^{-D\lambda_n^2\theta} \cos(\beta_n y)\cos(\Omega_m z) \qquad 48$$

and as the general two-dimensional solution

$$M = \sum_{m=1}^{\infty} \sum_{n=1}^{\infty} B_{mn} e^{-D\lambda_n^2\theta} \cos(\beta_n y)\cos(\Omega_m z) \qquad 49$$

where $B_{mn} = B_m \cdot B_n$ 50

Eq. (49) may be rewritten as follows

$$M(\theta,y,z) = \sum_{n=1}^{\infty} B_n e^{-D\beta_n^2\theta} \cos(\beta_n y) \sum_{m=1}^{\infty} B_m e^{-D\Omega_m^2\theta} \cos(\Omega_m z) \qquad 51$$

Note that only positive values of β_n and Ω_m need be considered since negative values give dependent particular solutions.

The average moisture content of the block of wood is:

$$M_{AV}(\theta) = \int_{-L}^{L} \int_{-\ell}^{\ell} M(\theta,y,z)\,dydz/4\ell L \qquad 52$$

Integration of Eq. (51) and substitution of the result in Eq. (52) yields:

$$M_{AV}(\theta) = \sum_{n=1}^{\infty} \frac{B_n}{\ell\beta_n} e^{-\beta_n^2 D\theta} \sin(\beta_n \ell) \sum_{m=1}^{\infty} \frac{B_m}{L\Omega_m} e^{-\Omega_m^2 D\theta} \sin(\Omega_m L) \qquad 53$$

The coefficients B_m and B_n on the right hand side of Eq. (51) are found by substituting Eq. (51) into the initial condition Equation 17,

$$1 = \sum_{n=1}^{\infty} B_n \cos(\beta_n y) \sum_{m=1}^{\infty} B_m \cos(\Omega_m z) \qquad 54$$

Multiplying both sides of Eq. (54) by $\int_0^{\ell} \cos(\beta_j y)\,dy$, we have

$$\int_0^{\ell} \cos(\beta_j y) = \sum_{m=1}^{\infty} B_m B_n \cos(\Omega_m z) \cdot \int_0^{\ell} \cos(\beta_j y)\cos(\beta_n y)\,dy \qquad 56$$

From standard orthogonality procedure (39)

$$\int_0^{\ell} \cos(\beta_n y)\cos(\beta_j y)dy = 0, \quad \text{when} \quad n \neq j \tag{57}$$

therefore, n = j.

Integration of Eq. (56) gives

$$F = B_n B \sum_{m=1}^{\infty} B_m \cos(\Omega_m z) \tag{58}$$

where

$$F = \sin(\beta_n \ell)/\beta_n$$

and

$$B = \{\frac{\ell}{2} + \frac{\sin(2\beta_n \ell)}{4\beta_n}\} \tag{59}$$

Multiplying both sides of Eq. (58) with $\int_0^L \cos(\Omega_k z)dz$ we get

$$F \int_0^L \cos(\Omega_k z)dz = B \cdot B_m \cdot B_n \int_0^L \cos(\Omega_m z)\cos(\Omega_k z)dz \tag{60}$$

If $k \neq m$,

$$\int_0^L \cos(\Omega_m z)\cos(\Omega_k z) = 0 \qquad 61$$

Therefore k = m, and Eq. (60) after integration becomes

$$AA = B_m \cdot B_n \cdot BB \cdot B \qquad 62$$

where

$$AA = F \sin(\Omega_m L)/\Omega_m$$

and

$$BB = \{\frac{L}{2} + \frac{\sin(2\Omega_m L)}{4\Omega_m}\} \qquad 63$$

Combining Eqs. (63) and (62) with Eq. (59) gives

$$B_{mn} = B_m \cdot B_n = \frac{\sin \beta_n \ell}{\{\frac{\beta_n \ell}{2} + \frac{\sin 2\beta_n \ell}{4}\}} \cdot \frac{\sin \Omega_m L}{\{\frac{\Omega_m L}{2} + \frac{\sin 2\Omega_m L}{4}\}} \qquad 64$$

Numerical solution of Eq. (53) in conjunction with Eq. (64) gives the average moisture content of the block as a function of time.

2. Heat transfer

By separation of variables

$$\bar{T} = \phi_1(\theta)\phi_2(y)\phi_3(z) \qquad 65$$

where ϕ_1, ϕ_2, and ϕ_3 are functions of θ, y, and z, respectively.

As in the case of mass transfer, Eq. (1) leads to the following equation, which is analogous to Eq. (43) for mass transfer:

$$\bar{T} = Ae^{-\alpha k^2 \theta}\cos(uy)\cos(vz) \qquad 66$$

where

A = constant of integration

α = thermal diffusivity

u,v = eigen values

$$k^2 = u^2 + v^2 \qquad 67$$

To find the constant u (eigen value), substitute Eq. (66) and Eq. (49) into Eq. (12), setting z = 0 and y = ℓ,

$$u_n e^{-\alpha k^2 \theta}\sin(u_n \ell) + a \sum_{m=1}^{\infty} \sum_{n=1}^{\infty} \beta_n B_{mn} \sin(\beta_n \ell) e^{-D\lambda^2 \theta}$$

$$= be^{-\alpha k^2 \theta}\cos(u_n \ell) \qquad 68$$

where u_n is the number of solutions, n being an integer.

By a similar method we find

$$v_m e^{-\alpha k^2 \theta} \sin(v_m L) + a \sum_{n=1}^{\infty} \sum_{m=1}^{\infty} \Omega_m B_{mn} \sin(\Omega_m L) e^{-D\lambda_n^2 \theta}$$

$$= b e^{-\alpha k^2 \theta} \cos(v_m L) \qquad 69$$

with v_m as solutions, m being an integer.

It follows from Eq. (67) that

$$k_n^2 = u_n^2 + v_m^2 \qquad 70$$

The general solution of Eq. (1) can now be written as follows:

$$\overline{T}(\theta, y, z) = \sum_{m=1}^{\infty} \sum_{n=1}^{\infty} A_{mn} e^{-\alpha k_n^2 \theta} \cos(u_n y) \cos(v_m z) \qquad 71$$

Since the coefficient $A_{mn} = A_m \cdot A_n$. 72

Eq. (71) may be written as follows:

$$\overline{T}(\theta, y, z) = \sum_{n=1}^{\infty} A_n e^{-\alpha u_n^2 \theta} \cos(u_n y) \sum_{m=1}^{\infty} A_m e^{-\alpha v_m^2 \theta} \cos(v_m z) \qquad 73$$

Equations (71) and (73) are analogous to mass transfer

Eqs. (49) and (51). The coefficients $A_{mn} = A_m \cdot A_n$ are found by the same method as used in the case of mass transfer with the following result:

$$A_{mn} = \frac{\sin(u_n \ell)}{\{\frac{u_n \ell}{2} + \frac{\sin 2u_n \ell}{4}\}} \cdot \frac{\sin(v_m L)}{\{\frac{v_m L}{2} + \frac{\sin 2v_m L}{4}\}} \qquad 74$$

The average wood temperature is given by:

$$\overline{T}_{AV}(\theta) = \int_{-\ell}^{\ell} \int_{-L}^{L} \overline{T}(\theta, y, z)\, dy dz / 4\ell L \qquad 75$$

Integration of Eq. (73) in conjunction with Eq. (74) and substitution of the result in Eq. (75) yields

$$\overline{T}_{AV}(\theta) = \sum_{n=1}^{\infty} \frac{A_n}{\ell u_n} e^{-\alpha u_n^2 \theta} \sin(u_n \ell) \sum_{m=1}^{\infty} \frac{A_m}{L v_m} e^{-\alpha v_m^2 \theta} \sin(v_m L) \qquad 76$$

Equation (76) is analogous to mass transfer Eq. (53) and can be solved numerically to get the average temperature of the wooden block as a function of drying time.

3.6 Calculation Procedure

In applying the preceding mathematical model to analysis of experimental data, the mass and heat diffusivities

(D in Eq. (53) and α in Eq. (76)) were treated as loose parameters. The values of these parameters were determined for each run by searching for the value required in the theoretical equations to give a good match (least-squares fit) between calculated and observed results of average moisture content and average temperature, each as a function of time.

1. Computer program

Digital computer programs for numerical solution of Eqs. (53) and (76) were written for predicting the average moisture content and average temperature, both as a function of time, for a block of wood undergoing unsteady-state drying. An additional program was written for computing and plotting moisture distribution (Eq. 51) as a function of time. A list of the Fortran programs used is shown in Appendix A, while the theoretical results of average moistures and temperatures together with corresponding experimental data appear in Appendix B. Theoretical result of moisture distribution within the block after different periods of drying time are included in Appendix D.

2. Mass transfer

For calculating average moisture content as function of time by Eq. (53), the Newton method of iteration (29) was employed to find eigen values (β_n and Ω_m), i.e., the roots of Eqs. (45.1) and (46.1). The constant $C = \left(\frac{k_g P_{vp} S^{-1}}{D\rho_{so}}\right)$ in Eq. (23) is a function of diffusivity D, which is unknown.

Fortunately the value of C for the experimental conditions of the present work was always > 100 and the eigen values for C > 100 are approximately the same as in the case of C = ∞, (30). Hence, even large changes in mass-transfer coefficient k_g, vapor pressure of water at the surface P_{vp}, and solid density ρ_s, have very little effect on the final result of eigen values. The slope of the equilibrium curve (desorption isotherm for Western Hemlock), S taken from Fig. (6) to be about 0.2 for moisture content of 5-6% which was experimentally found to be the moisture content close to the surface of the wood.

The mass transfer coefficient k_g, for use in Eq. (23) was calculated from the following equation given by Beek (4, p. 433)

$$\frac{K_{Gw}}{U_{mf}} \varepsilon_{mf} S_c^{2/3} = C^* \{ \frac{U_{mf} d_p \mu}{\rho(1-\varepsilon_{mf})} \}^{-m^*} \qquad 77$$

where $C^* = 0.7$, $m^* = 0$, and $S_c = 2.57$ for gas fluidized bed, $R_e^* = \frac{U_{mf} d_p \rho}{\mu(1-\varepsilon_{mf})}$ (300-12,000), and ε_{mf} (0.50-0.95), hence Eq. (77) may be rewritten:

$$\frac{K_{Gw}}{U_{mf}} \varepsilon_{mf} \cdot (2.57)^{2/3} = 0.7 \qquad 78$$

where K_{Gw} = mass-transfer coefficient, ft./hr.

Eq. (77) is valid for mass transfer between a fluidized bed and a wall or an object. The properties of the fluidized bed used are given in Table (4). For the present system with viscosity (μ) and density (ρ) of air at the bed temperature (T_b = 217°F) the value of the mass transfer coefficient by k_g works out to 128 lbm./ft.^{2}hr.atm. The average moisture content obtained after one hour of drying was used as the starting moisture content of the falling-rate period so as to exclude the initial heating-up period from the calculations.

3. Heat transfer

In order to calculate average wood temperature as a function of time using Eq. (76), the Newton method of iteration (29) was employed to find eigen values (u_n, and v_m), i.e., the roots of Eqs. (68) and (69). However, the existence of the terms $\partial M/\partial y$ and $\partial M/\partial z$ in Eqs. (12), (13), (14), and (15) made the boundary conditions non-linear. In order to simplify the problem, the following approximate procedure was adopted: The average wood temperature measured experimentally after one hour of drying was used as the starting temperature of the first interval. The drying time was then divided into intervals of one hour. For each interval, $\partial M/\partial y$ and $\partial M/\partial z$ were assumed constant and were evaluated at the mid point of that interval, taking time θ = 0, at the beginning of the interval. The eigen values (u_n and v_m) for each interval were then evaluated using Eqs. (68) and (69). Taking the final temperature at the end of a time interval to be the

initial temperature at the beginning of the next interval, and assuming that the initial temperatures of each interval is uniform throughout the block, it then becomes possible to determine the coefficients A_{mn} of the interval under consideration using Eq. (74). A more accurate approximation could have been obtained if, instead of the uniform distribution assumed, the actual temperature distribution at the end of the previous interval had been used in the usual orthogonality procedure for finding these coefficients. To check the validity of the approximation procedure used, the calculation was repeated using a shorter time interval (1/2 hr.). The results for half-hour and one-hour intervals, shown in Fig. (7), are seen to be within 2% of each other.

In Eqs. (68) and (69),

$$a = \frac{\Lambda D \rho_s m_0}{k_s (T_b - T_0)} \quad \text{and} \quad b = \frac{h}{k_s}$$

The heat of evaporation Λ as a function of average surface temperature of wood during the falling-rate period was read from the Steam Table (32) and the effective diffusivity D, was obtained from the mass transfer calculations described in the previous section. The density and thermal conductivity of wood were obtained from the literature (see Table 5) at average moisture and temperature conditions over the drying period.

The value of heat transfer coefficient (h) was calculated using the following correlation proposed by Wender and

Fig.7

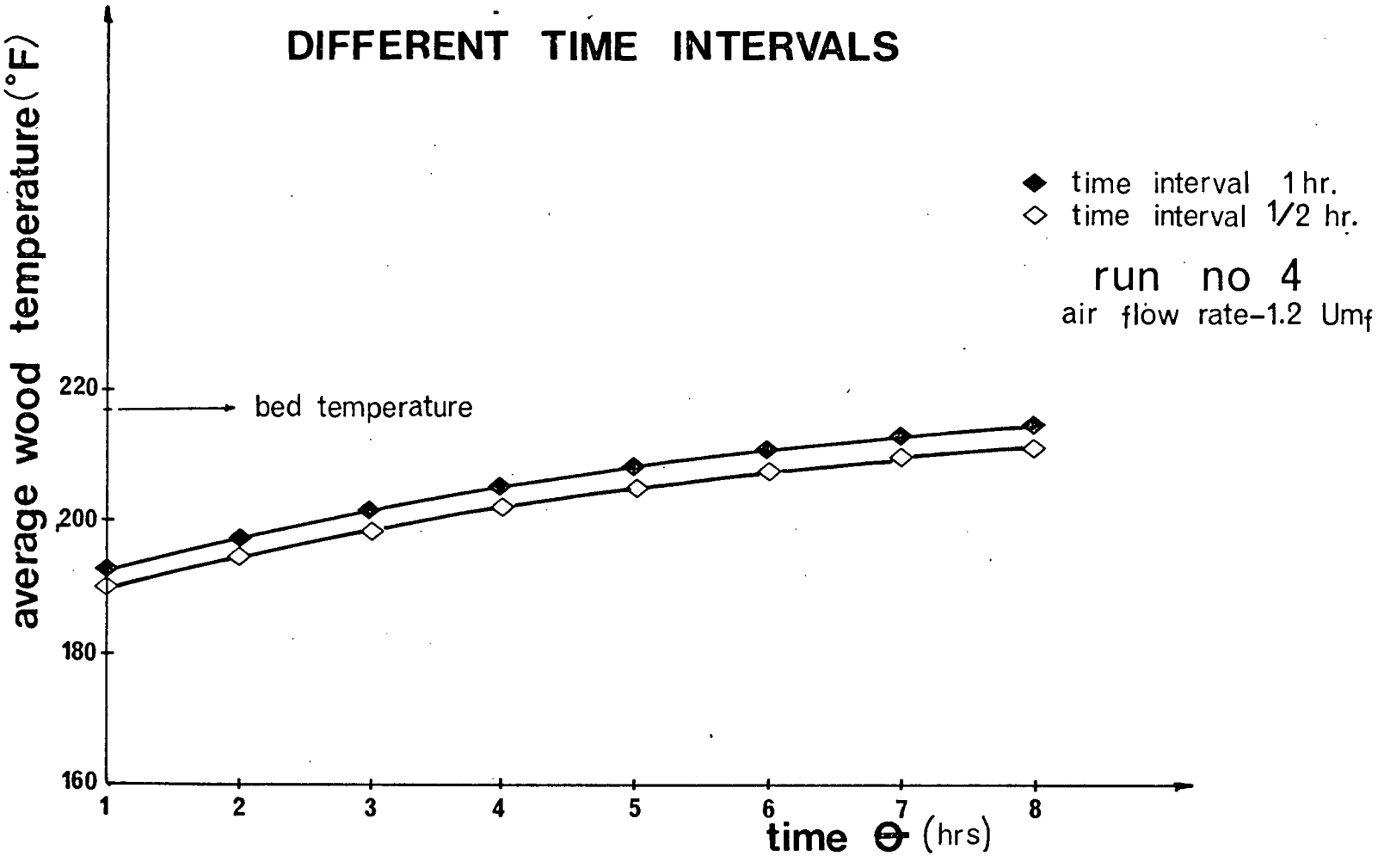
AVERAGE WOOD TEMPERATURE vs. TIME
CALCULATED BY EQ. 76 USING
DIFFERENT TIME INTERVALS
average wood temperature (°F)
time interval 1 hr.
time interval 1/2 hr.
run no 4
air flow rate-1.2 Umf
bed temperature
220
200
180
160
1
2
3
4
5
6
7
8
time Θ (hrs)

Cooper (3, p. 272) for fluidized bed to immersed vertical tube heat transfer:

$$\frac{hd_p}{k} = 0.01844\ C_R(1-\varepsilon_f)\left(\frac{C_{pg}\rho}{k}\right)^{0.43} \cdot \left(\frac{d_p\rho U}{\mu}\right)^{0.23} \left(\frac{C_{psand}}{C_{pg}}\right)^{0.8} \left(\frac{\rho_{sand}}{\rho}\right)^{0.66} \qquad 79$$

for

$$\frac{d_p\rho U}{\mu} = 10^{-2} - 10^{2}$$

(Re no. in present experiments ~ 12)

where C_R = correction factor for non-axial location of immersed tubes

= 1, for a vertical tube positioned at the bed's axis (our case).

The fluidization conditions used in this work were within the range of variables on which Eq. (79) is based.

CHAPTER 4

EXPERIMENTAL STUDY

4.1 Equipment

The equipment used is illustrated in Fig. (8). Air is supplied from the mains through globe valve C and rotameter D, (calibration chart in Appendix C) to the electrical heater E, where it is heated to the desired temperature. Hot air then enters the fluidized bed column H, which consists of a 5.75" diameter x 3' high stainless steel pipe fitted with a sight glass I, through a multiorifice gas distributor G. The distributor has 17 orifices of 0.6" diameter and is backed with a 60 mesh screen to avoid leakage of solids through the holes.

Iron-constantan thermocouples J were used to measure the temperature of the bed at different locations as well as temperatures within the wooden block at positions shown in Fig. (9). A standard Delmhorst resistance moisture meter capable of measuring moistures up to 65% dry-basis was used to measure the moisture content of the wood during drying. The calibration chart for the moisture meter provided by the manufacturer is included in Appendix C.

The calibration was checked by comparing moisture contents measured by the meter against results obtained by the oven-drying method (see Table 1), and the two were found to

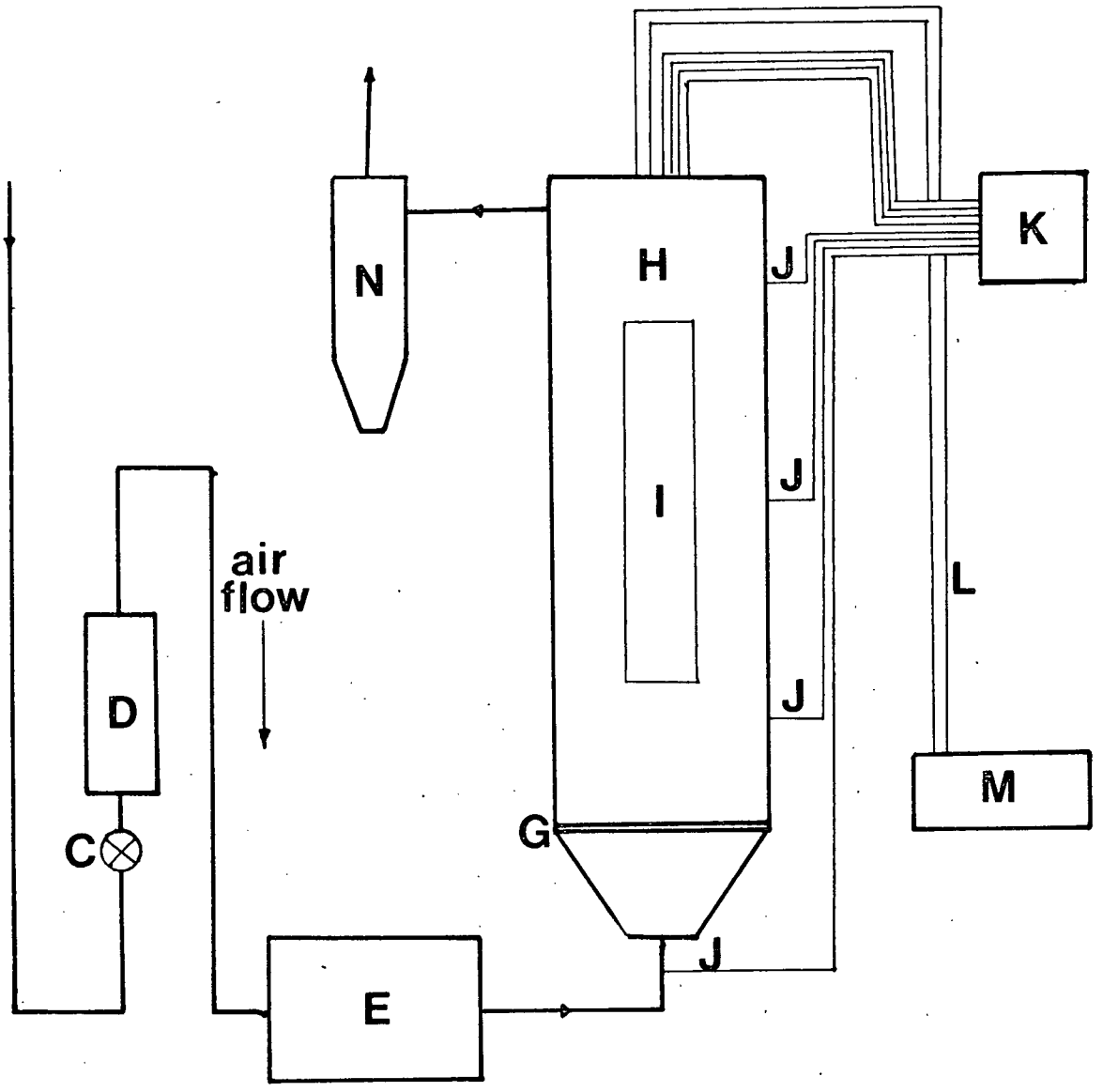

C- globe valve
D- rotameter
E- electrical heater
G- distributor
H- cylindrical column
I- sight window
J- thermocouples
K- temperature indicator
L- electrodes
M- moisture meter
N- cyclone

FIG. 8 DIAGRAM OF EQUIPMENT

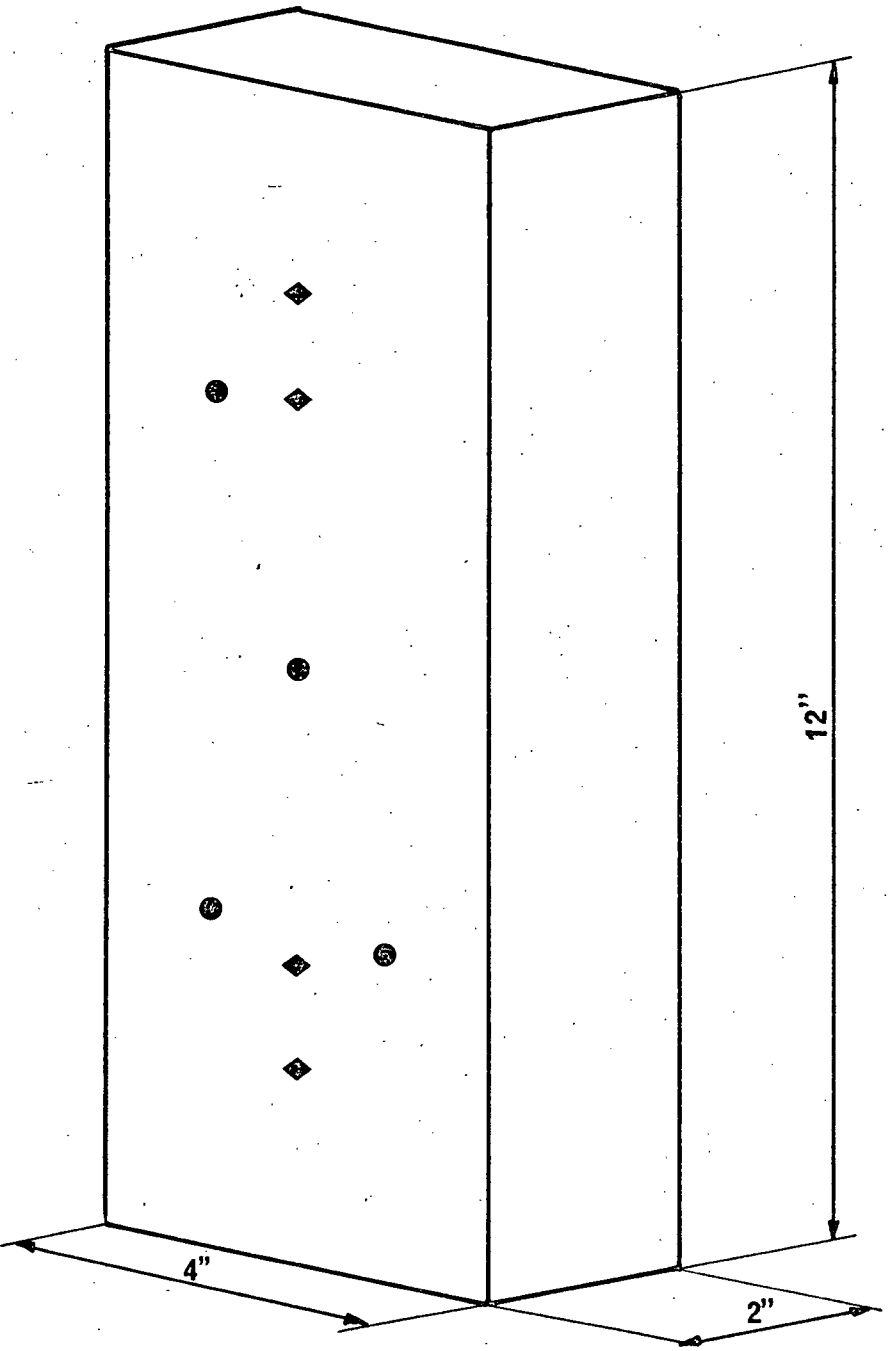

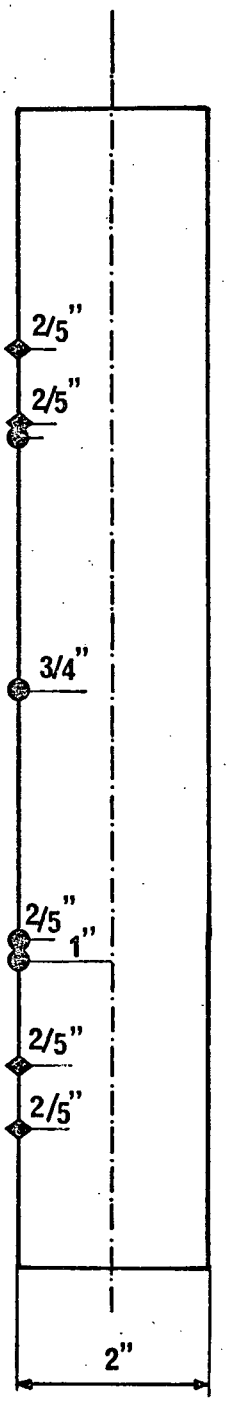

● thermocouples
◈ electrodes

FIG. 9 LOCATION OF THERMOCOUPLES AND ELECTRODES
note - standard block called a 2" x 4" actually is 1,5" x 3,5"

be within about 5% of each other.

TABLE 1. ACCURACY OF MOISTURE METER

	Final Moisture Content (%)	
Run No.	Meter Reading*	Oven-Drying Method
1	15	15.6
12	15	15.8
2	20	20.8
3	37.5	38.1
4	15	15.8
5	15	15.7
6	15	15.5
7	15	15.9
8	15	15.3
11	27	27.9

* Electrodes located at a distance of 1/5th the block thickness from the surface.

4.2 Procedure

Blocks of Western Hemlock, 2 in. x 4 in. x 1 ft. long containing 70% to 90% moisture (dry basis) were provided, and examined after drying, by MacMillan Bloedel Research Ltd. The samples were cut across the grain, and were free of knots, pitch, streaks, spits or other defects. Both ends of the sample were sealed with epoxy resin and covered with

1/16" thick asbestos cloth (two-dimensional drying) to prevent transfer of moisture and heat along the grain. In some experiments, either the edges (y direction) or the large sides (z direction) were additionally insulated in the same manner to achieve one-dimensional drying. The asbestos cloth was secured to the wood with wire. The samples, after insulating, were marked for identification, placed in polyethylene bags and stored in a constant humidity room (temperature 40°F, RH ≃ 50%) until further processing. The fluidized bed, of -20 + 30 mesh Ottawa sand (ρ_b = 89.03 lbm./ft.^{3} and ρ_{sand} = 164.2 lbm./ft.^{3}) was operated with the same bed depth (16" settled), and at a constant air flow rate (U = 1.2 U_{mf}) for all runs except run no. 7 (U = 1.3 U_{mf}) and run no. 8 (U = 1.1 U_{mf}). The observed minimum fluidization velocity, U_{mf}, was 1.3 ft./sec. The bed temperature was varied from one run to the other (175, 190, 204, and 217°F) by controlling the temperature of the inlet air.

The test sample, previously weighed and fitted with the moisture measuring electrodes and thermocouples, (Fig. 9), was mounted in a specially designed holder (Fig. 10), and was inserted into the preheated bed operating at steady-state conditions. The sample was positioned in the bed so that it was fully submerged and was well removed from the wall and base of the column, as shown in Figure (10).

The temperature of the bed, temperatures at different points in the test sample, as well as the average moisture content of the sample, were recorded at regular time intervals.

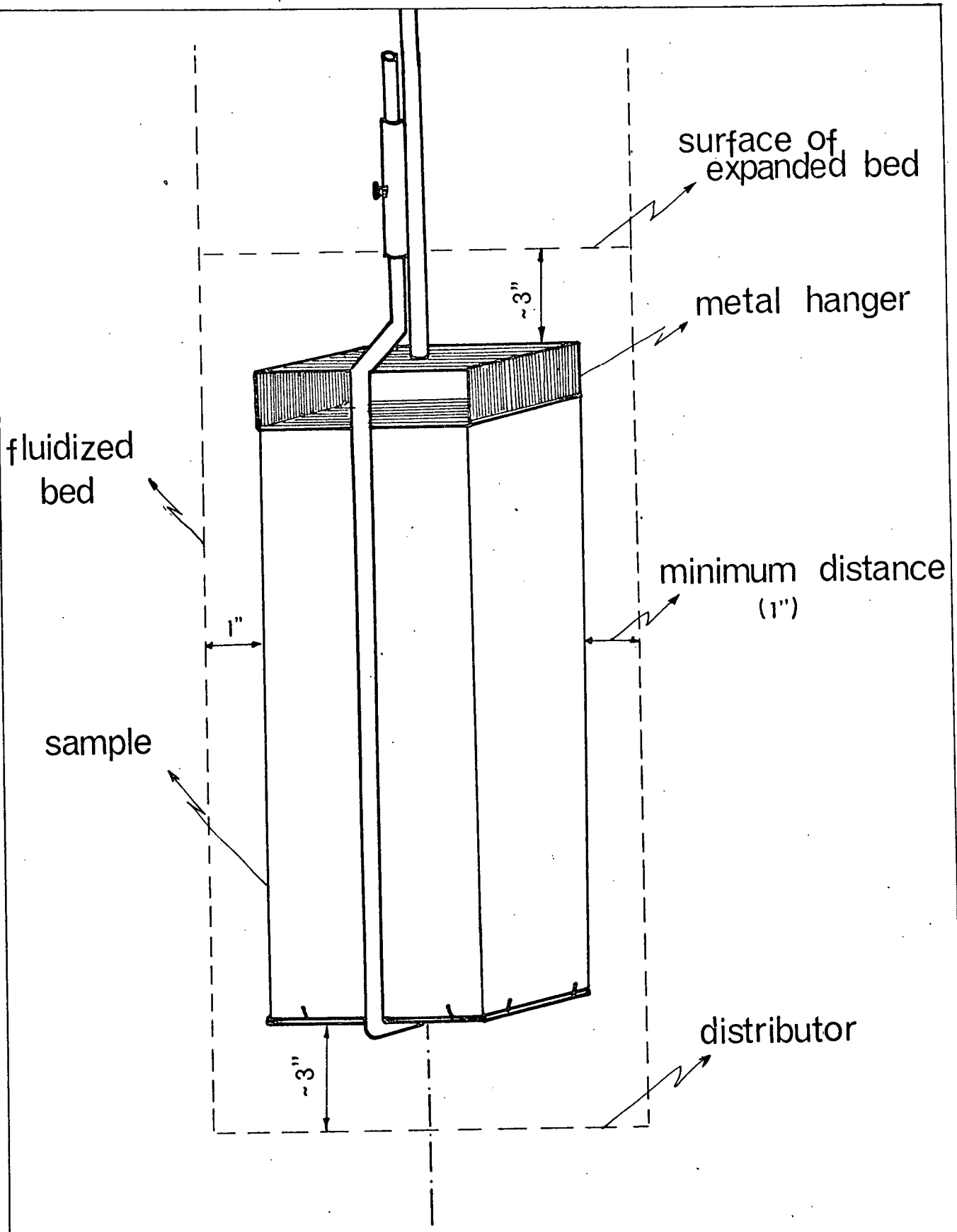

Fig.10 POSITION OF SAMPLE IN FLUIDIZED BED

The holes for the (1/8" dia.) electrodes were drilled undersize to insure a tight fit, and the electrodes were inserted into the wood through a rubber seal ring in order to avoid condensation or evaporation in the hole during decreasing relative humidity conditions. When the lumber reached the desired final moisture content of around 15%, the sample was removed from the bed and weighed immediately. The initial moisture content of the sample was determined by the oven-drying method (drying to constant weight at 212°F), since initial moistures were outside the upper limit measurable by the moisture meter (65%). The final moisture contents were also determined by the above method as a check of the correctness of the moisture meter readings (see Table 1).

The average moisture content of the test sample was determined using the procedure suggested by Dunlop and Bell (ref. 16, p. 185). These authors found, by integrating the roughly parabolic moisture content profiles of drying wood, that "the moisture content in a plane located at one-fifth of the thickness of the material from its surface is usually very near the average of the piece." The moisture content of the wood samples in the experiments were therefore obtained by placing the meter electrodes at the above distance from one of the uninsulated surfaces for the case of one-dimensional drying and from the front surface in the case of two-dimensional drying.

The data in Table (1) provide experimental support for assuming that the moisture meter indeed gave values close to

the average moisture content of the block, in conformity with the rule suggested by Dunlop and Bell. Further confirmation of this procedure over a wider moisture range was obtained by measuring moisture contents at two positions in the block 2/5" (1/5 x thickness) and 1" (centre of block), using two pairs of electrodies. The centre values were converted to average moisture contents by using the following equation given by Brown et al. (35, p. 86):

$$M_c = 3/2(M_a - M_s) + M_s \qquad 80$$

where M_c, M_s, and M_a are moisture contents (%) at the centre, surface, and average, respectively.

The average values (M_a) from Eq. (80), with M_s taken as 4%, show remarkably good agreement with results obtained at the 2/5" position, (see Table 2).

Eleven runs were performed with bed temperatures ranging from 175 to 217°F and U/U_{mf} from 1.1 to 1.3. In order to check the quality of the wood after drying, five extra samples were dried at bed temperatures of 190, 204 (two samples) and 217°F (two samples). After drying, the blocks of Hemlock were tested for drying defects. During the drying the following types of damage can occur in wood:

1. Casehardening is caused by too rapid drying in which the zones near the surface of the wood shrink more (passes F. S. P. faster) than the inner

TABLE 2. AVERAGE MOISTURE CONTENT FROM EQ. (80) VERSUS VALUES MEASURED AT 2/5" FROM SURFACE

θ	m_a(%)	M_c(%)	M_a from Eq. (80)(%)
Time	Distance from the Surface		
(Hr.)	2/5"	1"	
1	47.1	68.8	47.2
2	39.0	58.7	40.5
3	36.0	53.5	37.0
4	33.5	49.9	34.6
5	31.5	46.6	32.4
6	29.6	43.7	30.5
7	27.8	41.2	28.8
8	26.3	38.4	26.9
9	25.0	36.5	25.7
10	23.7	34.3	24.5
11	22.4	32.6	23.1
12	21.4	31.0	22.0
13	20.0	28.9	20.6
14	19.2	27.8	19.9
15	18.0	26.1	18.7
16	17.1	23.8	17.7
17	16.3	23.3	16.9
18	15.0	21.2	15.5

portion of the wood. The shell of the wood is in tension while the core is in compression (a). Surface checking (Fig. 12) related to casehardening can occur at this point. As the drying proceeds the core dries below F.S.P., shrinkage starts which creates tension stresses greater than those in the shell. Hence, the shell is now in compression and the core in tension (b) (see Fig. 11, ref. 16, p. 93).

The tensile stresses built up in casehardening may be of such magnitude that rupture in tension perpendicular to the grain may ensue.

2. Surface checks, Fig. (12) (16, p. 91) are longitudinal openings, frequently developed along the wood rays, and can be observed on the tangential surfaces. The cause of the surface checking is more rapid drying of the wood surface than the interior of the wood.
3. Honeycomb, Fig. (13) (16, p. 94) occurs when the internal tensile forces due to improper drying reach the breaking point. Breaks usually start at the interfaces between wood rays and adjoining longitudinal tissues, the short radial cracks thus formed open. This is a defect which is not always visable externally.

After drying, the blocks of Hemlock were tested for casehardening and examined externally for evidence of the

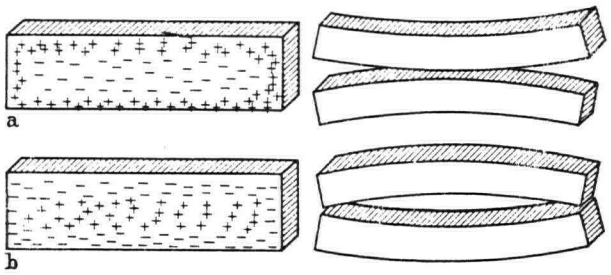

Fig.11 .Stress conditons in drying leading to case hardening

Fig.12. Surface checks

Fig 13 Honeycomb deffect in the wood

surface checking and internally under the microscope for honeycombing and the rupture in tension perpendicular to the grain. The procedure for the casehardening test is as follows (6): From the test piece, cut a small section about 3/8 in. wide from the centre of the board. Cut slots in the section with a hand saw, as shown in Fig. (14). After a few minutes, an evaluation of the stresses, can be made,

(c) If the outer prongs have turned in noticeably, the stock is stressed.

(d) If the outer prongs are straight, the wood is stress free.

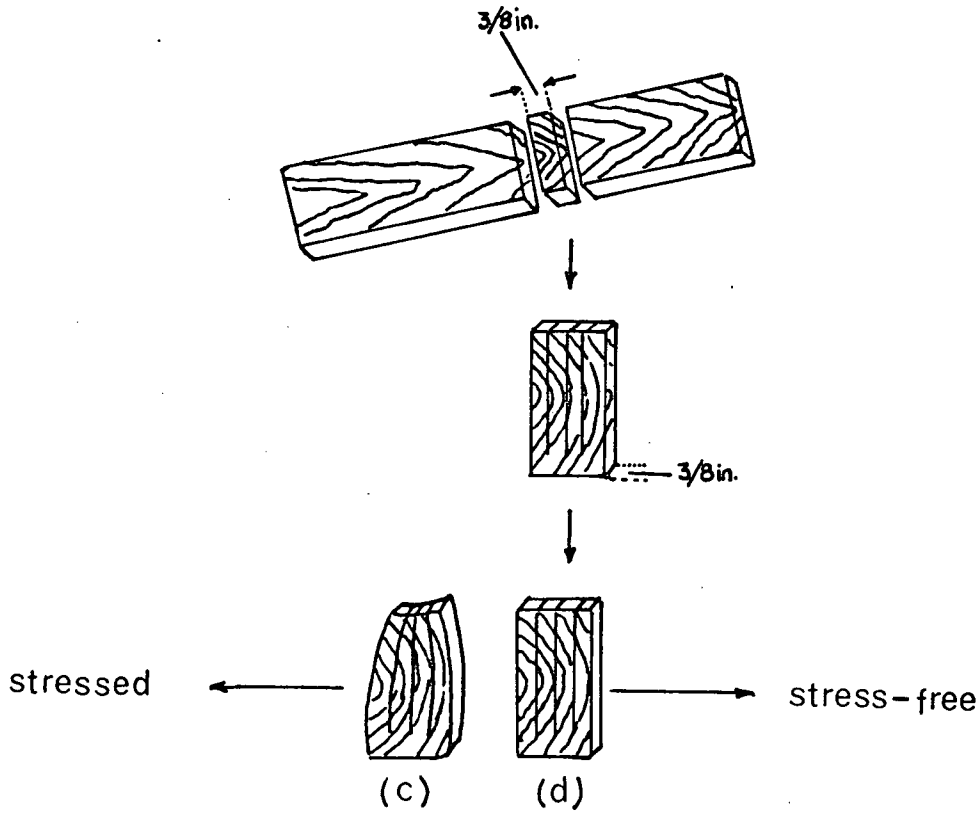

Fig.14. CASEHARDENING TEST

4.3 Results

The experimental results are summarized in Table (3), typical curves are shown in Figures (15) to (24) and detailed data, theoretical as well as experimental, for all the runs are tabulated in Appendix B, Tables (I) to (XII). Figures (15), (17), (18) and (19) also include theoretical curves of average moisture content versus time for comparison. Average block temperature data are shown in Fig. (24), the experimental results being arithmatic average values of temperatures measured at four different positions in the block. The values of time required to attain final M.C. of 15%, listed in Table (3), were mostly determined experimentally, but some were obtained by extrapolating the moisture content versus time curve to 15% M.C. (Figs. 15, 17, and 18).

The properties of the fluidized bed used are given in Table (4), and the properties of Western Hemlock in Table (5) with viscosity and density of air taken at the bed temperature (T_b = 217°F), the bed-to-surface mass transfer coefficient (k_g) for the sand bed used was calculated by Eq. (78) (Ch. 3) to be 128 lbm./ft.^{2}hr.atm., and the heat transfer coefficient (h) by Eq. (79) (Ch. 3) to be 43.01-43.47 BTU/hr.ft.^{2}°F.

Values of effective mass diffusivity (D) and thermal diffusivity (α) were obtained by searching for the value required in Eq. (53) (mass transfer) and Eq. (76) (heat transfer) to give the best (least squares) fit between theore-

TABLE 3. SUMMARY OF EXPERIMENTAL RESULTS

Run No.	U/U_{mf}	I.M.C. %	Bed. Temp. T_b	Time Required to Attain ≃ 15% M.C. θ (hr.)	Drying Direction
1	1.2	86	217	18	y
12	1.2	88	204	25	y
2	1.2	89	190	38	y
3	1.2	81	217	60	z
10	1.2	85	204	85	z
4	1.2	85	217	8	y + z
5	1.2	91	204	14	y + z
6	1.2	84	190	24.5	y + z
9	1.2	85	175	35	y + z
7	1.1	87	217	8.5	y + z
8	1.3	78.5	217	8.5	y + z
11 (no bed)	1.2	85	217	25	y + z

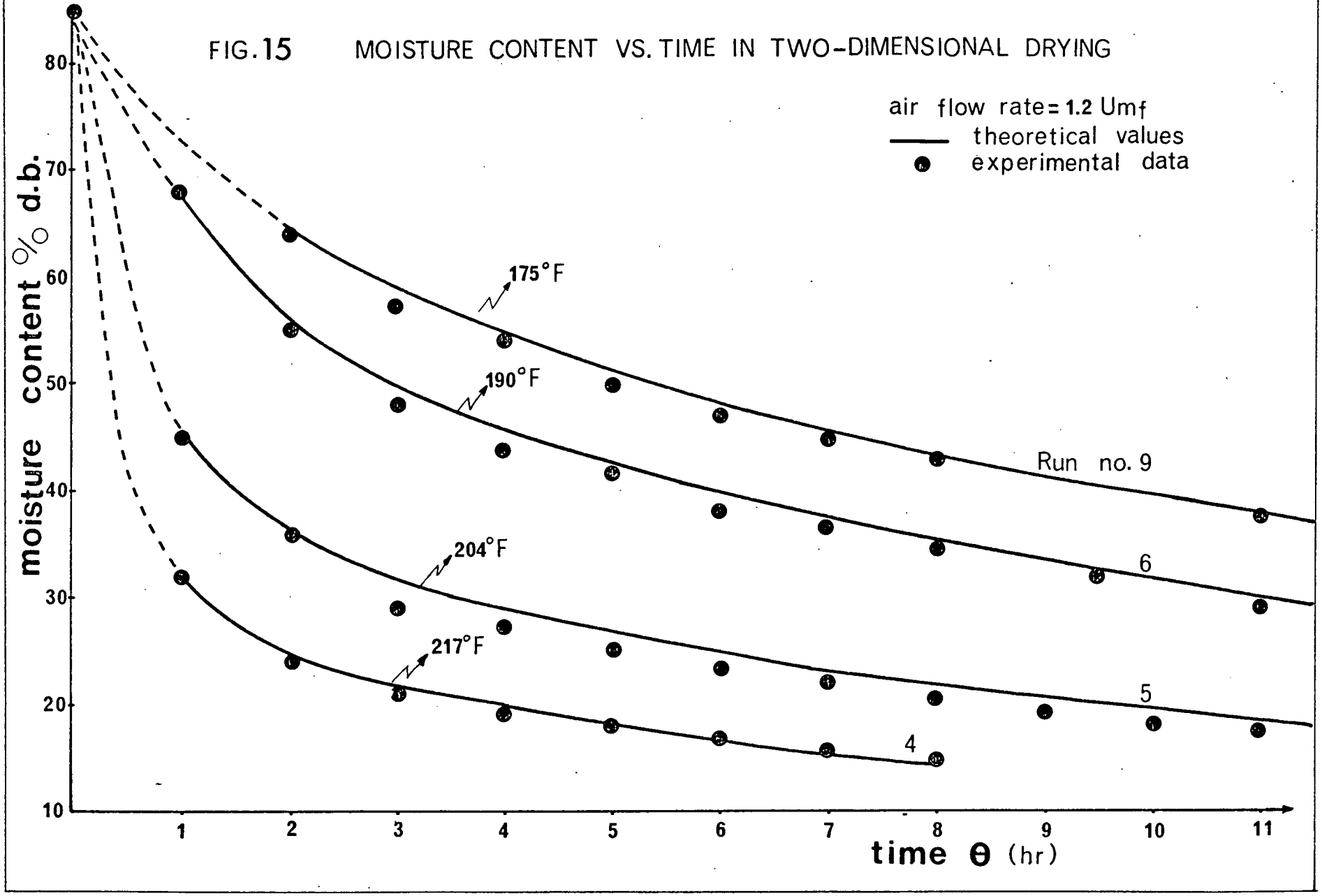
FIG. 15 MOISTURE CONTENT VS. TIME IN TWO-DIMENSIONAL DRYING
air flow rate = 1.2 Umf
theoretical values
experimental data
moisture content % d.b.
80
70
60
50
40
30
20
10
175°F
190°F
204°F
217°F
Run no. 9
6
5
4
1
2
3
4
5
6
7
8
9
10
11
time θ (hr)

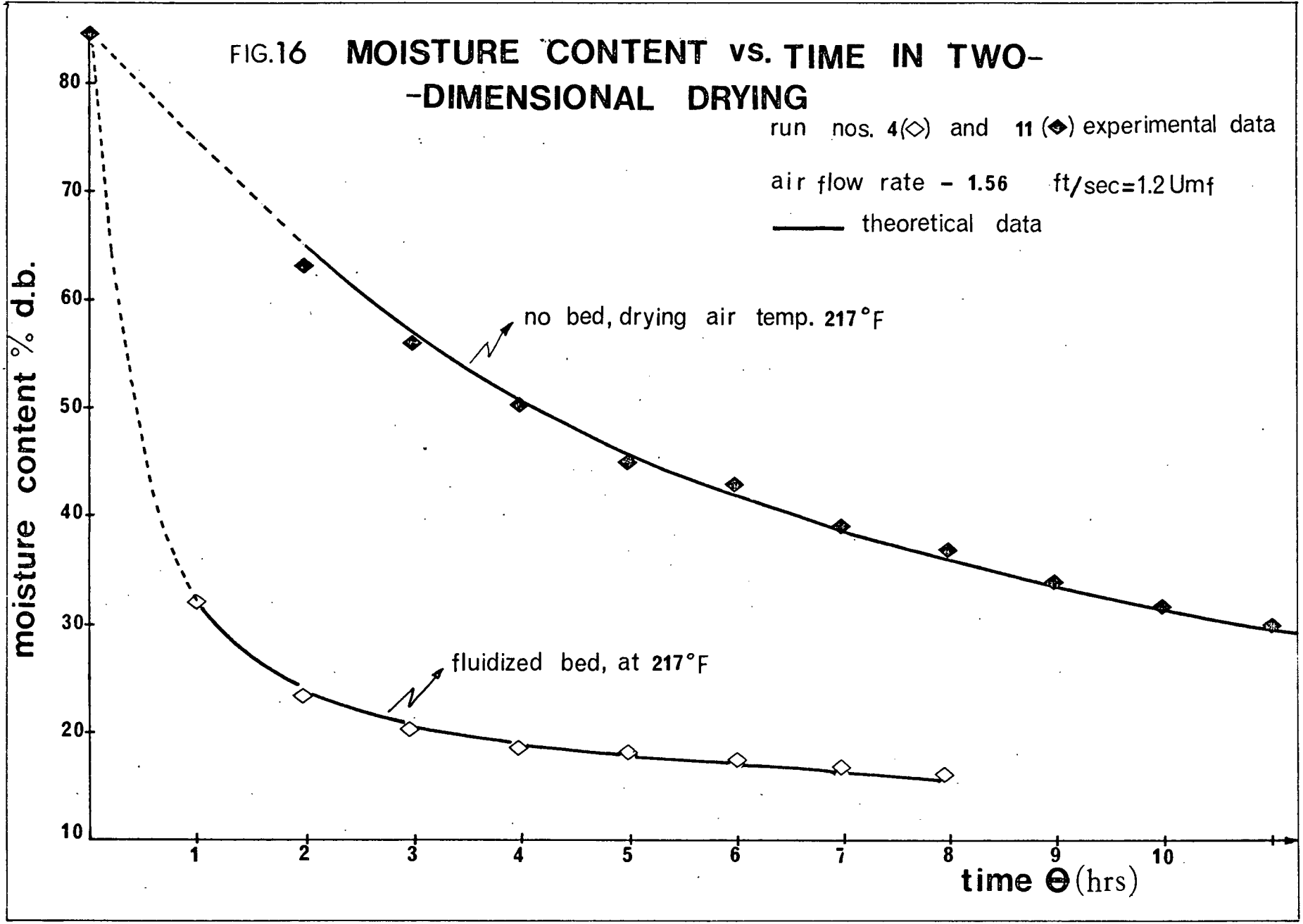
FIG.16 MOISTURE CONTENT vs. TIME IN TWO--DIMENSIONAL DRYING
run nos. 4(◇) and 11 (◆) experimental data
air flow rate - 1.56 ft/sec=1.2 Umf
theoretical data
no bed, drying air temp. 217°F
fluidized bed, at 217°F
moisture content % d.b.
80
70
60
50
40
30
20
10
1
2
3
4
5
6
7
8
9
10
time Θ (hrs)

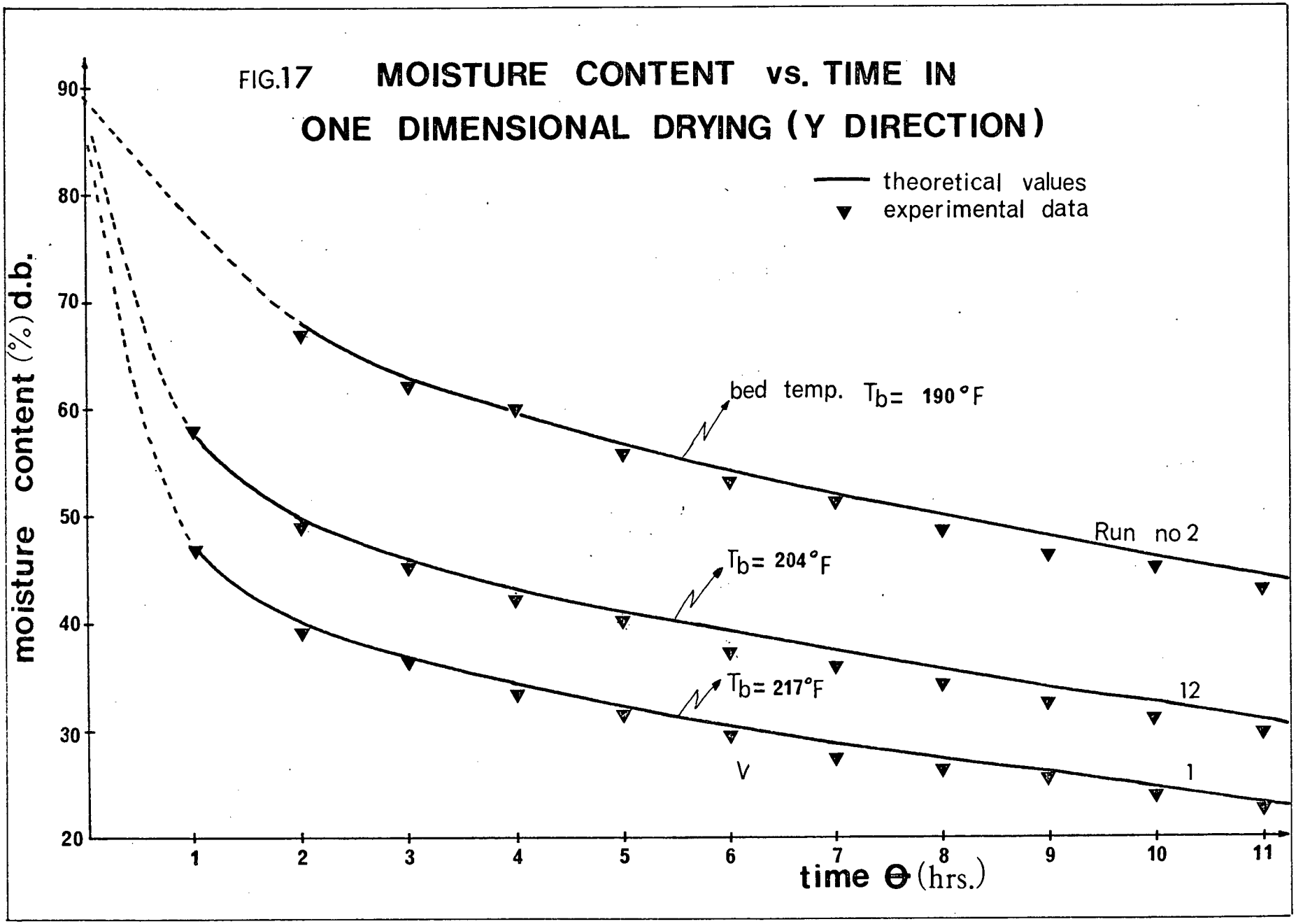
FIG.17 MOISTURE CONTENT vs. TIME IN ONE DIMENSIONAL DRYING (Y DIRECTION)
theoretical values
experimental data
moisture content (%) d.b.
90
80
70
60
50
40
30
20
bed temp. T_b= 190°F
Run no 2
T_b= 204°F
12
T_b= 217°F
V
1
1
2
3
4
5
6
7
8
9
10
11
time Θ (hrs.)

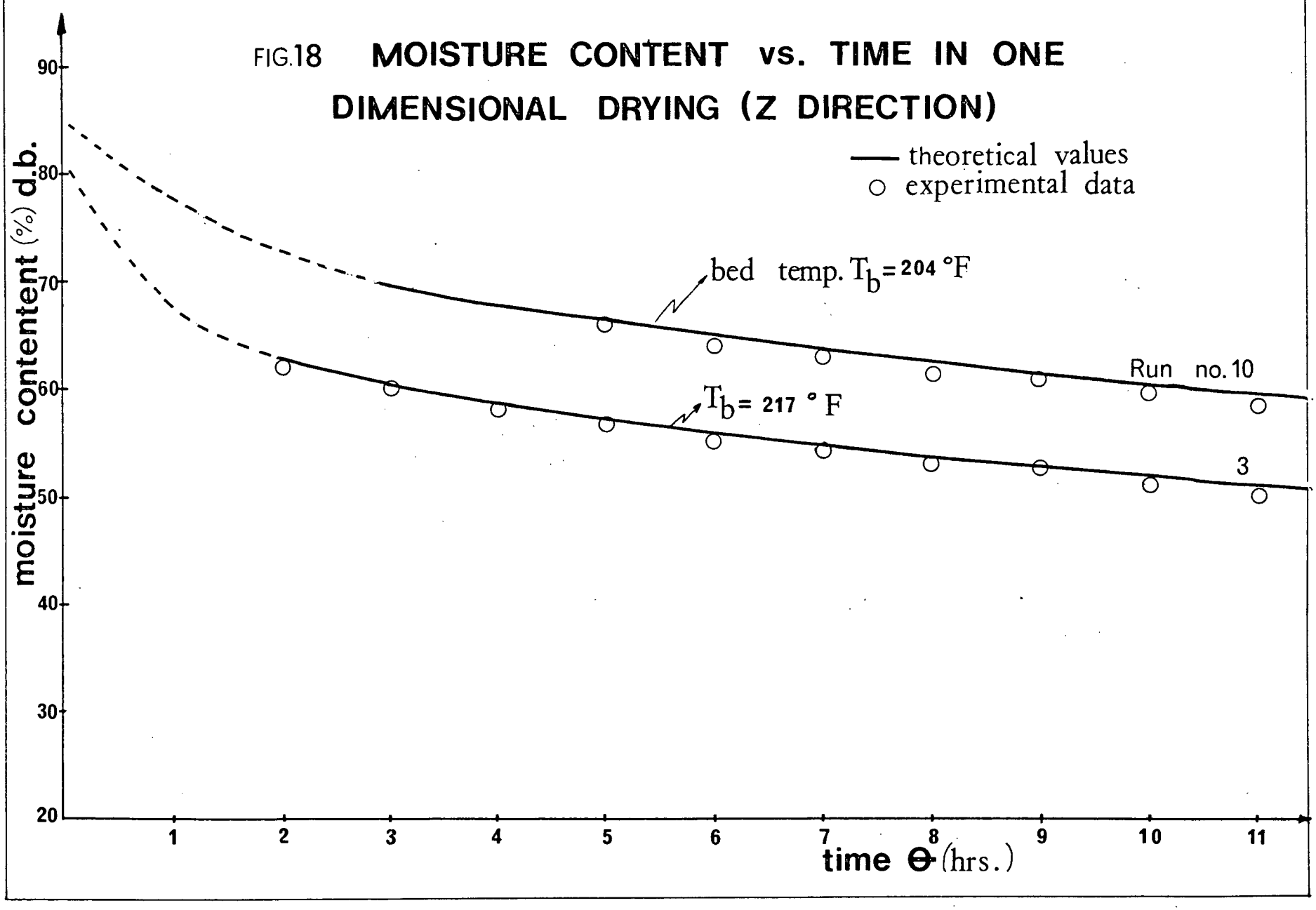
FIG.18 MOISTURE CONTENT vs. TIME IN ONE DIMENSIONAL DRYING (Z DIRECTION)
theoretical values
experimental data
bed temp. T_b = 204 °F
Run no. 10
T_b = 217 °F
3
moisture contentent (%) d.b.
time θ (hrs.)
90
80
70
60
50
40
30
20
1
2
3
4
5
6
7
8
9
10
11

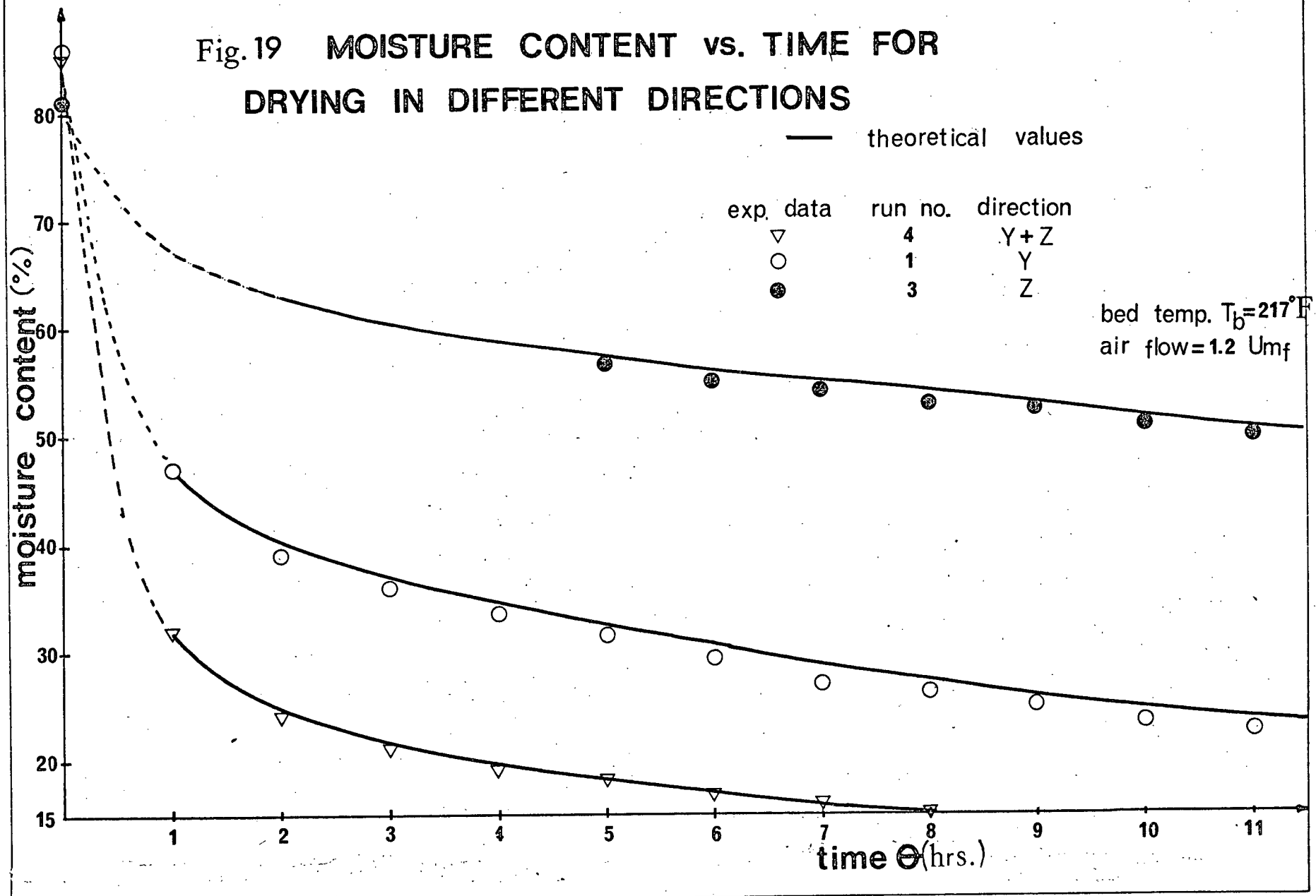
Fig. 19 MOISTURE CONTENT vs. TIME FOR DRYING IN DIFFERENT DIRECTIONS
theoretical values
exp. data
run no.
direction
4
Y + Z
1
Y
3
Z
bed temp. T_b=217°F
air flow=1.2 U_{mf}
moisture content (%)
80
70
60
50
40
30
20
15
1
2
3
4
5
6
7
8
9
10
11
time Θ (hrs.)

Fig. 20

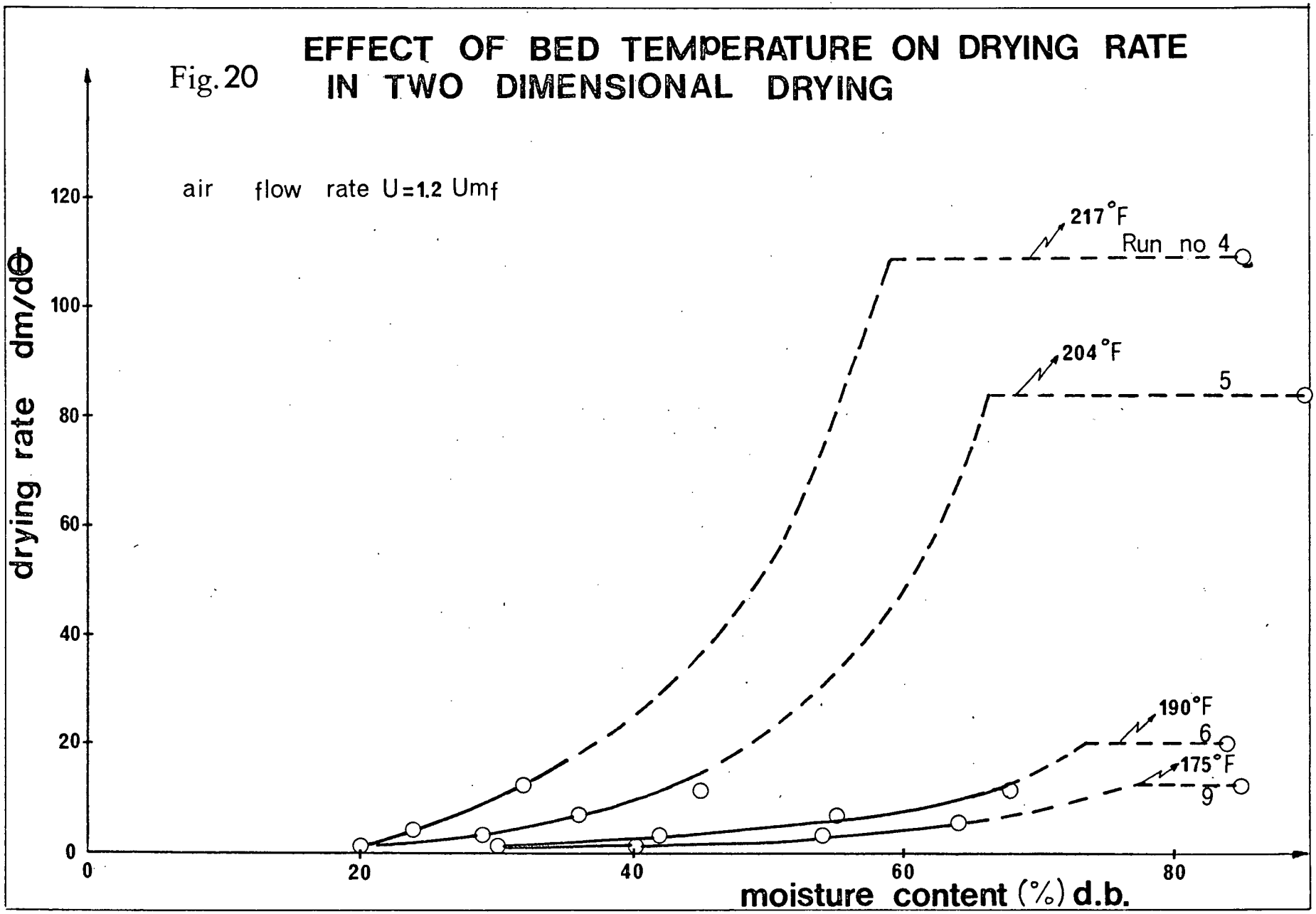
EFFECT OF BED TEMPERATURE ON DRYING RATE
IN TWO DIMENSIONAL DRYING
air flow rate U=1.2 Umf
drying rate dm/dΘ
moisture content (%) d.b.
0
20
40
60
80
100
120
217°F
Run no 4
204°F
5
190°F
6
175°F
9

Fig. 21

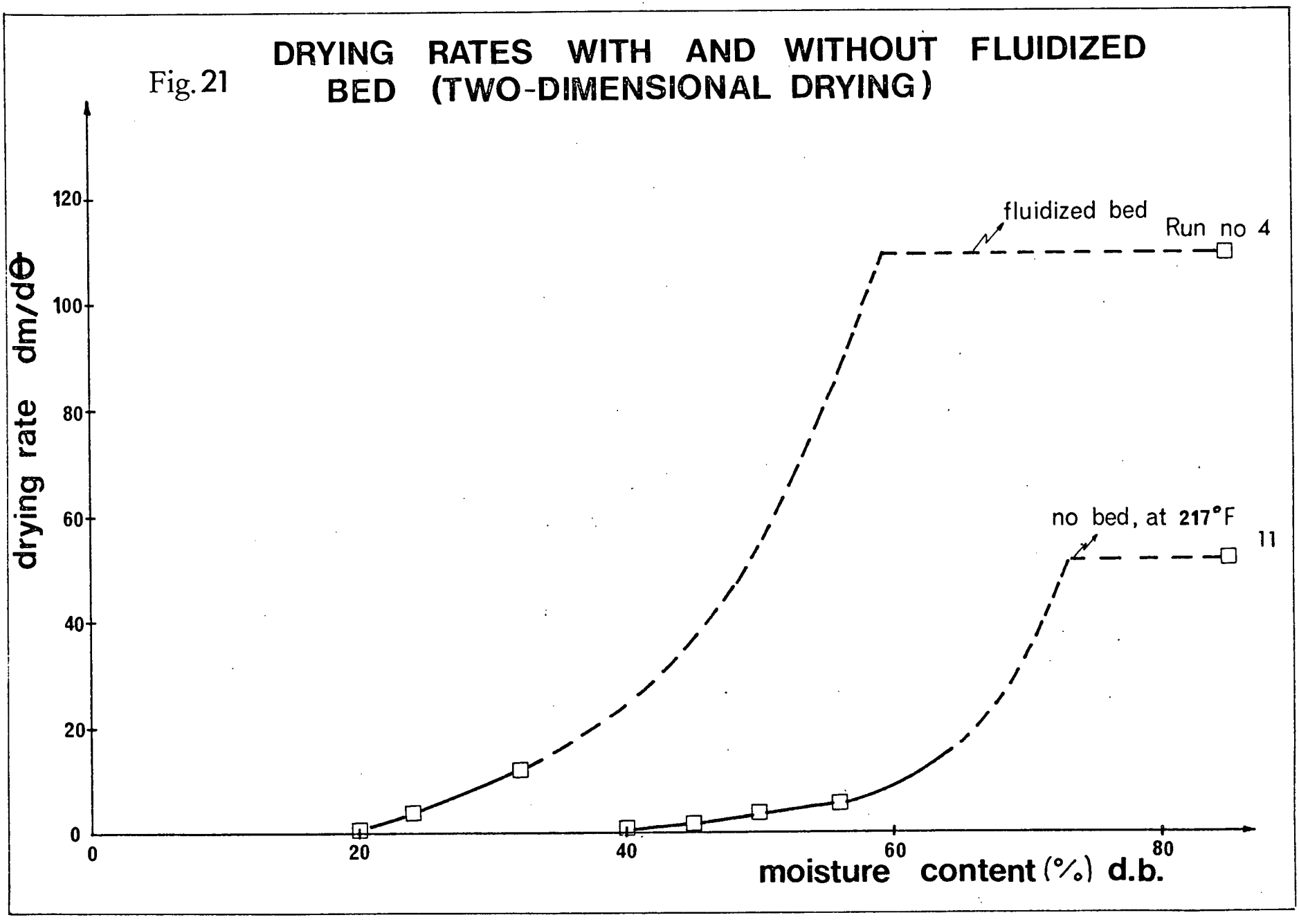
DRYING RATES WITH AND WITHOUT FLUIDIZED BED (TWO-DIMENSIONAL DRYING)
drying rate dm/dΘ
120
100
80
60
40
20
0
fluidized bed
Run no 4
no bed, at 217°F
11
0
20
40
60
80
moisture content (%) d.b.

Fig. 22 DRYING TIME FOR MOISTURE RANGE (≈90 to 15%) vs. BED TEMPERATURE (two-dimensional drying)

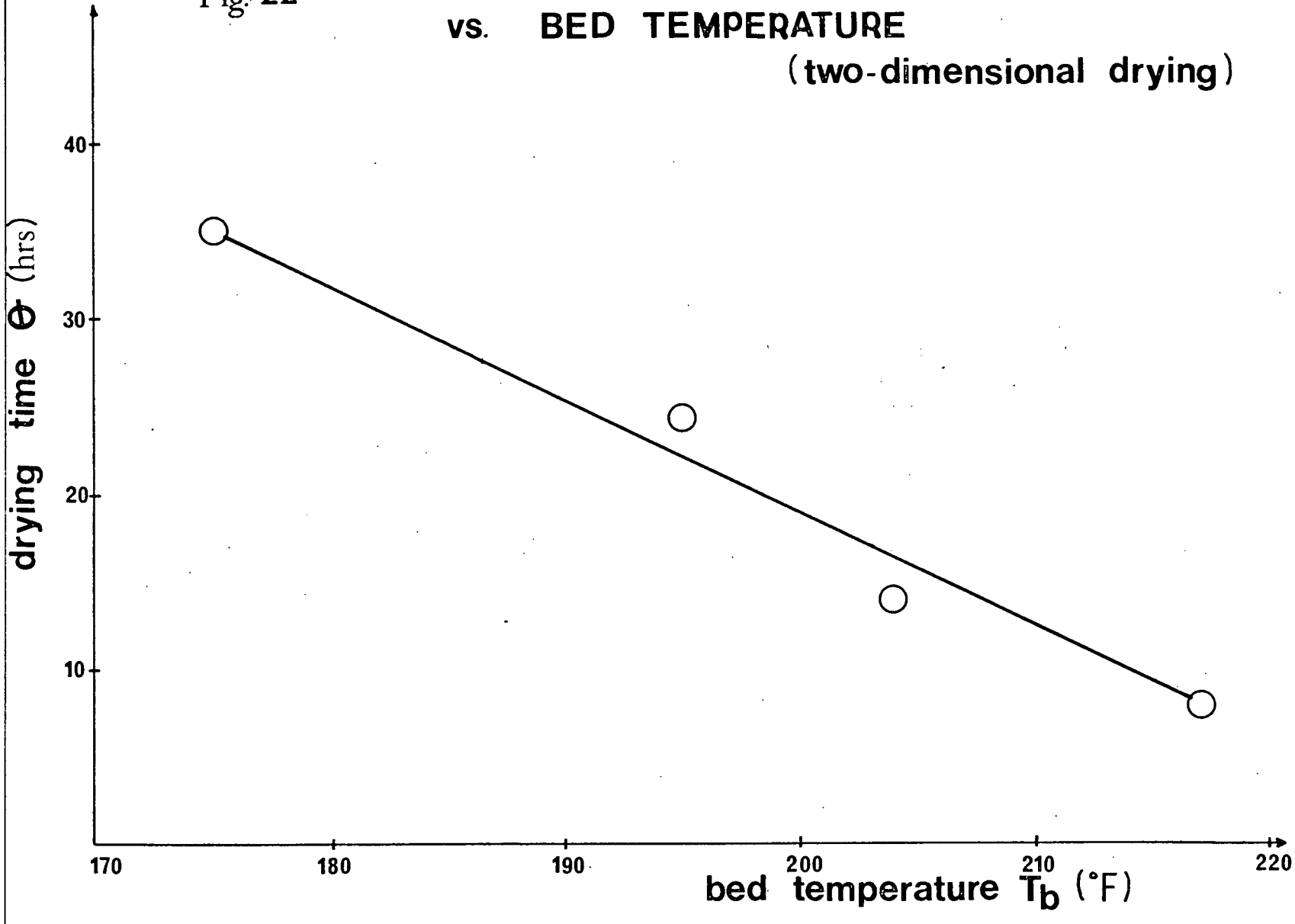

TEMPERATURE HISTORY OF LUMBER DURING TWO DIMENSIONAL DRYING

Fig.23

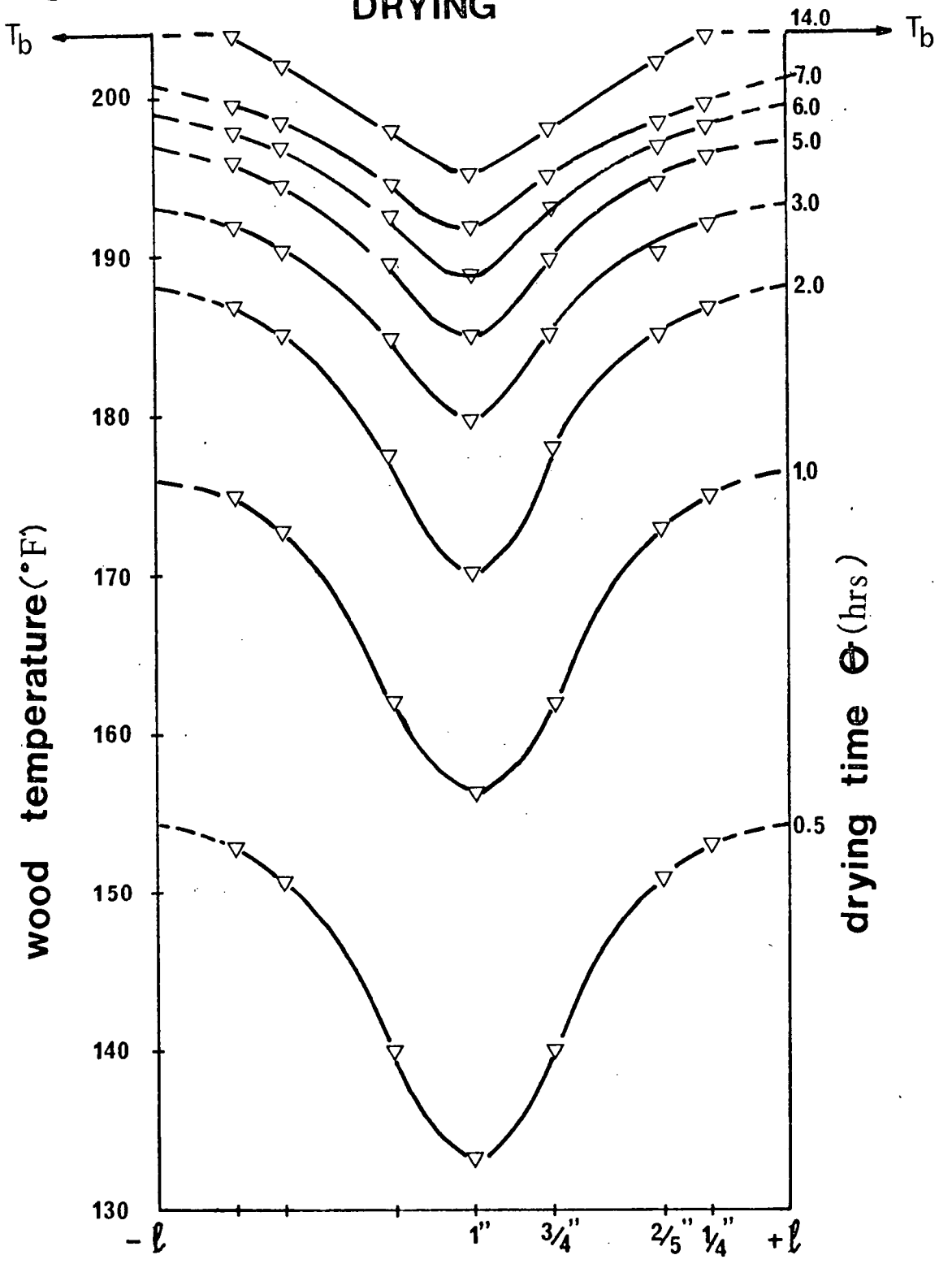

run no 5 ; T_b = 204°F (experimental data) ; air flow, U = 1.2 U_{mf} ; 2ℓ = 2"

Fig.24 AVERAGE WOOD TEMPERATURE vs. TIME IN TWO-DIMENSIONAL DRYING

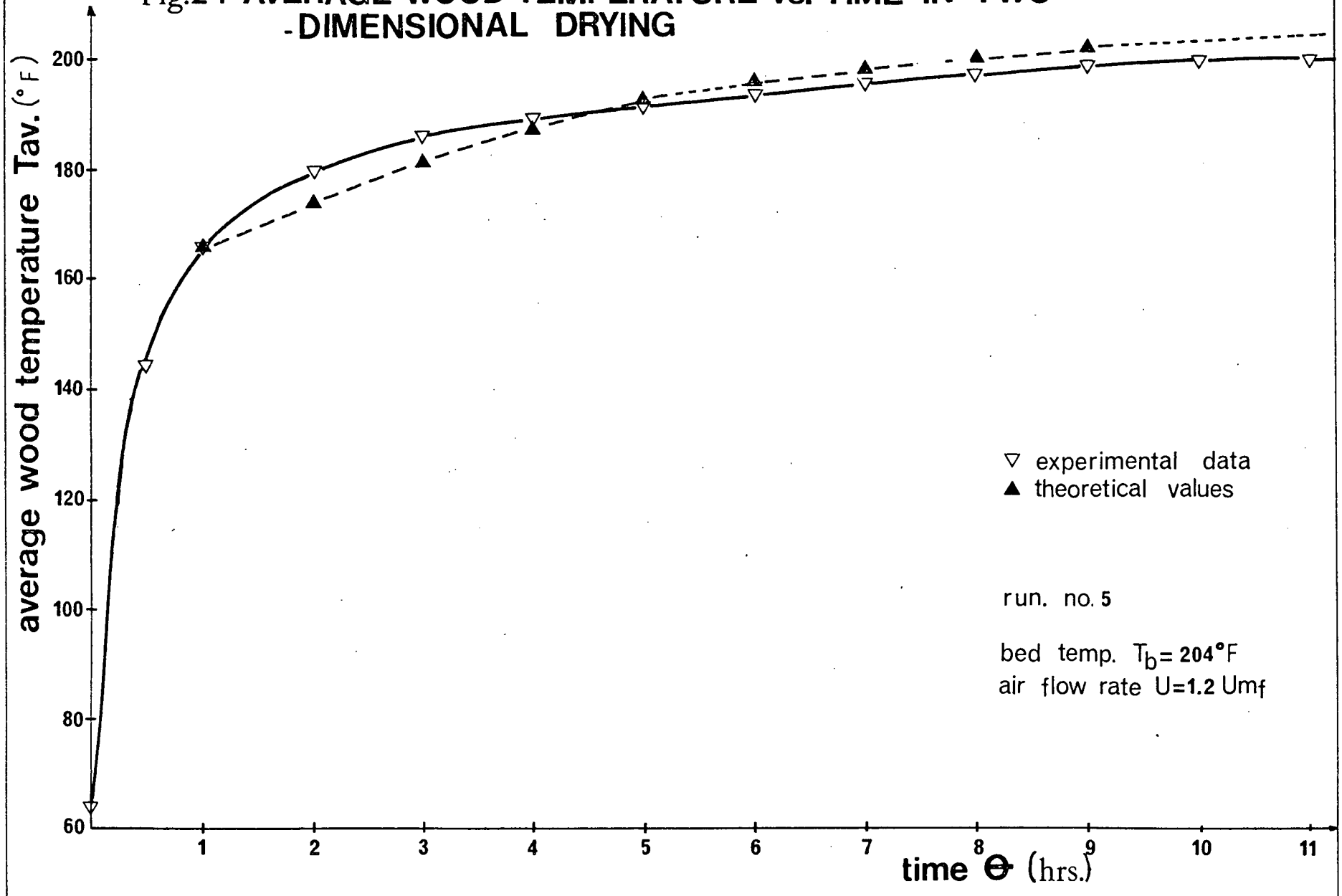

TABLE 4. PROPERTIES OF THE FLUIDIZED BED

Diameter of particles (d_p)	0.718 mm (-20 +30 mesh)
Minimum fluidization vel. (U_{mf})	1.3 ft./sec.
Height of bed at U_{mf} (L_{mf})	17"
Height of settled bed (L_m)	16"
Void fraction at U_{mf} (ε_{mf})	0.46
Operating velocities (U)	1.43, 1.56, and 1.69 ft./sec.
Height of expanded bed (L_f)	20", 22", and 23"
Void fraction at U (ε_f)	0.6, 0.64, and 0.65
Bulk density of sand (ρ_b)	89.0 lbm./ft.^{3}
Particle density of sand (ρ_{sand})	164.2 lbm./ft.^{3}
Specific heat of sand (C_{psand})	0.191 BTU/lbm.°F

TABLE 5. PROPERTIES OF WESTERN HEMLOCK

Specific gravity (oven-dry basis) (35, p. 14)	≃	0.4
Density of wet wood (16, p. 167) (32.5% M.C.) (ρ_s)	≃	30 lbm./ft.^{3}
Specific heat of wet wood (16, p. 246) (32.5% M.C.) (C_{ps})	≃	0.42 BTU/lbm.°F
Thermal conductivity (35, p. 112) (32.5% M.C.) (k_s)	≃	0.08 BTU/ft.hr.°F

TABLE 6. FLUIDIZED BED-TO-SURFACE HEAT TRANSFER COEFFICIENTS h(BTU/ft.^{2}hr.°F) CALCULATED BY EQ. (79)

Run No.	Bed Temp. °F	Air Velocity U/U_{mf}	h BTU/ft.^{2}hr.°F
4	217	1.2	42.3
5	204	1.2	43.3
6	190	1.2	43.4
9	175	1.2	43.4
7	217	1.1	43.0
8	217	1.3	43.5
11 (bed)	217	1.2	4.2

tical and experimental results. The diffusivity values thus obtained for each run are tabulated in Table (7).

Figure (25) gives a comparison between mass diffusivities found in this work and values obtained by other investigators (37, p. 128). Biggerstaff (37) measured the rates of drying of small, specimens of Eastern Hemlock sapwood from the fiber saturation point to the oven-dry condition at temperatures ranging from 50° to 120°C. A forced-convection oven was used to dry the samples. Diffusion coefficients were calculated from the square of the loss in moisture-time basis. The sensitivity of the M.C. versus time prediction to the value of diffusivity is illustrated in Fig. (26), and of wood temperature versus time prediction to the value of thermal diffusivity in Fig. (27).

TABLE 7. VALUES OF EFFECTIVE MASS DIFFUSIVITY (D) AND THERMAL DIFFUSIVITY (α) FOUND BY LEAST SQUARE FIT OF THEORETICAL AND EXPERIMENTAL DRYING CURVES

Run No.	Bed Temp. T_b °F	Moisture Range %	Operating Air Velocity U/U_{mf}	Direction of Drying	Mass Diffusivity $D \cdot 10^4$ ft.^{2}/hr.	Thermal Diffusivity $\alpha \cdot 10^3$ ft.^{2}/hr.
1	217	(47.1-15)	1.2	y	1.4	-
12	204	(58-15)	1.2	y	1.2	-
2	190	(67-20)	1.2	y	1.0	-
3	217	(62-37.5)	1.2	z	1.4	-
10	204	(69-45)	1.2	z	1.2	-
4	217	(32-15)	1.2	y + z	1.4	2.5
5	204	(45-15)	1.2	y + z	1.2	3.0
6	190	(68-15)	1.2	y + z	1.0	3.5
9	175	(64-15)	1.2	y + z	0.8	4.0
7	217	(33-15)	1.1	y + z	1.4	2.0
8	217	(33-15)	1.3	y + z	1.4	2.5
11 (no bed)	217	(63-23)	1.2	y + z	1.4	2.5

Fig. 25 DIFFUSION COEFFICIENTS FROM LITERATURE (37, FIG. 5) AND DIFFUSION COEFFICIENTS FOUND IN THIS WORK vs. DRYING TEMPERATURE

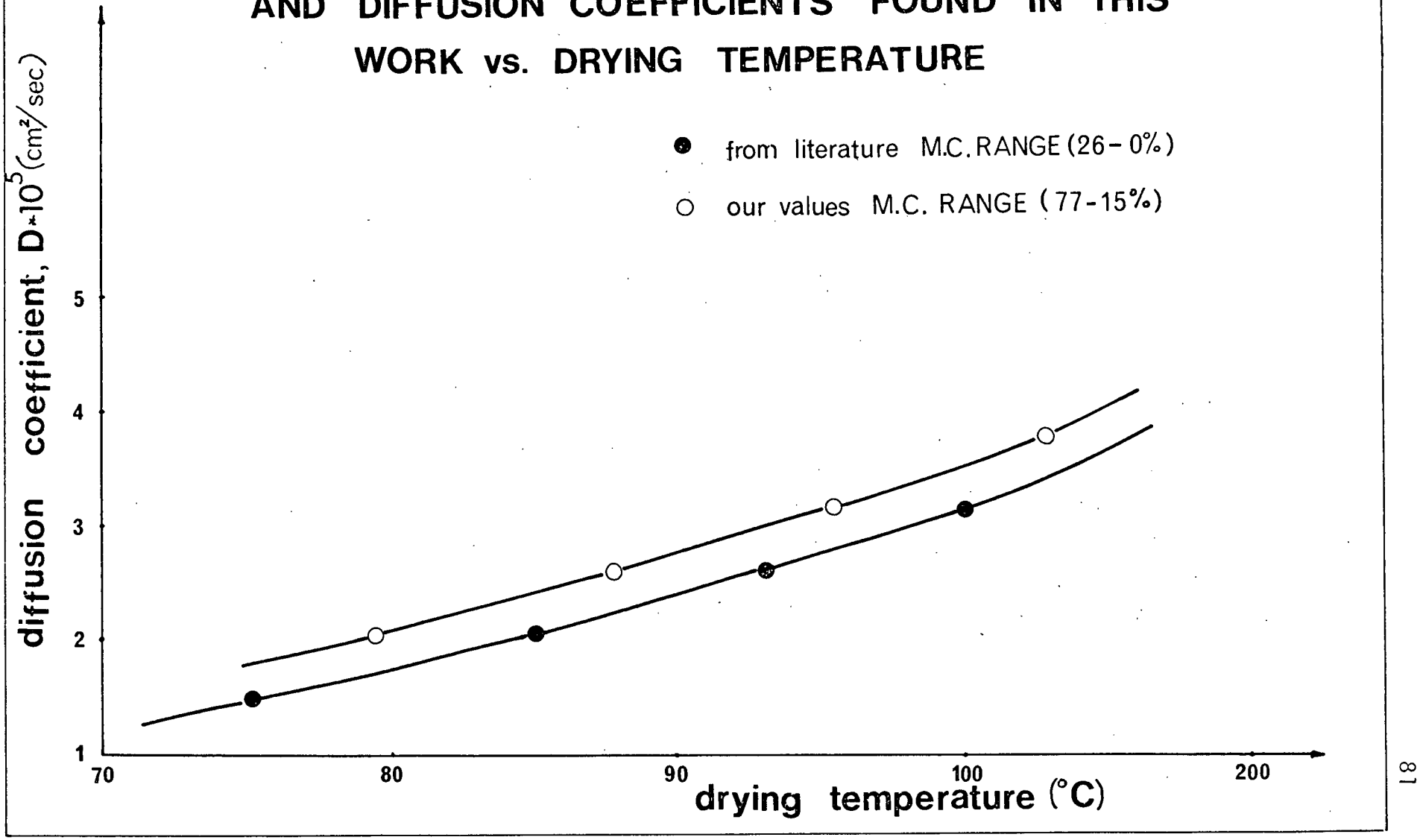

Fig. 26

SENSITIVITY OF M.C. vs. TIME PREDICTION TO VALUES OF DIFFUSIVITY

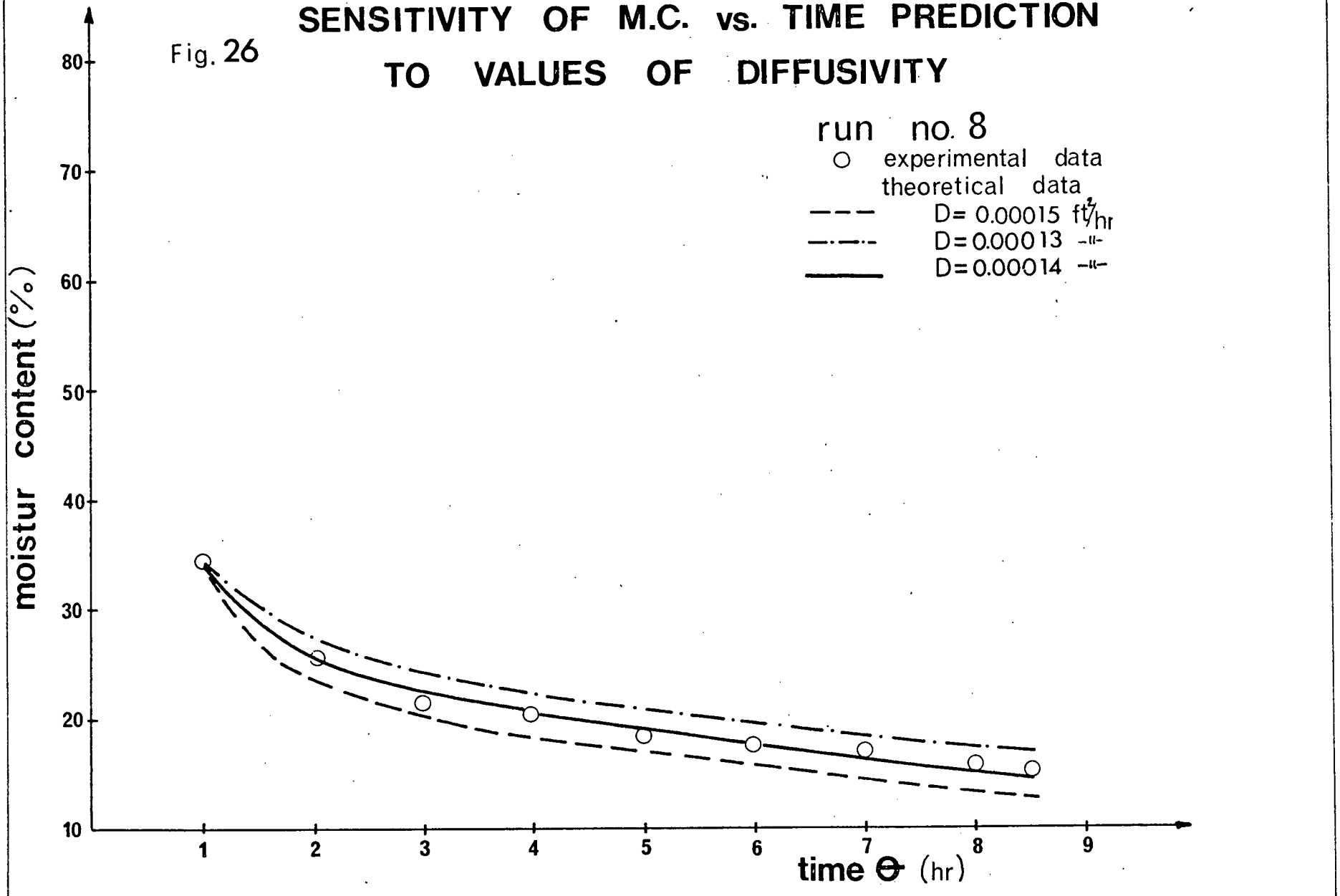

Fig. 27

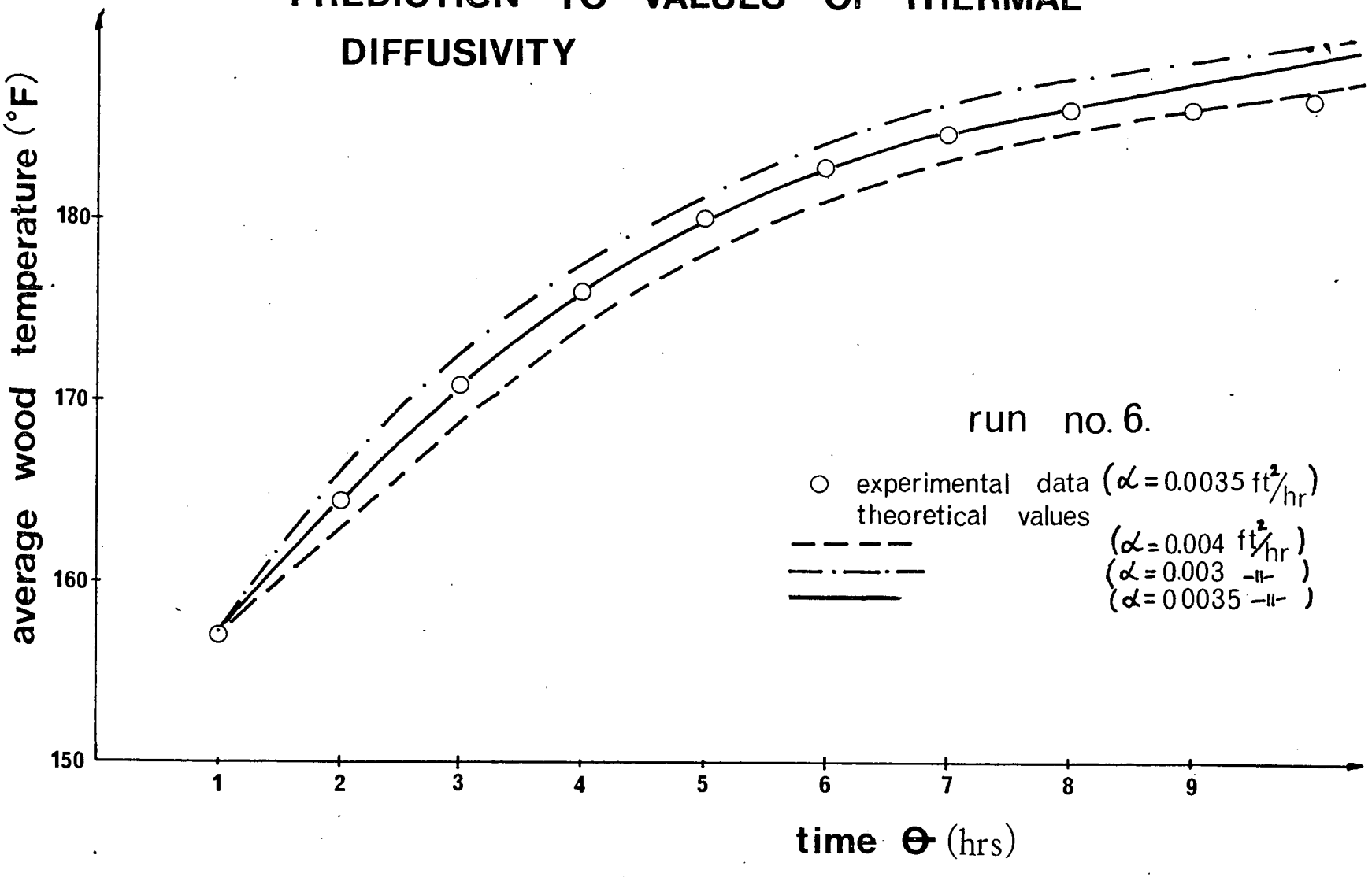
SENSITIVITY OF AVERAGE WOOD TEMP. vs. TIME PREDICTION TO VALUES OF THERMAL DIFFUSIVITY
average wood temperature (°F)
180
170
160
150
1
2
3
4
5
6
7
8
9
time θ (hrs)
run no. 6.
experimental data (α = 0.0035 ft²/hr)
theoretical values
(α = 0.004 ft²/hr)
(α = 0.003 -"-)
(α = 0.0035 -"-)

CHAPTER 5

DISCUSSION OF RESULTS

5.1 Controlling Mechanism

The drying curves in Fig. (20), which are drawn from the data in Fig. (15), show two stages: a constant rate period, followed by a falling rate period. However, the first moisture measurement was made after one or two hours of drying so that the shape of the M.C. versus time curves (Figs. 15, 17, and 18) during the initial one or two hours, when the constant-rate period might have existed, is not known. According to drying theory, the drying rate during the first period is governed by evaporation of moisture from the solid surface, and during the second period by diffusion of bound water through the solid. The surface temperature of wood, estimated by extrapolating the measured temperature profiles (Fig. 23 and Appendix B, Tables I to XII), rose to values higher than the adiabatic saturation temperature of the drying air in less than half an hour. Thus, the constant-rate period, if it existed, lasted only for a very short time. Above the fiber saturation point (F.S.P. $\simeq$ 30% M.C. (16)), the cell cavities contain varying amounts of free water, but they are never filled with it. However, the cell walls are saturated with water. As long as the cell walls are saturated with water, no unbalanced force exists which

would tend to cause diffusion from regions of high concentration to those of low concentration (35).

The agreement obtained between experimental and theoretical values of M.C., starting after one or two hours of drying (Fig. 15) suggests that apparent F.S.P. could be as high as 65% M.C. at the lower drying temperature used. It is possible that during the first period, above the fiber saturation point, drying was governed by the external mass transfer rate as well as by the internal movement of free water from the cell cavities. In view of the difficulty in judging when the constant rate period ended, it was assumed in all calculations that the falling rate period started after one or two hours of drying, even though at high temperatures (217°F, 204°F, Fig. 15) it actually started earlier.

5.2 Effect of Operating Variables

1. Bed temperature

The strong influence of bed temperature on drying rate can be seen from the data in Fig. (15) which have been replotted in Fig. (22) as drying time for the moisture range ≃ 80 to 15% versus bed temperature. Fig. (22) shows that increasing the bed temperature from 175°F to 217°F caused the drying time to decrease from 35 hrs. to 8 hrs. The effect of bed temperature is reflected in diffusivity values (Table 7), which increased from 0.00008 ft.^{2}/hr. at 175°F to 0.00014 ft.^{2}/hr. at 217°F.

2. Air flow rate

Variation in air flow rate up to 30% above the minimum fluidization rate had little effect on drying time as shown in Table (3). It was observed that at an operating velocity 20% above U_{mf}, temperatures at different locations in the bed were very uniform. Either increasing or decreasing the air flow rate ($U = 1.3\ U_{mf}$ or $U = 1.1\ U_{mf}$) caused temperature differences to arise within the bed, although in appearance the bed seemed to be as well fluidized as at $U = 1.2\ U_{mf}$.

3. Fluidized bed-drying versus air-drying

Figures (16) and (21) show the effect of the presence of the fluidized bed on drying time. Both runs were operated at the same bed temperatures (T_b = 217°F), the same air flow rate ($U = 1.2\ U_{mf}$ = 1.56 ft./sec.), and the same I.M.C. (85%). Without the bed, the time required to take moisture down to 15% was 25 hours (obtained by extrapolation) while with the bed, the time required was only 8 hours. This comparison underlines the main advantage of drying lumber in a fluidized bed of inert particles which arises from the much higher heat transfer coefficients obtainable with fluidized beds (43 BTU/hr.ft.^{2}°F, see Table 6) than with convective heat transfer (4 BTU/hr.ft.^{2}°F).

As pointed out earlier, the constant $C = \frac{k_g P_{vp} S^{-1}}{D \rho_{So}}$ in Eq. (45.1), used in finding the mass transfer eigen values, is always large and in fact approaches infinity. This implies

that the internal resistance to mass transfer in wood ($\propto D^{-1}$) under convective drying conditions is always much greater than the external resistance ($\propto k_g^{-1}$). In other words, the diffusion model predicts that the drying process in the falling-rate period should be independent of the external environment. It should therefore be expected that for a given drying temperature, the average moisture content-time curves for different fluidized bed velocities, and even in the absence of the bed, should yield the same diffusivity values. As can be seen from Table (7) (run nos. 7, 8, 4, and 11) this is indeed the case. The good agreement obtained between the experimental and theoretical results, and the insensitivity of diffusivity values to changes in the external conditions, would seem to substantiate the validity of the diffusion model for the falling-rate period. Although the external conditions have no observable effect on drying during the falling-rate period, they are obviously of great importance at the beginning of drying as shown by the much more rapid initial drying in the fluidized bed than in air alone (Fig. 16).

5.3 Quality Tests

In order to check the quality of dried wood, five wood samples after drying were tested (by MacMillan Bloedel Research Ltd.). The results of the test are shown in Table (8).

It can be seen from Table (8) that the blocks of Western Hemlock dried at bed temperature of 204°F and below did not

suffer any defects during drying, while the quality of wood dried at 217°F was adversely affected. A photograph illustrating the appearance of samples subjected to the stress test is shown in Fig. (28).

TABLE 8. RESULTS OF QUALITY TESTS ON FLUIDIZED BED DRIED WOOD

Run No.	Bed Temp. (°F)	Drying Time (hr.)	Moisture Range (%)	Quality
13	190°F	≃25	≃80-≃15	No drying defects
14	204°F	≃14	≃80-≃15	No drying defects
15	204°F	≃15	≃80-≃15	No drying defects
16	217°F	≃8	≃80-≃15	Drying defects 1. Casehardening 2. Very small and narrow honeycombing 3. Same surface checks
17	217°F	≃9	≃90-≃15	Drying defects 1. Casehardening 2. Very small and narrow honeycombing

5.4 Theory Versus Experiment

1. Mass transfer

Figures (15), (17), and (18) show good agreement between measured moisture contents of wood during drying and values calculated by the theoretical model described in Chapter 3. Similar agreement was obtained for all other runs

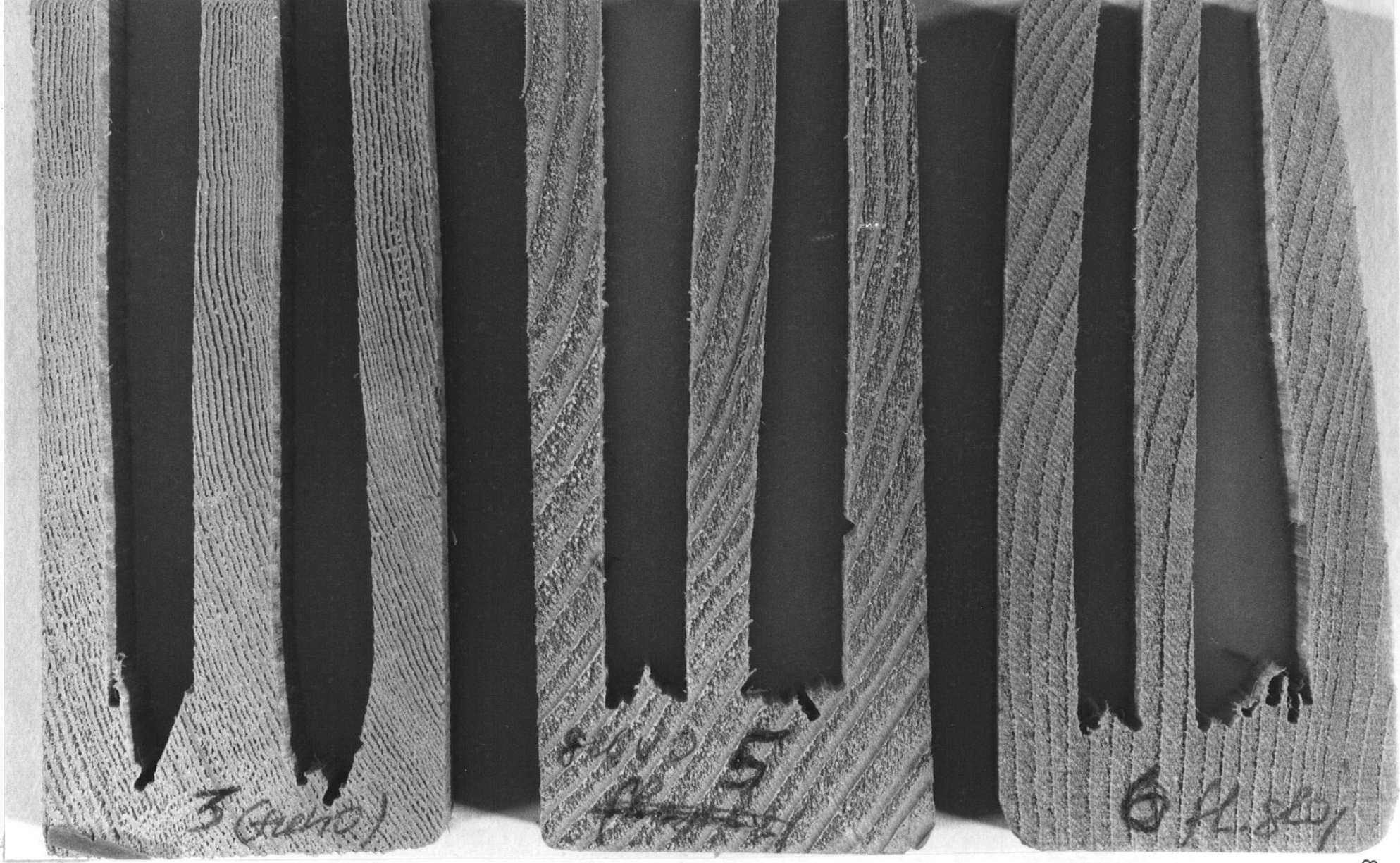

T_b= 204°F T_b=204°F T_b=217°F

Fig.28 **QUALITY TEST**

also, detailed data for which are presented in Appendix B. The effective diffusivity D for each run, which is the value required in Eq. (53) to give the best fit between the theoretical curves and the experimental data, are tabulated in Table (7). The magnitude of these values, as well as their temperature dependence, is consistent with published values of diffusivity of water in wood, as can be seen in Fig. (25).

It has been found that after a given drying time, the average moisture content during two-dimensional drying ($M.C._{yz}$) approximately equals the product of average moisture contents during drying in the y direction ($M.C._{y}$) and in the z direction ($M.C._{z}$). The theoretical basis for the above finding is the following equation, (38, p. 80):

$$X = f(\frac{D\theta}{\ell^2}) f(\frac{D\theta}{L^2}) \qquad 81$$

for diffusion controlled drying of a rectangular bar of thickness 2ℓ and width 2L, with sealed ends, where X = fraction of water unremoved, dimensionless.

Consider for example the data for run nos. 4, 1, and 3 (Appendix B) in the first 8 hours of drying, presented in Table (9). Data for the other runs (Appendix B) show a similar behavior.

It was also found that diffusion coefficients in y, z, and y + z directions (Table 7) were the same for the same bed temperature.

TABLE 9. COMPARISON BETWEEN EXPERIMENTAL ($M.C._{yz}$) AND CALCULATED MOISTURE CONTENTS FOR BED TEMP. = 217°F AND U = 1.2 U_{mf}

Time (hr.)	$M.C._y$ (%)	$M.C._z$ (%)	$M.C._{yz}$ (%)	$M.C._y \times M.C._z$ (%)
1	47.1	68 (extrap.)	32	31.9
2	39	62	24	24.2
3	36	60	21	21.6
4	33.5	68.1	19	19.5
5	31.5	56.6	18	17.8
6	29.6	55.1	17	16.3
7	27.8	54.2	16	15.1
8	26.3	53	15	14

2. Heat transfer

Good agreement was obtained between experimental and theoretical average wood temperatures as illustrated in Fig. (24) and shown by the data in Appendix B. The average thermal diffusivity α for each run was determined, as for mass transfer, by matching the theoretical curve with experimental data. The results for two-dimensional drying are tabulated in Table (7). The sensitivity of the average wood temperature versus time prediction to the value of thermal diffusivity is shown in Fig. (27). The values of α found in this work (0.002-0.004 $ft.^2/hr.$) are of the same order as the value

calculated from wood properties in literature ($\alpha = k_s/\rho_s C_{ps} = 0.006$). The inverse dependence of thermal diffusivity α with wood temperature found in this work would be explained if k_s increases with temperature at a slower rate than C_{ps}.

3. Distribution of moisture during drying

Figures (29) and (30) show typical distributions of moisture content within the wooden block in the y and z directions after one hour and two hours of drying respectively, calculated by Eq. (51), at 217°F with starting M.C. of 32%-dry basis, (corresponding to experimental run no. 4). Similar curves for hourly intervals up to 8 hrs. are included in Appendix D. Because of symmetry, the moisture profiles are given only for one quadrant ($y = 0, \ell/2; z = 0, L/2$) of the block of wood. No measurements of moisture distribution within the block were made but average moisture contents based on the predicted profiles, calculated by Eq. (53), gave good agreement with experimentally obtained values (Appendix B), providing support for the validity of Eq. (51).

θ, THETA = 1.0 HRS.

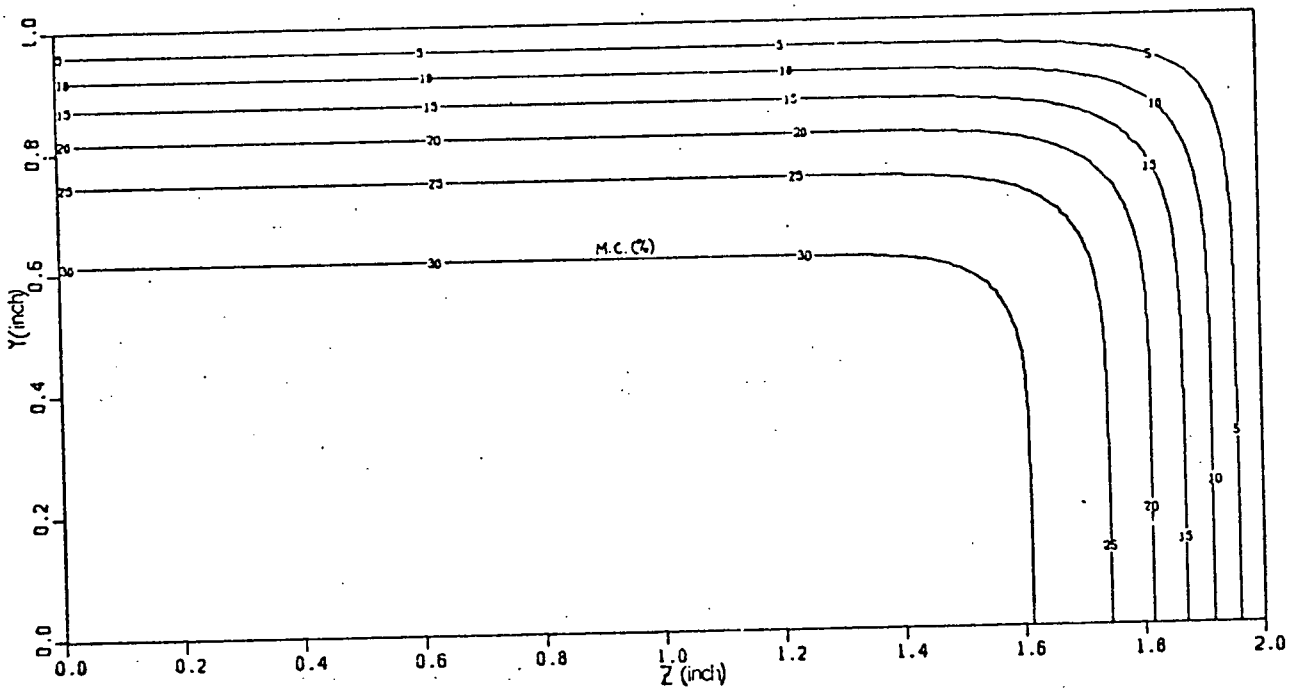

Fig.29. DISTRIBUTION OF MOISTURE IN WOOD

THETA = 2.0 HRS.

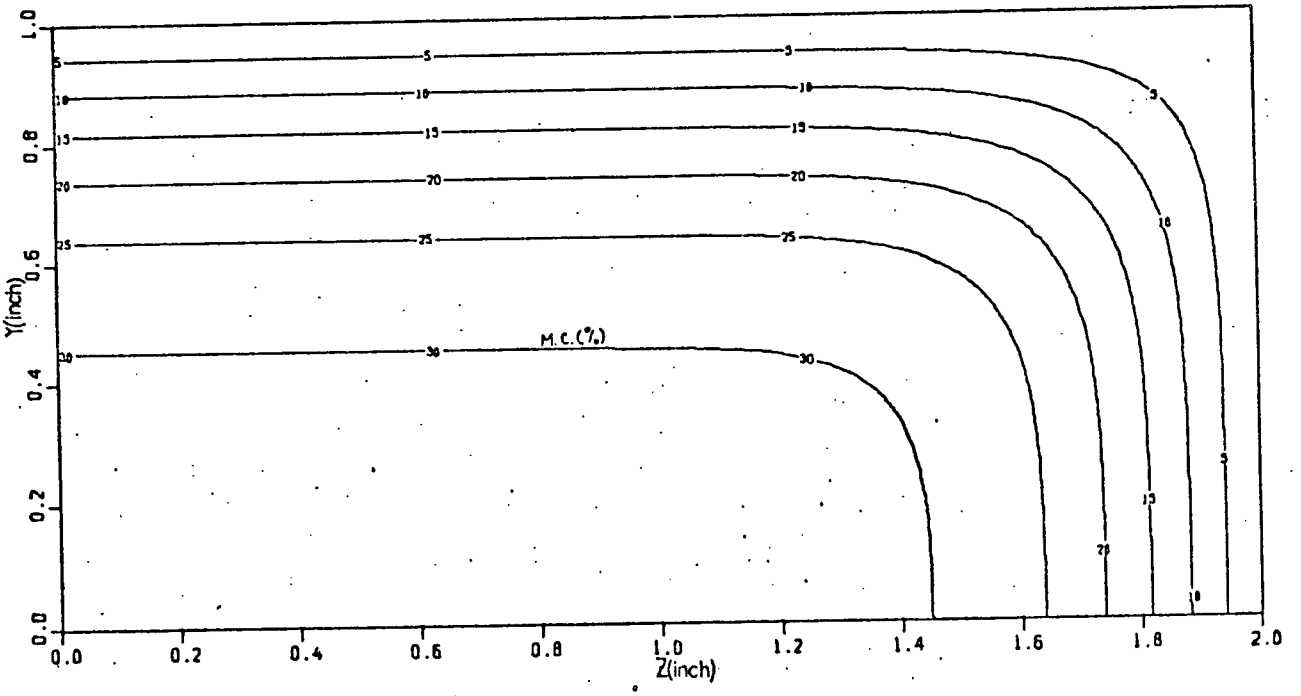

Fig.30. DISTRIBUTION OF MOISTURE IN WOOD

CHAPTER 6

COMPARISON WITH KILN DRYING

6.1 Drying Time

Table (10) shows comparative results of drying Hemlock in a fluidized bed and in a kiln at approximately the same air dry bulb temperature. The kiln drying data for 2"x10"x3' (end-coated) Western Hemlock are those reported by Solomon (34) who worked with an experimental kiln of internal size 3 ft. wide x 3 ft. long x 6 ft. deep.

The drying time in the fluidized bed is seen to be much smaller than in the kiln. The air velocity in the kiln (34) is much greater than in the fluidized bed, but the calculated heat transfer coefficient for the kiln (h = 15.1 BTU/hr.ft.^{2}°F) is much smaller than for the fluidized bed (h = 43 BTU/hr.ft.^{2}°F), due to the contribution of particle convection to fluidized bed heat transfer. Note that the air wet bulb temperature during the kiln drying was lower than during fluidized bed drying.

In addition, the uniform and easily controlled temperature of a fluidized bed should give more uniform drying and hence, should result in better quality of dried lumber.

6.2 Economics

A conceptual scheme for fluidized bed drying of lumber

TABLE 10. FLUIDIZED BED VS. KILN DRYING OF HEMLOCK

	Temperature		Air Flow		I.M.C.	Time Required to Dry to 15% M.C.
	Dry Bulb (°F)	Wet Bulb (°F)	$\frac{ft.^3}{min.}$	$\frac{ft.}{sec.}$	(%)	(hr.)
Fluidized bed*	204	≃88	18.72	1.56	85	14
Kiln (34)	160-218	150-200	5400	10	60	80

* Data for run no. 5.

on the industrial scale is costed in Table (11). The following design basis was used for sizing and costing the drying plant:

1. Capacity: 36 million FBM/yr. where Feet Board Measure (FBM) is a unit ≡ 1"x1"x1'
2. Moisture range: 91% (dry-basis) to 15% (dry-basis)
3. Drying air temperature = 204°F
4. Drying time = 14 hrs.
5. Batch size = 5140 pieces of lumber, 2"x4"x20'
6. Loading and unloading time = 2 hrs.
7. Working days/yr. = 350
8. Bed material = -20 +30 mesh sand
9. Air velocity (= 1.2 U_{mf}) = 1.56 ft./sec.
10. Size of fluidized bed, based on 1" spacing between boards. = 30 ft. dia. x 30 ft.

The capital cost of an equivalent kiln drying facility (3 double kilns, 36 million FBM/yr.) is estimated at $600,000 and its operating cost at $10/MFBM (42). Thus the fluidized bed is seen to offer a considerable economic advantage in capital cost.

Note that MFBM is a unit ≡ 1000 (1"x1"x1') lumber.

TABLE 11. ECONOMICS OF FLUIDIZED BED DRYING OF LUMBER

CAPITAL COST		
	Description	Cost ($)
1. Equipment cost*	30' dia. x 30' high. m.s. vessel plus blower, direct fired air heater, cyclones, piping and ducting.	158,000
2. Installation cost* incl. supports structure, electricals, insulation, contractors fee (100% of equipment cost)		158,000
3. Loading-unloading equipment cost (ref. 41)		100,000
Capital Cost		416,000

* Cost data taken from reference (40, 1967) and up-dated using the Marshal and Steven's inflation index from Chemical Engineering.

TABLE 11. (CONTINUED)

OPERATING COST

Item	Usage	Unit Price	Cost ($/yr.)
1. Electricity for air blower 52200 cfm at 17 psi	15,000,000 kwh/yr.	1.2 c/kwh	180,000
2. Fuel cost* 52200 cfm from 70°F to 250°F	58,000 $\times 10^6$ BTU/yr.	\$4.10/6.3 $\times 10^6$ BTU	38,000
3. Maintenance cost (5% of capital cost)			20,800
4. Labor cost	1 man/shift	\$8/hr.	67,000
5. Supervision (30% of labor cost)			20,000
6. Depreciation cost (10% of capital cost)			41,600
Operating Cost			370,000 ≈ \$10/MFBM

* Fuel consumption has been estimated without allowing for recycling of the air, and therefore represents the upper limit of heat requirement. Note that \$4.10/6.3 x 10^6 BTU is for net heating value, based on equivalent price of oil and natural gas.

CHAPTER 7

CONCLUSIONS

The following conclusions can be drawn from the results of this investigation.

1. The time taken to dry Western Hemlock of 2"x4" size immersed in a fluidized bed of sand at 204°F, from a moisture content of 91% (dry-basis) to 15%, was found to be 14 hours as against 25 hours for air drying with air temperature of 217°F and at air velocity of 1.56 ft./sec.
2. The rate of drying showed a marked increase with increasing fluidized bed temperature (range studied: 175-217°F), but wood dried at bed temperatures above 204°F suffered a loss in quality, evidenced by case-hardening, surface checking and small and narrow honeycombing in the interior of the wood.
3. Variation in air flow rate up to 30% above the minimum flow required for fluidization did not show any noticeable effect on the rate of drying.
4. The temperature and moisture history of wood during drying suggested that in drying from ≃85% to 15% moisture, the constant rate period, if it existed, lasted for a very short period (< 1/2 hr.).
5. A theoretical model to describe the drying process

in the falling rate period, based on liquid diffusion for internal mass transfer, was formulated. The model takes into account simultaneous transfer of heat, externally by convection and internally by conduction.

Predictions from the model, with assigned values of mass diffusivity and thermal diffusivity, showed good agreement with experimental data on variation of moisture content and temperature (average values for the block) with drying time. Moisture profiles within the drying block were also calculated.

The diffusivity values required for obtaining the best fit between theoretical predictions and experimental results were found to be consistent with literature values for wood, for both mass and heat diffusion.

6. A rough estimate of the cost of fluidized bed drying on the industrial scale shows that the method offers substantial economies in the capital cost when compared with the conventional kiln drying process. The operating cost works out to a value similar to that for kiln drying, but is likely to be reduced by improvements in the design of the fluidized bed drier, e.g. use of a rectangular unit, positioning the lumber horizontally in the drier, recirculation of the air, etc.

NOMENCLATURE

Symbol		Units
A	Surface area	$ft.^2$
A_{mn}	Coefficient of a series in Eq. (71)	
a	Constant defined by (Eq. 10, Ch. 3)	
b_1	Coefficient in (Eq. 9, Ch. 2) bed temperature dependent	
b	Constant defined by (Eq. 11, Ch. 3)	$ft.^{-1}$
B_{mn}	Coefficient of a series in Eq. (53)	
C	Constant defined by Eq. (23)	$ft.^{-1}$
C^*	Constant in Eq. (77)	
C_R	Correction factor of nonaxial location of immersed tubes, Eq. (79)	
C_{ps}	Specific heat of wet wood	BTU/lbm.°F
C_{pg}	Specific heat of gas	BTU/lbm.°F
C_{psand}	Specific heat of sand	BTU/lbm.°F
d_p	Particle diameter	ft.
D	Effective diffusivity of water in wood	$ft.^2/hr.$
D_e	Effective diffusivity of water vapor through dry wood layer	$ft.^2/hr.$

Symbol		Units
F.S.P.	Fiber saturation point	
h	Heat transfer coefficient across gas film	BTU/ft.^{2}hr.°F
I.M.C.	Initial moisture content	%
k	Thermal conductivity of air	BTU/ft.hr.°F
k_s	Thermal conductivity of wet wood	BTU/ft.hr.°F
k_g	Mass transfer coefficient across gas film	lbm./hr.ft.^{2}atm.
K_{Gw}	Mass transfer coefficient	ft./hr.
K_1	Constant in (Eq. 5, Ch. 2)	hr.$^{-1}$
k_1	Coefficients in (Eq. 8, Ch. 2) bed temperature dependent	
k_n	$= \sqrt{u_n^2 + v_m^2}$, eigen values	ft.$^{-1}$
ℓ	Half thickness of wood	ft.
L	Half width of wood	ft.
L_i	Thickness of wood - Wen and Loos model	ft.
ΔL_i	Thickness of dry layer	ft.
L_{mf}	Height of bed at U_{mf}	inch.
L_m	Height of settled bed	inch.
L_f	Height of expanded bed	inch.
M_w	Molecular wt. of water	lb.moles
M.C.	Moisture content	%

Symbol		Units
M.C.y	Average M.C. in y direction	%
M.C.z	Average M.C. in z direction	%
M.C.yz	Average M.C. in y+z directions	%
m_a	Average moisture content	%
M_c	Moisture content at the centre of wood	%
M_s	Moisture content ~ at the surface of wood	%
M_a	Average M.C. calculated by Eq. (80)	%
$M=M(\theta,y,z)$	Dimensionless moisture content $= \frac{m-m_\infty}{m_0-m_\infty}$, function of θ and directions	
m	Moisture content at any time	$\frac{\text{lbm. water}}{\text{lbm. dry-wood}}$
m_0, m_∞	Moisture content of wood at $\theta = 0$, and $\theta \to \infty$, respectively	$\frac{\text{lbm. water}}{\text{lbm. dry-wood}}$
m_s	Moisture content at surface	$\frac{\text{lbm. water}}{\text{lbm. dry-wood}}$
m_c	Critical moisture content	$\frac{\text{lbm. water}}{\text{lbm. dry-wood}}$
%m	Percentage moisture content	%
M_{AV}	Average moisture content, dimensionless	
$dm/d\theta = (dm/d\theta)_{fall.}$	Drying rate in falling-rate period	%/hr.

Symbol		Units
m^*	Constant in Eq. (77)	
$(dm/d\theta)_c$	Drying rate in constant-rate period	$\frac{\text{lbm. water}}{\text{lbm. dry-wood, hr.}}$
N_w	Flux of water vapor	lbmoles/hr.ft.^{2}
P_{vp}	Vapor pressure at surface	atm.
P_s	Partial pressure of water at surface	atm.
P_b	Partial pressure of water in bed	atm.
P_{ds}	Vapor pressure of water at T_{ds}	atm.
P_f	Vapor pressure of water at T_f	atm.
P_g	Partial pressure of water in gas	atm.
P_{sc}	Vapor pressure of water at T_{sc}	atm.
q	Flux of heat transfer	BTU/ft.^{2}hr.
Re^*	$= \frac{Ud_p\rho}{\mu(1-\varepsilon_f)}$ Reynolds no., dimensionless	
R	Gas constant	atm. ft.^{3}/lbmoles°F
Sc	Slope of desorption isotherm (Eq. 20), (Fig. 6)	
S_1	Thickness of veneer (Eq. 7, Ch. 2)	mm
Sc	Schmidt no., dimensionless	
T_g	Gas dry-bulb temperature	°F

Symbol		Units
T_{sc}	Surface temp. during evaporation in constant-rate period	°F
T_{ds}	Surface temp. of dry layer	°F
T_f	Temp. of interface between wet and dry layers	°F
T_b	Bed temperature	°F
T_s	Surface temp. during falling-rate period	°F
t	Bed temp. (Eq. 7, Ch. 2)	°C
$\overline{T}$	$= \frac{T_b - T}{T_b - T_0}$, dimensionless temperature	
T_a	Average temp. in the wood, (Eqs. 11, 12, Ch. 2)	°F
$\overline{T}_{AV}(\theta)$	Average wood temp., dimensionless	
T	Temp. at any point inside wood	°F
T_0	Initial temp. of block	°F
U	Operating air velocity	ft./sec.
U_{mf}	Minimum fluidization velocity	ft./sec.
u_n	Eigen values - heat transfer (y direction)	$ft.^{-1}$
v_m	Eigen values - heat transfer (z direction)	$ft.^{-1}$
X	Fraction of moisture unremoved, dimensionless	

Symbol		Units
x	Direction of flow along the grain	ft.
y	Direction of flow across the grain	ft.
z	Direction of flow across the grain	ft.
β_n	Eigen values - mass transfer (y direction)	$ft.^{-1}$
Ω_m	Eigen values - mass transfer (z direction)	$ft.^{-1}$
λ_n	$= \sqrt{\beta_n^2 + \Omega_m^2}$, eigen values - mass transfer	$ft.^{-1}$
ρ_{sand}	Particle density of sand	$lbm./ft.^3$
ρ_b	Bulk density of sand	$lbm./ft.^3$
ρ_w	Initial wt. of water per unit volume	$lbm./ft.^3$
ρ_s	Density of wet wood	$lbm./ft.^3$
ρ_{s0}	Density of oven-dry wood	$lbm./ft.^3$
ρ	Density of air	$lbm./ft.^3$
μ	Viscosity of air	lbm./ft.hr.
ε_{mf}	Void fraction at U_{mf}	
ε_f	Void fraction at U	
α	$= k_s/\rho_s C_{ps}$, thermal diffusivity	$ft.^2/hr.$

Symbol		Units
θ	Time	hr.
τ	Time, (Eq. 7, Ch. 2)	sec.
Λ	Latent heat of vaporization	BTU/lbm.
$\psi_1(\theta), \psi_2(y), \psi_3(z)$	Functions of θ, y, z respectively - mass transfer	
$\phi_1(\theta), \phi_2(y), \phi_3(z)$	Functions of θ, y, z respectively - heat transfer	

REFERENCES

1. Loos, W.E., Forest Product Journal 21, 44 (1971).

2. Babailov, V.E. and Petri, V.N., Lesnoi Journal 1, No. 1, 85 (1974).

3. Levenspiel, O. and Kunii, D., "Fluidization Engineering", Wiley & Sons, Inc., New York (197).

4. Davidson, J.E. and Harrison, D., "Fluidization", Academic Press, London and New York (1971).

5. Ziegler, E.N., Koppel, L.B., and Brazetton. W.T., Ind. Eng. Chem. 3, No. 2, May, 95, (1964); 3, No. 4, Nov., 325, (1964).

6. Brown, W.H., "An Introduction to the Seasoning of Timber", Vol. 1, Pergamon Press, The MacMillan Company, New York (1965).

7. Perry, R.H., and Chilton, C.H., "Chemical Engineers Handbook", Fifth Edition, MacGraw Hill, New York (1974).

8. Peck, R.E., and Wasan, D.T., Advances in Chem. Eng. 9, 247, 306, Academic Press (1974).

9. Sherwood, T.K., Ind. Eng. Chem., 21, 12 (1929).

10. Newman, A.B., Trans. A.I.Ch.E., 27, 210-333 (1931).

11. Bramhall, G., "Fick's Laws and Bound Water Diffusion", (Paper in Press), Forest Product Research Branch, Department of Forestry of Canada, Vancouver.

12. Ceaglske, N.H., and Hougen, O.A., Trans. A.I.Ch.E., 33, 283 (1937).

13. Fulford, G.D., Can. J. Chem. Eng. 47, 378 (1969).

14. Kisakurek, B., Peck, R.E., and Cakaloz, T., Can. J. Chem. Eng., 53, February, 53 (1975).

15. Stamm, A.J., "Wood and Cellulose Science", Ronald Press Company, New York (1964).

16. Kollmann, F.F.P., and Côté, W.A., "Principles of Wood Science and Technology", (I Solid Wood), Springer-Verlag, New York (1968).

17. Lebedev, P.D., Int. J. Heat Mass Transfer, 1, 294 (1961).

18. Kumar, I.J., and Narang, H.N., Int. J. Heat Mass Transfer, 9, 95 (1966); Ibid., 10, 1095 (1967).

19. Valchar, J., pp. 409-418 in Proc. 3rd Internat. Heat Transfer Conference, Chicago, Aug. 1966, 1, A.S.M.E.-A.I.Ch.E., New York (1966), (cited in ref. 13).

20. Krischer, O., "Die Wissenschaftlichen Grundlagen der Trockhungstechnik", 2nd Edition, Springer, Berlin (1963), (cited in ref. 13).

21. Lykov, A.V., "Heat and Mass Transfer in Capillary-Porous Bodies", Pergamon Press, Oxford (1966), (cited in ref. 13).

22. Wen, C.Y., and Loos, W.E., Wood Science, 2, No. 2, 87 (1969).

23. Leva, M., and Grummer, M., Ind. Eng. Chem. 40, 415 (1948), (cited in ref. 5).

24. Leva, M., Weintraub, M., and Grummer, M., Chem. Eng. Progr., 45, 563 (1949), (cited in ref. 5).

25. Leva, M., General Discussion of Heat Transfer, London, September, (1951), (cited in ref. 5).

26. Dow, W.M., and Jakob, M., Chem. Eng. Progr. 47, 637 (1951), (cited in ref. 5).

27. Van Heerden, C., Nobel, A.P.P., and Van Krevelen, D.W., Chem. Eng. Sci. 1, No. 2, 51 (1951), (cited in ref. 5).

28. Van Heerden, C., Nobel, A.P.P., and Van Krevelen, D.W., Ind. Eng. Chem. 45, 1237 (1953), (cited in ref. 5).

29. Carahan, B., Luther, H.A., and Wilkes, J.O., "Applied Numerical Methods", John Wiley & Sons, New York (1970).

30. Carslaw, H.S., and Jaeger, J.C., "Conduction of Heat in Solids", Clarendon Press, (1947).

31. Soloman, M., Forest Product Lab, Vancouver, Personal Communication.

32. Keenan, J.H., and Keyes, F.G., "Thermodynamic Properties of Steam", John Wiley & Sons, New York (1948).

33. Toomey, R.D., and Johnstone, H.F., Chem. Eng. Prog. Symposium Series, 49, No. 5, 51 (1953).

34. Soloman, M., Forest Products Journal, 15, No. 3, 122 (1965).

35. Brown, H.P., Panshin, A.J., and Forsaith, C.C., "Textbook of Wood Technology", Vol. II, McGraw-Hill Book Company, Inc., New York (1952).

36. Panshin, A.J., and Zeeuw, C., "Textbook of Wood Technology", Vol. I, McGraw-Hill Book Company, New York (1964).

37. Biggerstaff, T., Forest Product Journal, 15, No. 3, 127 (1965).

38. Treybal , R.E., "Mass-Transfer Operations", McGraw-Hill, New York, (Second Edition).

39. Wylie, C.R., "Advanced Engineering Mathematics", McGraw-Hill Book Company, New York (1960).

40. Clark, W.E., Chemical Engineering, 74-1, No. 6, 178 (1967).

41. Personal Communication from Dr. V. Mathur, MacMillan Bloedel Research, Vancouver.

42. Tam, S., "Drying of Lumber in a Fluidized Bed", B.A.Sc. Thesis, U.B.C. (1974).

APPENDIX A

COMPUTER PROGRAMS

No. 1 Average Moisture Content Calculated by Eq. (53)

No. 2 Average Wood Temperature Calculated by Eq. (76)

No. 3 Distribution of Moisture Calculated by Eq. (51)

Note : Sample computer outputs are presented in Appendix D.

Symbols used in the following programmes:

1. Calculation of average moisture content - Programme No. 1

LZ ≡ L = 2"

LY ≡ ℓ = 1"

MA → dimensionless average moisture content in y + z direction

MCO ≡ M_0 → average exptl. moisture content at the beginning of falling-rate period (lbm./lbm. dry wood)

MT → average theor. M.C. in the wood at any time (lbm./lbm. dry-wood)

ME → average exptl. M.C. in the wood at any time (lbm./lbm. dry-wood)

TET ≡ θ → drying time (hrs.)

D ≡ D → diffusion coefficient ($ft.^2/hr.$)

BET ≡ β → eigen value in y direction ($ft.^{-1}$)

OM ≡ Ω → eigen value in z direction ($ft.^{-1}$)

MY → dimensionless average M.C. in y direction

MZ → dimensionless average M.C. in z direction

2. Calculation of average wood temp. - Programme No. 2

TA → dimensionless average wood temp. in y + z direction

TY → dimensionless average wood temp. in y direction

TZ → dimensionless average wood temp. in z direction

TT → average theor. wood temp. at any time (y + z directions), (°F)

TE → average exptl. wood temp. at any time (y + z directions), (°F)

PMY ≡ $\partial M/\partial y$

PMZ $\equiv \partial M/\partial z$

TETT → time in the mid point of each interval, used to calculate $\partial M/\partial y$ and $\partial M/\partial z$, (hrs.)

ALFA $\equiv \alpha$ → thermal diffusivity ($ft.^2/hr.$)

U $\equiv u$ → heat eigen value in y direction ($ft.^{-1}$)

V $\equiv v$ → heat eigen value in z direction ($ft.^{-1}$)

3. Moisture distribution in the wood - Programme No. 3

TB $\equiv T_b$ → bed temperature, (°F)

C $\equiv k_g P_{vp} S^{-1}/\rho_s D$ ($ft.^{-1}$)

MY → dimensionless moisture content as function of y direction and θ

MZ → dimensionless moisture content as function of z direction and θ

M → dimensionless moisture content as function of y, z directions and θ

MC → distribution of moisture during drying (lbm./lbm. dry-wood)

PROGRAM: No. 1

FORTRAN IV G COMPILER MAIN 10-21-75 11:40:31 PAGE 0001

```
            C       MAIN PROGRAM
 0001               IMPLICIT REAL*8(A-H,O-Z)
 0002               DIMENSION OM(2000),BET(2000),TET(50),ME(50),MT(50)
 0003               REAL*8 LZ,LY,MY,MZ,MA,MCO,ME,MT
 0004               READ(5,4) IRUN,TB,C
 0005               READ(5,1) I1,K
 0006               DO 300 J=1,K
 0007               READ(5,17) TET(J),ME(J)
 0008            17 FORMAT(2F10.5)
 0009           300 CONTINUE
 0010               TETO=TET(1)
 0011               DO 400 J=1,K
 0012               TET(J)=TET(J)-TETO
 0013           400 CONTINUE
 0014               WRITE(6,5) IRUN,TB,C
 0015           4   FORMAT(I4,2F 12.5)
 0016           5   FORMAT(1H1,5X,'RUN NO=',I5/3X,'BED TEMP.=',F10.5/5X,'C=',F12.5/)
 0017               WRITE(6,2)
 0018            2  FORMAT(7X,'TET              ME              MT              O
                   1          SIG'//)
 0019            1  FORMAT(2I4)
 0020               MCO=ME(1)
 0021               LY=1./12.
 0022               LZ=1./6.
 0023               DO 3000 I=1,1000
 0024               CALL AV(C,X,LY,I)
 0025               BET(I)=X
 0026               CALL AV(C,X,LZ,I)
 0027               OM(I)=X
 0028           3000 CONTINUE
 0029               D=0.0
 0030            7  D=D+0.00001
 0031               SIG=0.0
 0032               DO 500 J=1,K
 0033               N=1
 0034               MY=0.0
 0035           13   BETT=BET(N)*LY
 0036               BM=2.*DSIN(BETT)/(BETT+DSIN(2.*BETT)/2.)
 0037               FY=D*(BET(N)*BET(N))
 0038                     BY=BM*DSIN(BETT)/BETT
 0039               XY=BY*DEXP(-FY*TET(J))
 0040               MY=MY+XY
 0041               IF(N.EQ.1) GO TO 8
            C       CHECK THE CONVERGENCE
 0042               CON=XY/MY
 0043               IF(DABS(CON).LT.0.00001) GO TO 100
 0044               IF(N.LT.1000) GO TO 8
 0045               WRITE(6,11)
 0046            11 FORMAT(1X,'MY NCT CONVERGED')
 0047               GO TO 100
 0048            8  N=N+1
 0049               GO TO 13
 0050           100 MZ=0.0
 0051               N=1
 0052            6  OMT=OM(N)*LZ
 0053               BN=2.*DSIN(OMT)/(OMT+DSIN(2.*OMT)/2.)
 0054               FZ=D*(CM(N)*OM(N))
 0055               BZ=BN*DSIN(OMT)/GMT
```

```
FORTRAN IV G COMPILER        MAIN            10-21-75        11:40:31

0056                XZ=BZ*DEXP(-FZ*TET(J))
0057                MZ=MZ+XZ
0058                IF(N.EQ.1) GO TO 9
                C       CHECK THE CONVERGENCE
0059                CON=XZ/MZ
0060                IF(DABS(CON).LT.0.00001) GO TO 200
0061                IF(N.LT.1000) GO TO 9
0062                WRITE(6,12)
0063             12 FORMAT(1X,'MZ NOT CONVERGED')
0064                GO TO 200
0065              9 N=N+1
0066                GO TO 6
                C       AVERAGE MOISTURE CONTENT
0067            200 MA=MY*MZ
0068                MT(J)=MA*MCO
0069                WRITE(6,3) TET(J),ME(J),MT(J)
0070              3 FORMAT(3F 15.6)
0071                SIGS=(ME(J)-MT(J))*(ME(J)-MT(J))
0072                SIG=SIGS+SIG
0073            500 CONTINUE
0074                WRITE(6,19)D,SIG
0075             19 FORMAT(45X,2F10.5)
0076                IF(D.GT.0.001) GO TO 21
0077                GO TO 7
0078             21 STOP
0079                END

 TOTAL MEMORY REQUIREMENTS 008A62 BYTES

 COMPILE TIME =       0.4  SECONDS
```

```
FORTRAN IV G COMPILER        MAIN            10-21-75        11:40:31

            C       SUBPROGRAM
0001                SUBROUTINE AV(C,X,L,I)
0002                IMPLICIT REAL*8(A-H,O-Z)
0003                REAL*8 L
0004                F12(A)=A*DTAN(A*L)-C
0005                PI=3.141593
0006                H=0.001
0007                X1=((I-1)*PI/L)+PI/(2.*L)-0.0001
0008              2 X2=X1-H
0009                A1=F12(X1)
0010                A2=F12(X2)
0011                AM=A1*A2
0012                IF(AM.LT.0.0) GO TO 10
0013                X1=X2
0014                GO TO 2
            C       NEWTON METHOD ITERATION
0015             10 X=(X1*A2-X2*A1)/(A2-A1)
0016                IF(DABS(X-X2).LT.0.00001) GO TO 7
0017                X1=X2
0018                X2=X
0019                A1=F12(X1)
0020                A2=F12(X2)
0021                GO TO 10
0022              7 RETURN
0023                END

 TOTAL MEMORY REQUIREMENTS 000396 BYTES

 COMPILE TIME =       0.1  SECONDS
```

PROGRAMME No. 2

```
FORTRAN IV G COMPILER        MAIN              12-01-75        22:48:47

C      MAIN PROGRAM
C       CALCULATION OF  AVERAGE TEMP. IN Y AND Z DIRECTION
0001          IMPLICIT REAL*8(A-H,O-Z)
0002           DIMENSION BET(100),OM(100),TET(50),
             1TETT(50),TE(50),TT(50),PMY(50),PMZ(50)
0003          REAL*8 LY,LZ
0004          READ(8,4) IRUN,TB,D,A,B
0005          WRITE(6,5) IRUN,TB,D
0006          READ(8,1) K
0007        4 FORMAT(I4,4F10.5)
0008        1 FORMAT(I4)
0009        5 FORMAT(1H1,5X,'RUN NO.=',I5/3X,'BED TEMP.=',F10.5/5X,
           2 'D=',F10.5/)
0010          DO 600 J=1,K
0011          READ(8,17) TET(J),TE(J),TETT(J)
0012       17 FORMAT(3F10.5)
0013       600 CONTINUE
0014          C=1000.0
0015          WRITE(6,2)
0016        2  FORMAT(7X,'TET                TE                TT
           3ALFA             SIG'//)
0017          LY=1./12.
0018          LZ=1./6.
0019           DO 3000 I=1,100
0020          CALL EVM(C,X,LY,I)
0021          BET(I)=X
0022          CALL EVM(C,Y,LZ,I)
0023          OM(I)=Y
0024          WRITE(7,7) X,Y
0025        7 FORMAT(2F10.3)
0026       3000 CONTINUE
0027          DO 300 J=1,K
0028          SY=0.0
0029          SZ=0.0
0030          SY1=0.0
0031          SZ1=0.0
0032          DO 700 I=1,100
0033          BETT=BET(I)*LY
0034          OMT=OM(I)*LZ
0035          BM=2.*DSIN(BETT)/(BETT+DSIN(2.*BETT)/2.)
0036          BN=2.*DSIN(OMT)/(OMT+DSIN(2.*OMT)/2.)
0037          FY=D*(BET(I)*BET(I))
0038          FZ=D*(OM(I)*OM(I))
0039          BY=BM*BET(I)*DSIN(BETT)
0040          BZ=BN*OM(I)*DSIN(OMT)
0041          XY=BY*DEXP(-FY*TETT(J))
0042          XZ=BN*DEXP(-FZ*TETT(J))
0043          XY1=BM*DEXP(-FY*TETT(J))
0044          XZ1=BZ*DEXP(-FZ*TETT(J))
0045          SY=SY+XY
0046          SZ=SZ+XZ
0047          SY1=SY1+XY1
0048          SZ1=SZ1+XZ1
0049        700 CONTINUE
0050          PMY(J)=SY*SZ
0051          PMZ(J)=SY1*SZ1
0052          WRITE(9,8) PMY(J),PMZ(J)
0053        8 FORMAT(2F10.5)
```

```
FORTRAN IV G COMPILER        MAIN            12-01-75        22:48:47

0054          300  CONTINUE
0055               ALFA=0.0
0056           27  ALFA=ALFA+0.0005
0057               TO=TE(1)
0058                TT(1)=TE(1)
0059               SIG=0.0
0060               DO 500 J=1,K
0061               N=1
0062               TY=0.0
0063               U=0.0
0064          13   CALL EVH(A,B,PMY(J+1),LY,U,N)
0065               WRITE(10,22) U
0066          22   FORMAT(F 10.3)
0067               UT=U*LY
0068               BM=2.*DSIN(UT)/(UT+DSIN(2.*UT)/2.)
0069                FY=ALFA*(U*U)
0070               BY=BM*DSIN(UT)/UT
0071               XY=BY*DEXP(-FY)
0072               TY=TY+XY
0073               IF(N.EQ.1) GO TO 88
           C        CHECK THE CONVERGENCE
0074               CON=XY/TY
0075               IF(DABS(CON).LT.0.00001) GO TO 100
0076               IF(N.LT.100) GO TO 88
0077               WRITE(6,11)
0078            11 FORMAT(1X,'TY NOT CONVERGED')
0079               GO TO 100
0080            88  N=N+1
0081               GO TO 13
0082           100 TZ=0.0
0083               N=1
0084               V=0.0
0085          6    CALL EVH(A,B,PMZ(J+1),LZ,V,N)
0086               WRITE(10,22) V
0087               VT=V*LZ
0088               BN=2.*DSIN(VT)/(VT+DSIN(2.*VT)/2.)
0089               FZ=ALFA*(V*V)
0090               BZ=BN*DSIN(VT)/VT
0091               XZ=BZ*DEXP(-FZ)
0092               TZ=TZ+XZ
0093               IF(N.EQ.1) GO TO 9
           C        CHECK THE CONVERGENCE
0094               CON=XZ/TZ
0095               IF(DABS(CON).LT.0.00001) GO TO 200
0096               IF(N.LT.100) GO TO 9
0097               WRITE(6,12)
0098            12 FORMAT(1X,'TZ NOT CONVERGED')
0099               GO TO 200
0100            9  N=N+1
0101               GO TO 6
           C        AVERAGE TEMPERATURE
0102           200 TA=TY*TZ
0103               TT(J+1)=TB-TA*(TB-TO)
0104                TO=TT(J+1)
0105               WRITE(6,33) TET(J),TE(J),TT(J)
0106            33 FORMAT(3F15.6)
0107               IF(J.EQ.1) GO TO 500
0108               SIGS=(TE(J)-TT(J))*(TE(J)-TT(J))
```

```
FORTRAN IV G COMPILER        MAIN            12-01-75        22:48:47

 0109                SIG=SIGS+SIG
 0110          500   CONTINUE
 0111                WRITE(6,19) ALFA,SIG
 0112           19   FORMAT(45X,2F10.5)
 0113                IF(ALFA.GT.0.01) GO TO 21
 0114                GO TO 27
 0115           21   STOP
 0116                END

  TOTAL MEMORY REQUIREMENTS 001BF6 BYTES

  COMPILE TIME =       0.6  SECONDS
```

```
FORTRAN IV G COMPILER        MAIN              12-01-75        22:48:48

             C       SUBPROGRAM
0001                 SUBROUTINE EVM(C,X,L,I)
0002                 IMPLICIT REAL*8(A-H,O-Z)
0003                 REAL*8 L
0004                 F12(A)=A*DTAN(A*L)-C
0005                 PI=3.141593
0006                 H=0.001
0007                 X1=((I-1)*PI/L)+PI/(2.*L)-0.0001
0008                 X1=((I-1)*PI/L)+PI/(2.*L)-0.0001
0009               2 X2=X1-H
0010                 A1=F12(X1)
0011                 A2=F12(X2)
0012                 AM=A1*A2
0013                 IF(AM.LT.0.0) GO TO 10
0014                 X1=X2
0015                 GO TO 2
             C       NEWTON METHOD ITERATION
0016              10 X=(X1*A2-X2*A1)/(A2-A1)
0017                 IF(DABS(X-X2).LT.0.00001) GO TO 7
0018                 X1=X2
0019                 X2=X
0020                 A1=F12(X1)
0021                 A2=F12(X2)
0022                 GO TO 10
0023               7 RETURN
0024                 END

 TOTAL MEMORY REQUIREMENTS 0003D6 BYTES

 COMPILE TIME =       0.1  SECONDS
```

```
FORTRAN IV G COMPILER        MAIN            12-01-75        22:48:48

                C       SUBPROGRAM
 0001                   SUBROUTINE EVH(A,B,S,L,X,I)
 0002                  IMPLICIT REAL*8(A-H,O-Z)
 0003                  REAL*8 L
 0004                  F12(G)=G*DSIN(G*L)+A*S-B*DCOS(G*L)
 0005                  H=1.
 0006                  IF(I.GT.1) GO TO 3
 0007                  X1=X
 0008                  GO TO 2.
 0009              3   X1=X+1.
 0010              2   X2=X1+H
 0011                  G1=F12(X1)
 0012                  G2=F12(X2)
 0013                  GM=G1*G2
 0014                  IF(GM.LT.0.0) GO TO 10
 0015                  X1=X2
 0016                  GO TO 2
                C       NEWTON METHOD ITERATION
 0017             10   X=(X1*G2-X2*G1)/(G2-G1)
 0018                  IF(DABS(X-X2).LT.0.00001) GO TO 7
 0019                  X1=X2
 0020                  X2=X
 0021                  G1=F12(X1)
 0022                  G2=F12(X2)
 0023                  GO TO 10
 0024              7   RETURN
 0025                  END

  TOTAL MEMORY REQUIREMENTS 0003E4 BYTES

  COMPILE TIME =       0.1  SECONDS
```

PROGRAM NO. 3

```
**LAST SIGNON WAS: 22:48:45    MON DEC 01/75
 USER "MAYA" SIGNED ON AT  09:42:26 ON MON DEC 22/75
$LIST M
     1      C      CALCULATION OF MOISTURE PROFILE IN THE WOOD
     2      C       MAIN PROGRAM
     3             IMPLICIT REAL*8(A-H,O-Z)
     4             DIMENSION OM(2000),BET(2000),Y(30),Z(60),MY(30),
    4.25          3 MZ(60),M(60,60),YP(60),ZP(60)
     5             REAL*8 LZ,LY,MY,MZ,MCO
    5.25           REAL*4 YP,ZP,M,CN
     6             READ(5,4) IRUN,TB,C
     7             WRITE(6,5)IRUN,TB
     8       4     FORMAT(I4,2F 12.5)
     9       5     FORMAT(1H1,5X,'RUN NO=',I5/3X,'BED TEMP=',F10.5/)
    13             MCO=0.32
    14             D=0.00015
    15             LY=1./12.
    16             LZ=1./6.
    17             DO 3000 I=1,2000
    18             CALL AV(C,X,LY,I)
    19             BET(I)=X
    20             CALL AV(C,X,LZ,I)
    21             OM(I)=X
```

```
22       3000 CONTINUE
22.25         YP(1)=2.5
22.5          DO 800 I=2,26
22.6          YP(I)=YP(I-1)+0.2
22.7     800  CONTINUE
22.8          ZP(1)=0.0
22.81         DO 900 J=2,51
22.82         ZP(J)=ZP(J-1)+0.2
22.83    900  CONTINUE
23            TET=1.0
24            DO 300 K=1,8
25            Y(1)=0.0
26            DO 400 I=1,26
27            N=1
28            MY(I)=0.0
29       13    BETT=BET(N)*LY
30            BM=2.*DSIN(BETT)/(BETT+DSIN(2.*BETT)/2.)
31            FY=D*(BET(N)*BET(N))
32            XY=BM*DEXP(-FY*TET)*DCOS(BET(N)*Y(I))
33            MY(I)=MY(I)+XY
34            IF(N.EQ.1) GO TO 8
35       C    CHECK THE CONVERGENCE
36            CON=XY/MY(I)
37            IF(DABS(CON).LT.0.0000000001) GO TO 100
38            IF(N.LT.2000) GO TO 8
39            WRITE(6,11)
40        11  FORMAT(1X,'MY NOT CONVERGED')
41            GO TO 100.
42        8   N=N+1
43            GO TO 13
44        100 Y(I+1)=Y(I)+LY/25.
45        400 CONTINUE
46            Z(1)=0.0
47            DO 500 J=1,51
48            N=1
49            MZ(J)=0.0
50         6  OMT=OM(N)*LZ
51            BN=2.*DSIN(OMT)/(OMT+DSIN(2.*OMT)/2.)
52            FZ=D*(OM(N)*OM(N))
53            XZ=BN*DEXP(-FZ*TET)*DCOS(OM(N)*Z(J))
54             MZ(J)=MZ(J)+XZ
55            IF(N.EQ.1) GO TO 9
56       C     CHECK THE CONVERGENCE
57            CON=XZ/MZ(J)
58            IF(DABS(CON).LT.0.0000000001) GO TO 200
59            IF(N.LT.2000) GO TO 9
60            WRITE(6,12)
61        12  FORMAT(1X,'MZ NOT CONVERGED')
62            GO TO 200
63         9  N=N+1
64            GO TO 6
65        200 Z(J+1)=Z(J)+LZ/50.
66        500 CONTINUE
67            DO 600 I=1,26
68            DO 700 J=1,51
69            M(J,I)=MY(I)*MZ(J)*MCO*100.
73.25    700   CONTINUE
73.5     600   CONTINUE
73.6          .CALL AXIS(0.0,2.5,'Z',-1,10.0,0.0,0.0,0.2)
73.7           CALL PLOT(10.0,2.5,3)
```

```
     73.71            CALL PLOT(10.0,7.5,2)
     73.72            CALL PLOT(0.0,7.5,2)
     73.82            CALL AXIS(0.0,2.5,'Y',1,5.0,90.0,0.0,0.2)
     73.83            CN=5.0
     73.84            DO 910 I=1,6
     73.85            CALL CNTOUR(ZP,51,YP,26,M,60,CN,3.0,CN)
     73.86            CN=CN+5.0
     73.87   910      CONTINUE
     74.12            CALL SYMBOL(0.5,8.0,0.28,'THETA =',0.0,7)
     74.37            CALL NUMBER(2.42,8.0,0.28,TET,0.0,1)
     74.62            CALL PLOT(14.0,0.0,-3)
     74.87            TET=TET+1.0
     74.97   300      CONTINUE
     75.25            CALL PLOTND
     76               STOP
     77               END
     78        C      SUBPROGRAM
     79               SUBROUTINE AV(C,X,L,I)
     80               IMPLICIT REAL*8(A-H,O-Z)
     81               REAL*8 L
     82               F12(A)=A*DTAN(A*L)-C
     83               PI=3.141593
     84               H=0.001
     85               X1=((I-1)*PI/L)+PI/(2.*L)-0.0001
     86          2    X2=X1-H
     87               A1=F12(X1)
     88               A2=F12(X2)
     89               AM=A1*A2
     90               IF(AM.LT.0.0) GO TO 10
     91               X1=X2
     92               GO TO 2
     93        C      NEWTON METHOD ITERATION
     94         10    X=(X1*A2-X2*A1)/(A2-A1)
     95               IF(DABS(X-X2).LT.0.00001) GO TO 7
     96               X1=X2
     97               X2=X
     98               A1=F12(X1)
     99               A2=F12(X2)
    100               GO TO 10
    101          7     RETURN
    104               END
END OF FILE


$SIG
```

APPENDIX B

SUMMARY OF EXPERIMENTAL DATA AND THEORETICAL RESULTS OF MOISTURE CONTENT VS. TIME AND TEMPERATURE VS. TIME FOR BEST-FIT VALUES OF D AND α

TABLE B-I. EXPERIMENTAL AND THEORETICAL DATA FOR RUN NO. 1

Time (hr.)	Wood Temperature, °F — Distance from Surface 1/4"	2/5"	3/4"	1"	Average Value	Average M.C. % — Exptl.	Theor. (Eq. 53)
0	61	61	61	61	61	86	
0.5	166	163	156	150	158.75		
1	195	192	185	180	176.0	47.1	47.1
2	199	196	190	185	192.5	39.0	39.6
3	203	200	194	190	196.75	36.0	36.43
4	210	208	200	196	203.50	33.5	34.04
5	214	212	204	197	206.75	31.5	32.01
6	215	213	205	198	207.75	29.6	30.03
7	216	215	209	199	209.75	27.8	28.62
8	217	216	200	200	210.5	26.3	27.14
9	"	"	"	"	"	25.0	25.76
10	"	"	"	"	"	23.7	24.48
11	"	"	"	"	"	22.4	23.27
12	"	"	"	"	"	21.4	22.13
13	"	"	"	"	"	20.0	21.04
14	"	"	"	"	"	19.2	20.0
15	"	"	"	"	"	18.0	19.04
16	"	"	"	"	"	17.1	18.11
17	"	"	"	"	"	16.3	17.23
18	"	"	"	"	"	15.0	16.39

Air flow: $U = 1.2\ U_{mf} = 1.56$ ft./sec.; Bed Temp., $T_b = 217°F$; $D = 1.4 \times 10^{-4}$ ft.^{2}/hr.
Drying Direction → y.

TABLE B-II. EXPERIMENTAL AND THEORETICAL DATA FOR RUN NO. 2

Time (hr.)	Wood Temperature, °F — Distance from Surface 1/4"	2/5"	3/4"	1"	Average Value	Average M.C. % — Exptl.	Theor. (Eq. 53)
0	60.5	60.5	60.5	60.5	60.5	89	
1/2	138	135	125	115	128.25		
1	156	153	145	139	148.25	78 (extrap.)	
2	174	172	164	158	165.25	67 (extrap.)	67.0
3	178	176	169	165	172.25	62	63.07
4	181	178	172	169	175.0	60	59.72
5	183	181	177	172	178.25	55.7	56.88
6	185	184	180	176	181.25	53.1	54.39
7	188	186	182	179	183.75	51.0	52.13
8	189	187	183	181	185	48.5	50.01
9	189	187	183	181	185	46.2	48.13
10	189	187	183	181	185	45.0	46.32
11	190	187	183	181	185.25	43.1	44.61
12	"	"	"	"	"	41.4	42.98
13	"	"	"	"	"	40.0	41.43
14	"	"	"	"	"	38.1	39.95

TABLE B-II. (CONTINUED)

Time (hr.)	Wood Temperature, °F — Distance from Surface 1/4"	2/5"	3/4"	1"	Average Value	Average M.C. % — Exptl.	Theor. (Eq. 53)
15	190	187	183	181	185.25	36.8	38.53
16	"	"	"	"	"	35.1	37.17
17	"	"	"	"	"	33.7	35.86
18	"	"	"	"	"	32.4	34.59
19	"	"	"	"	"	31.1	33.38
20	"	"	"	"	"	30.0	32.22
21	"	"	"	"	"	28.7	31.08
22	"	"	"	"	"	28.0	29.99
23	"	"	"	"	"	26.7	28.94
24	"	"	"	"	"	26.0	27.93
25	"	"	"	"	"	24.6	26.96
26	"	"	"	"	"	24.0	26.01
27	"	"	"	"	"	22.9	25.11
28	"	"	"	"	"	22.0	24.23
29	"	"	"	"	"	21.0	23.38
30	190	187	183	181	185.25	20.0	22.57

Air flow: $U = 1.2\ U_{mf} = 1.56$ ft./sec.; Bed Temp., $T_b = 190°F$; Drying Direction → y

$D = 1.0 \times 10^{-4}$ ft.^{2}/hr.

TABLE B-III. EXPERIMENTAL AND THEORETICAL DATA FOR RUN NO. 3

Time (hr.)	Wood Temperature, °F — Distance from Surface 1/4"	2/5"	3/4"	1"	Average Value	Average M.C. % — Exptl.	Theor. (Eq. 53)
0	61	61	61	61	61	81	
1/2	150	148	137	132	141.75		
1	168	165	156	150	159.75	67.9 (extrap.)	
2	172	170	160	155	164.24	62.0	62.0
3	183	181	173	168	174.00	60.0	60.21
4	192	190	183	175	182.66	58.1	58.48
5	197	195	188	181	188	56.6	57.03
6	202	202	194	188	195	55.1	55.74
7	206	204	196	190	196.66	54.2	54.58
8	212	211	204	197	204	53.0	53.51
9	216	214	207	199	206.66	52.6	52.52
10	217	216	209	200	208.0	51.0	51.58
11	"	"	"	"	"	50	50.70
12	"	"	"	"	"	49	49.86
13	"	"	"	"	"	48	49.06
14	"	"	"	"	"	47.5	48.29

TABLE B-III. (CONTINUED)

Time (hr.)	Wood Temperature, °F — Distance from Surface 1/4"	2/5"	3/4"	1"	Average Value	Average M.C. % — Exptl.	Theor. (Eq. 53)
15	217	216	209	200	208	46.5	47.55
16	"	"	"	"	"	46.2	46.83
17	"	"	"	"	"	45.2	46.15
18	"	"	"	"	"	44.5	45.48
19	"	"	"	"	"	44.0	44.83
20	"	"	"	"	"	43.0	44.19
21	"	"	"	"	"	42.6	43.57
22	"	"	"	"	"	42.0	42.97
23	"	"	"	"	"	41.2	42.39
24	"	"	"	"	"	40.0	41.81
25	"	"	"	"	"	39.9	41.25
26	"	"	"	"	"	39.6	40.70
27	"	"	"	"	"	39	40.17
28	"	"	"	"	"	38.5	39.64
29	"	"	"	"	"	38.2	39.13
30	217	216	209	200	208	37.5	38.62

Air Flow: $U = 1.2\ U_{mf} = 1.56$ ft./sec.; Bed Temp., $T_b = 217°F$; Direction of Flow → z; $D = 1.4 \times 10^{-4}$ ft.^{2}/hr.

TABLE B-IV. EXPERIMENTAL AND THEORETICAL DATA FOR RUN NO. 4

Time (hr.)	Wood Temperature, °F: Distance from Surface 1/4"	2/5"	3/4"	1"	Average Wood Temperature: Exptl.	Theor. (Eq. 53)	Average M.C. %: Exptl.	Theor. (Eq. 53)
0	61	61	61	61	61		85	
1/2	169	167	153	143	158			
1	202	200	190	180	193	193	32	32
2	209	207	200	190	201.5	197.6	24	24.5
3	213	212	206	194	206.25	201.89	21	21.64
4	214	215	208	198	207	205.37	19	19.56
5	217	216	210	200	208.75	208.11	18	17.86
6	217	216	211	200	211	210.23	17	16.42
7	"	"	"	"	"	211.87	16	15.16
8	"	"	"	"	"	213.12	15	14.04

Air Flow Rate: $U = 1.2\ U_{mf}$; Bed Temp., $T_b = 217°F$; Drying Direction → y + z;

$D = 1.4 \times 10^{-4}$ ft.^{2}/hr.; $\alpha = 2.5 \times 10^{-3}$ ft.^{2}/hr.

TABLE B-V. EXPERIMENTAL AND THEORETICAL DATA FOR RUN NO. 5

Time (hr.)	Wood Temperature, °F: Distance from Surface 1/4"	2/5"	3/4"	1"	Average Wood Temperature: Exptl.	Theor. (Eq. 53)	Average M.C. %: Exptl.	Theor. (Eq. 53)
0	64	64	64	64	64		91	
1/2	153	151	140	133	144.25			
1	175	173	162	156	166.5	166.5	45	45
2	187	185	178	170	180.0	174.37	36	35.49
3	192	190	185	180	186.75	181.55	29	31.84
4	194	192	187	182	188.75	187.22	27.2	29.15
5	196	195	190	185	191.75	191.56	25.1	26.96
6	198	197	193	189	194.25	194.82	23.5	25.09
7	199	198	195	192	196.0	197.26	22	23.45
8	200	199	196	194	197.25	199.06	20.5	21.98
9	204	202	198	195	197.75	200.39	19.3	20.65
10	"	"	"	"	"	201.68	18.3	19.43
11	"	"	"	"	"		17.6	18.30
12	"	"	"	"	"		16.8	17.26
13	"	"	"	"	"		15.8	16.28
14	204	202	198	195	197.75		15.0	15.38

Air Flow Rate: $U = 1.2\ U_{mf} = 1.56$ ft./sec.; Bed Temp., $T_b = 204°F$; $D = 1.2 \times 10^{-4}$ ft.^{2}/hr. $\alpha = 3.0 \times 10^{-3}$ ft.^{2}/hr.; Drying Direction → y + z.

TABLE B-VI. EXPERIMENTAL AND THEORETICAL DATA FOR RUN NO. 6

Time (hr.)	Wood Temperature, °F: Distance from Surface 1/4"	2/5"	3/4"	1"	Average Wood Temperature: Exptl.	Theor. (Eq. 76)	Average M.C. %: Exptl.	Theor. (Eq. 53)
0	60	60	60	60	60		84	
1/2	142	140	130	120	133			
1	165	163	153	148	157.25	157.25	68 (extrap.)	68
2	172	170	160	156	164.5	164.51	55	54.82
3	178	176	166	164	171.1	171.11	48	49.73
4	185.	183	172	165	176.25	176.23	44	45.96
5	188	186	176	170	180.10	180.05	41.8	42.88
6	190	188	180	174	182.9	182.85	38.0	40.24
7	190	188	183	179	184.9	184.89	36.8	37.92
8	190	188	185	182	186.4	186.36	34.5	35.83
9.5	"	"	"	"	"	189.92	32	33.04
11	"	"	"	"	"		29	30.57
12.5	"	"	"	"	"		27	28.35
15.5	"	"	"	"	"		24	24.49
16.5	"	"	"	"	"		23	23.35
17.5	"	"	"	"	"		21.5	22.26
19	"	"	"	"	"		20	20.75
20	"	"	"	"	"		19	19.79
21.5	"	"	"	"	"		18	18.46
22.5	"	"	"	"	"		17	17.63
23.5	"	"	"	"	"		16	16.83
24.5	190	188	185	182	186.4		15	16.07

Air Flow Rate: $U = 1.2\ U_{mf} = 1.56$ ft./sec.; Bed Temp., $T_b = 190°F$; Drying Direction → y + z
$D = 1.0 \times 10^{-4}$ ft.^{2}/hr.; $\alpha = 3.5 \times 10^{-3}$ ft.^{2}/hr.

TABLE B-VII. EXPERIMENTAL AND THEORETICAL DATA FOR RUN NO. 7

Time (hr.)	Wood Temperature, °F: Distance from Surface 1/4"	2/5"	3/4"	1"	Average Wood Temperature Exptl.	Theor. (Eq. 76)	Average M.C. % Exptl.	Theor. (Eq. 53)
0	71	71	71	71	71		87	
1/2	178	175	160	152	166.25		44	
1	209	205	195	185	198.55	198.55	33	33
2	212	209	200	192	200.31	201.76	25	25.49
3	214	211	203	195	205.7	204.81	22	22.64
4	216	214	206	198	208.4	207.36	19.5	20.54
5	217	215	206	202	210.0	209.42	18.6	18.84
6	217	216	210	205	212.0	211.06	17.5	17.39
7	217	216	210	205	212.0	212.36	16.8	16.12
8.5	217	216	210	205	212.0	113.98	15.0	14.5

Air Flow Rate: $U = 1.3\ U_{mf} = 1.69$ ft./sec.; Bed Temp., $T_b = 217°F$; Drying Direction → y + z; $D = 1.4 \times 10^{-4}$ ft.^{2}/hr.; $\alpha = 2.0 \times 10^{-3}$ ft.^{2}/hr.

TABLE B-VIII. EXPERIMENTAL AND THEORETICAL DATA FOR RUN NO. 8

Time (hr.)	Wood Temperature, °F: Distance from Surface 1/4"	2/5"	3/4"	1"	Average Wood Temperature: Exptl.	Theor. (Eq. 76)	Average M.C. %: Exptl.	Theor. (Eq. 53)
0	62	62	62	62	62		78.5	
0.5	179	177	162	154	168			
1	204	201	191	180	194	194	33.0	33
2	211	208	200	192	200	197.59	24.0	25.5
3	214.5	211.5	203	195	203.16	201.36	21.5	22.64
4	215	213	207	199	206.3	204.6	19.5	20.54
5	216	214	209	200	207.6	207.25	18.6	18.84
6	217	216	211	201	209.3	209.39	17.0	17.39
7	217	216	211	201	209.3	211.08	16.5	16.12
8.5	217	216	211	201	209.3	212.82	15	14.50

Air Flow Rate: $U = 1.1\ U_{mf} = 1.43$ ft./sec.; Bed Temp., $T_b = 217°F$; Drying Direction → y + z; $D = 1.4 \times 10^{-4}$ ft.^{2}/hr.; $\alpha = 2.5 \times 10^{-3}$ ft.^{2}/hr.

TABLE B-IX. EXPERIMENTAL AND THEORETICAL DATA FOR RUN NO. 9

Time (hr.)	Wood Temperature, °F: Distance from Surface 1/4"	2/5"	3/4"	1"	Average Wood Temperature: Exptl.	Theor. (Eq. 76)	Average M.C. %: Exptl.	Theor. (Eq. 53)
0	61	61	61	61	61		85	
1/2	126	124	113	105	117			
1	148	145	134	127	138.5	138.5	77 (extrap.)	
2	155	152	143	137	146.8	144.7	64	64
3	162	159	150	147	154.5	155.5	57	58.5
4	168	166	156	152	160.5	158.8	54.2	55.2
5	172	170	162	155	164.7	162.9	50	51.5
6	174	172	165	160	167.8	166.7	47	48.5
7	175	174	168	163	170	168.9	45.1	46.2
8	175	174	170	167	171.4	177.5	43.2	44.2
11	175	174	171	170	172.5	174.28	38	38.5
15	175	174	171	170	172.5	175.91	32.7	33.4
19	"	"	"	"	"		29	30.2
22	"	"	"	"	"		25.3	25.8
26	"	"	"	"	"		22	21.5
28	"	"	"	"	"		20	19.2
31	"	"	"	"	"		18	17.1
33	"	"	"	"	"		16.5	15.2
35	175	174	171	170	172.5		15	14

Air Flow Rate: $U = 1.2\ U_{mf} = 1.56$ ft./sec.; Bed Temp., $T_b = 175°F$; Drying Direction → y + z

$D = 0.8 \times 10^{-4}$ ft.^{2}/hr.; $\alpha = 2 \times 10^{-3}$ ft.^{2}/hr.

TABLE B-X. EXPERIMENTAL AND THEORETICAL DATA FOR RUN NO. 10

Time (hr.)	Wood Temperature, °F — Distance from Surface 1/4"	2/5"	3/4"	1"	Average Value	Average M.C. % — Exptl.	Theor. (Eq. 53)
0	71	71	71	71	71	85	
1/2							
1	152	150	139	132	143.25		
2	166	163	151	144	156.0		
3	177	175	165	158	168.75	69.0 (extrap.)	69.0
4	186	183	175	167	177.75	67.0 (extrap.)	67.64
5	195	193	182	174	186.00	66.0	66.09
6	199	197	186	179	190.25	64.1	64.74
7	200	198	187	180	191.50	63.1	63.51
8	202	200	190	184	194.00	61.4	62.38
9	203	201	191	184	194.75	61.0	61.33
10	204	202	192	185	195.75	59.7	60.34
11	"	"	"	"	"	58.4	59.41
12	"	"	"	"	"	57.4	58.52
13	"	"	"	"	"	56.6	57.66
14	"	"	"	"	"	56.0	56.85

TABLE B-X. (CONTINUED)

Time (hr.)	Wood Temperature, °F — Distance from Surface 1/4"	2/5"	3/4"	1"	Average Value	Average M.C. % — Exptl.	Theor. (Eq. 53)
15	204	202	192	185	195.75	55.0	56.07
16	"	"	"	"	"	54.2	55.31
17	"	"	"	"	"	53.4	54.58
18	"	"	"	"	"	53.0	53.87
19	"	"	"	"	"	52.0	53.19
20	"	"	"	"	"	51.5	52.51
21	"	"	"	"	"	51	51.86
22	"	"	"	"	"	50.2	51.23
23	"	"	"	"	"	49.4	50.61
24	"	"	"	"	"	48.7	50.0
25	"	"	"	"	"	48.2	49.41
26	"	"	"	"	"	47.3	48.82
27	"	"	"	"	"	47	48.25
28	"	"	"	"	"	46.6	47.70
29	"	"	"	"	"	45.7	47.15
30	204	202	192	185	195.75	45.0	46.61

Air Flow: $U = 1.2\ U_{mf} = 1.56$ ft./sec.; Bed Temp., $T_b = 204°F$; Drying Direction → z; $D = 1.2 \times 10^{-4}$ ft.^{2}/hr.

TABLE B-XI. EXPERIMENTAL AND THEORETICAL DATA FOR RUN NO. 11 (NO BED)

Time (hr.)	Wood Temperature, °F: Distance from Surface 1/4"	2/5"	3/4"	1"	Average Wood Temperature: Exptl.	Theor. (Eq. 76)	Average M.C. %: Exptl.	Theor. (Eq. 53)
0	61	61	61	61	61		85	
1					193	193		
2					201	197.55	63	62.6
3					206.5	201.82	56	55.6
4					207.0	205.29	50	50.4
5					209.0	208.04	45	46.2
6					210.0	210.17	43	42.7
7					211.0	211.82	39	39.6
8					211.0	213.08	37	36.8
9					"	213.84	34	34.3
10					"		31.5	32.0
11					"		30	29.88
12					"		27.5	27.94
13					"		26.0	26.15
14					"		25	24.48
15					211.0		23	22.93

Air Flow: U = 1.56 ft./sec.; Air Temp., = 217°F; Drying Direction → y + z;
$D = 1.4 \times 10^{-4}$ ft.^{2}/hr.; $\alpha = 2.5 \times 10^{-3}$ ft.^{2}/hr.

TABLE B-XII. EXPERIMENTAL AND THEORETICAL DATA FOR RUN NO. 12

Time (hr.)	Wood Temperature, °F — Distance from Surface 1/4"	2/5"	3/4"	1"	Average Value	Average M.C. % — Extpl.	Theor. (Eq. 53)
0	60	60	60	60	60	88	
1/2	152	149	137	130	142	72 (extrap.)	
1	173	170	160	152	163.75	58	58
2	185	183	176	168	178	49	49.4
3	187	185	178	170	180	45.1	45.84
4	192	189	184	179	186	42.3	43.11
5	195	192	187	183	189.25	40	40.8
6	197	195	190	185	191.75	37	38.77
7	199	197	193	189	194.5	35.9	36.93
8	200	198	195	192	196.25	34.2	35.24
9	202	199	196	193	197.5	32.4	33.67
10	204	202	198	195	199.75	31.0	32.22
11	"	"	"	"	"	29.5	30.81
12	"	"	"	"	"	28.1	29.49
13	"	"	"	"	"	27.0	28.24
14	"	"	"	"	"	25.5	27.05
15	"	"	"	"	"	24.3	25.91
16	"	"	"	"	"	23.5	24.82
17	"	"	"	"	"	22.3	23.78
18	"	"	"	"	"	21.3	22.78
19	"	"	"	"	"	20.6	21.83
20	"	"	"	"	"	19.7	20.92
21	"	"	"	"	"	18.8	20.04
22	"	"	"	"	"	17.8	19.21
23	"	"	"	"	"	17.0	18.40
24	"	"	"	"	"	16.0	17.64
25	204	202	198	195	199.75	15	16.9

Air Flow: $U = 1.2\ U_{mf} = 1.56$ ft./sec.; $D = 1.2 \times 10^{-4}$ ft.^{2}/hr.; Bed Temp., T_b = 204°F; Drying Direction → y.

APPENDIX C

CALIBRATION CHARTS

C-I. Rotometer

C-II. Moisture Meter

Fig.C-I **CALIBRATION CHART FOR THE ROTAMETER**

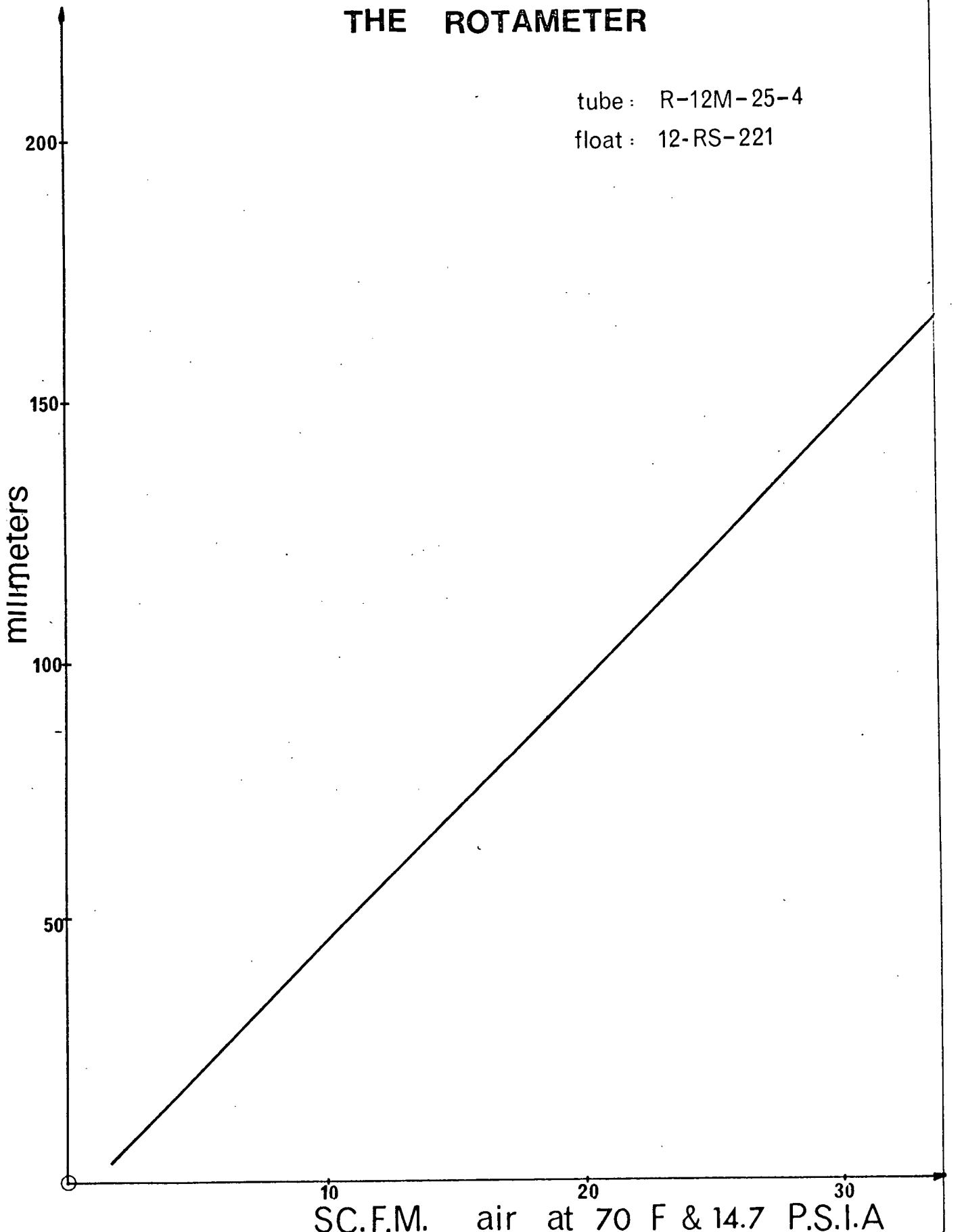

Fig.C-II

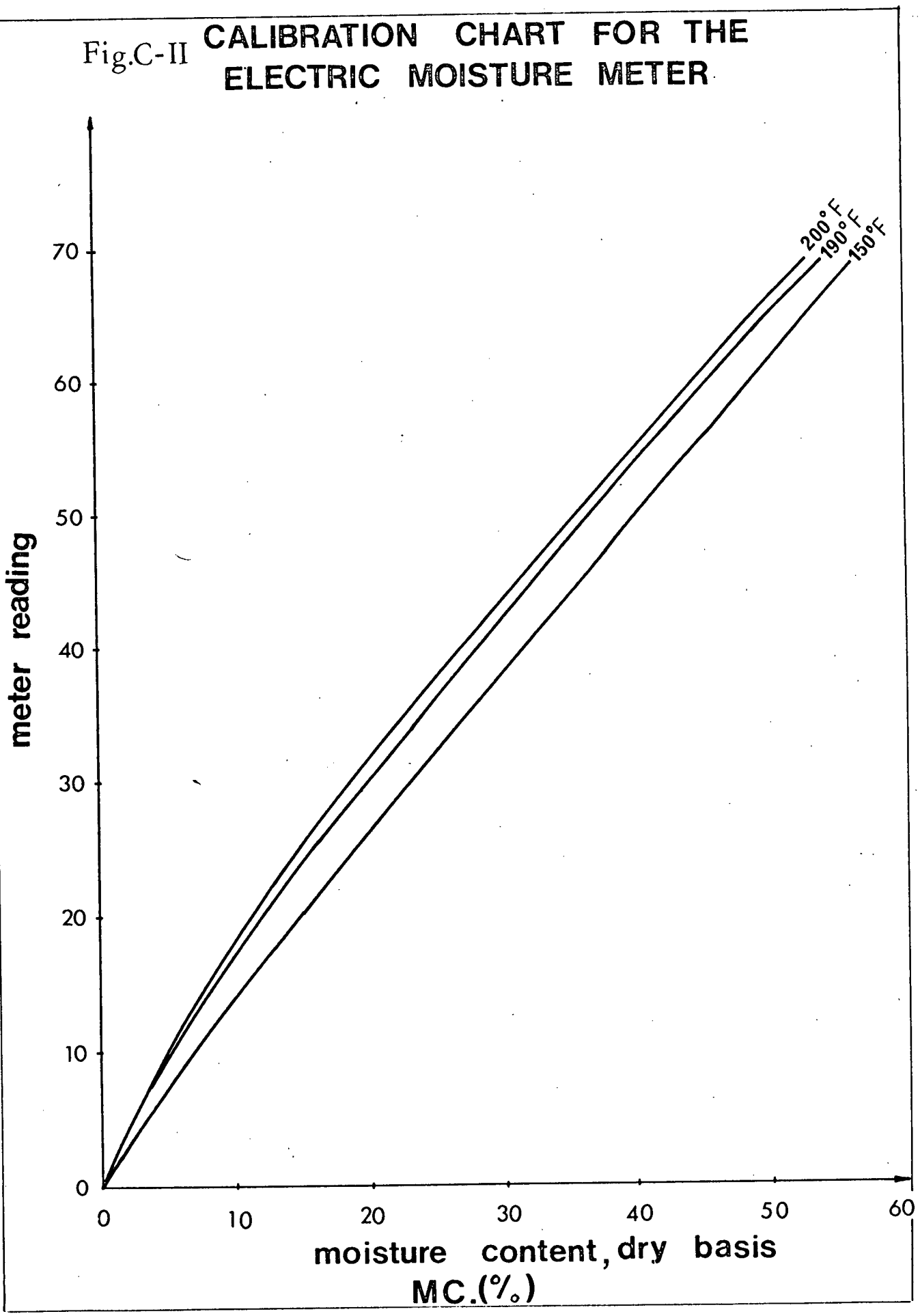
CALIBRATION CHART FOR THE ELECTRIC MOISTURE METER
200°F
190°F
150°F
meter reading
0
10
20
30
40
50
60
70
0
10
20
30
40
50
60
moisture content, dry basis
MC.(%)

APPENDIX D

No. 1 Moisture Distribution Data by Eq. (51)

No. 2 Computer Output - Average M.C. by Eq. (53)

No. 3 Computer Output - Average Wood Temp. by Eq. (76)

No. 1 Moisture Distribution Data by Eq. (51)

θ, THETA = 3.0 HRS.

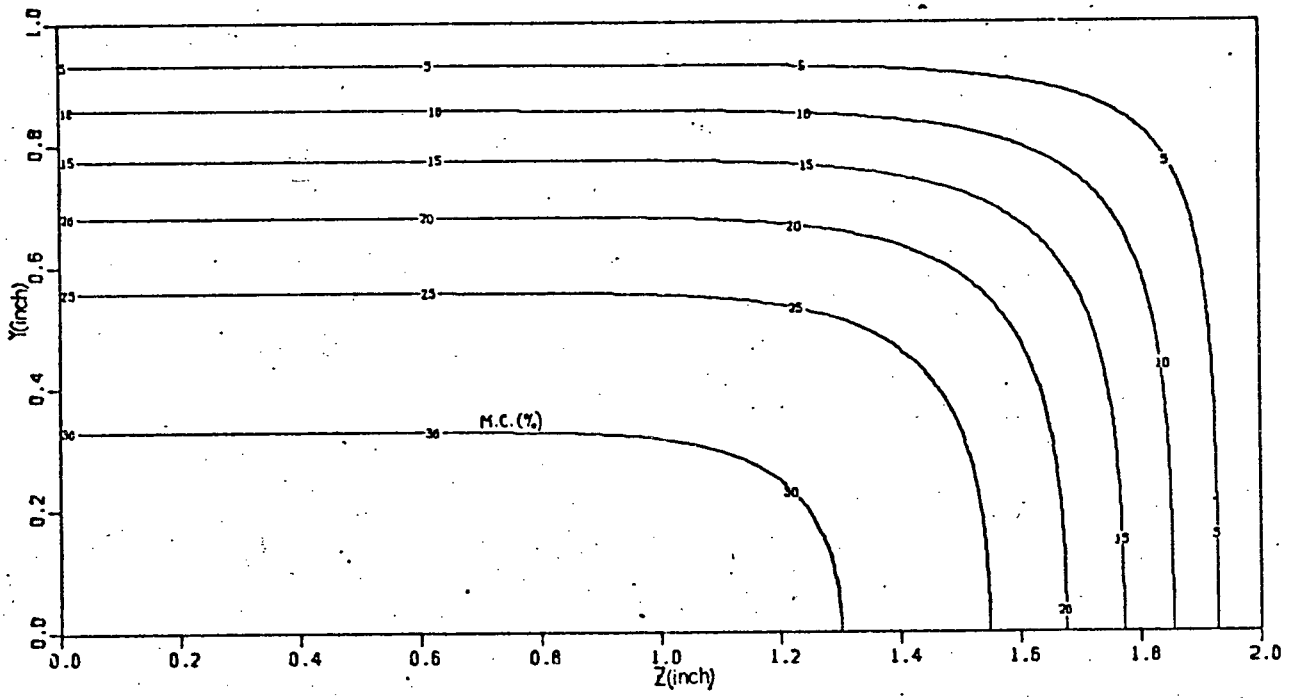

FIG. I

θ, THETA = 4.0 HRS.

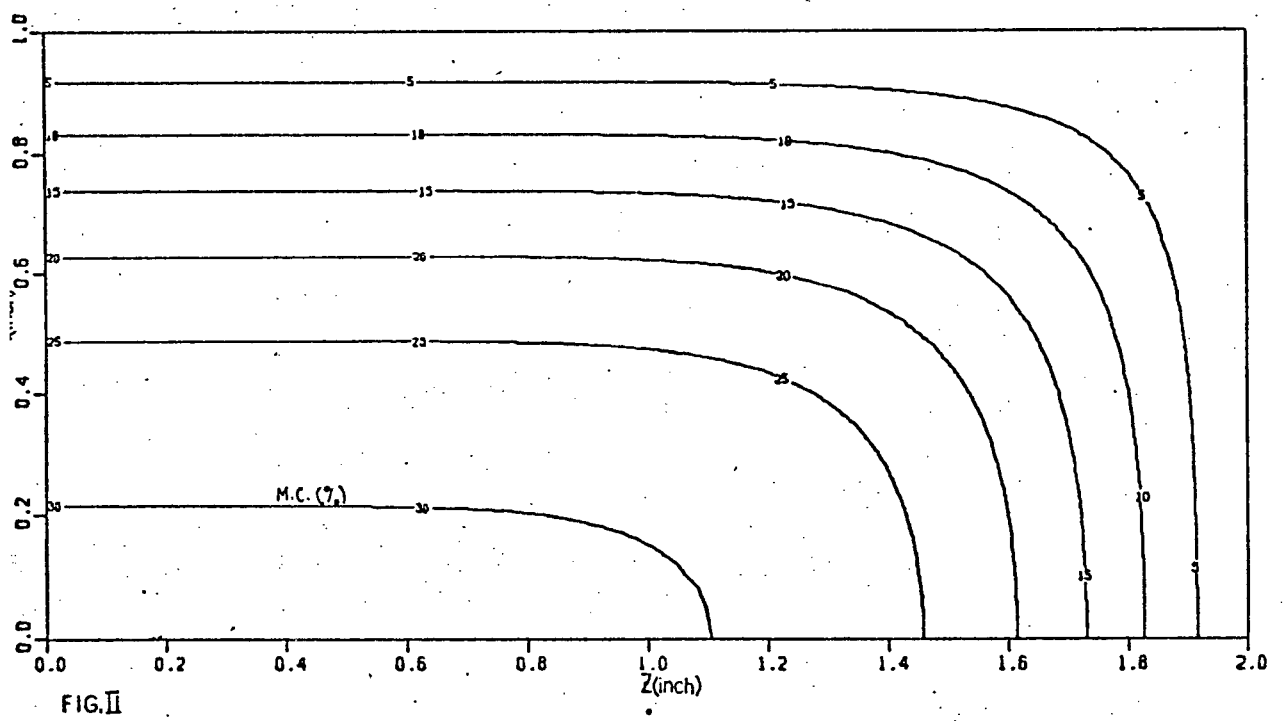

FIG. II

LEAF 146 OMITTED IN PAGE NUMBERING.

p. 146 does not exist

θ, THETA = 5.0 HRS.

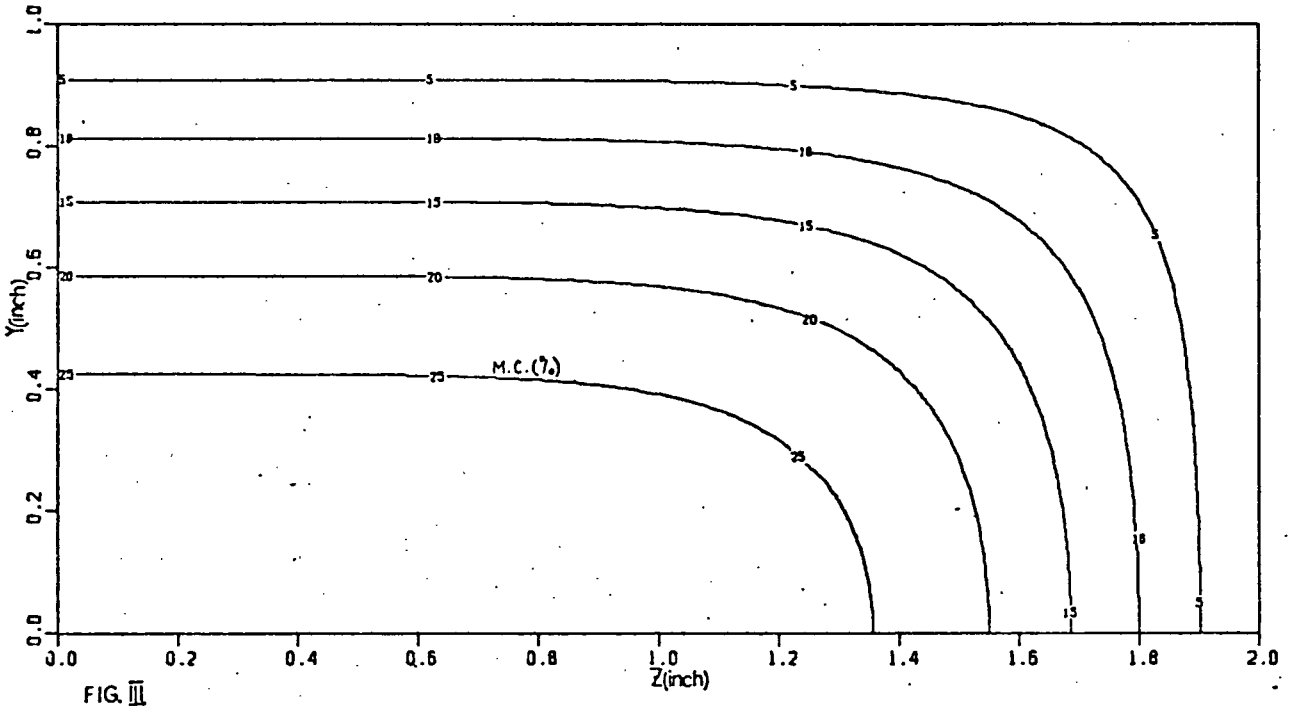

FIG. III

θ, THETA = 6.0 HRS.

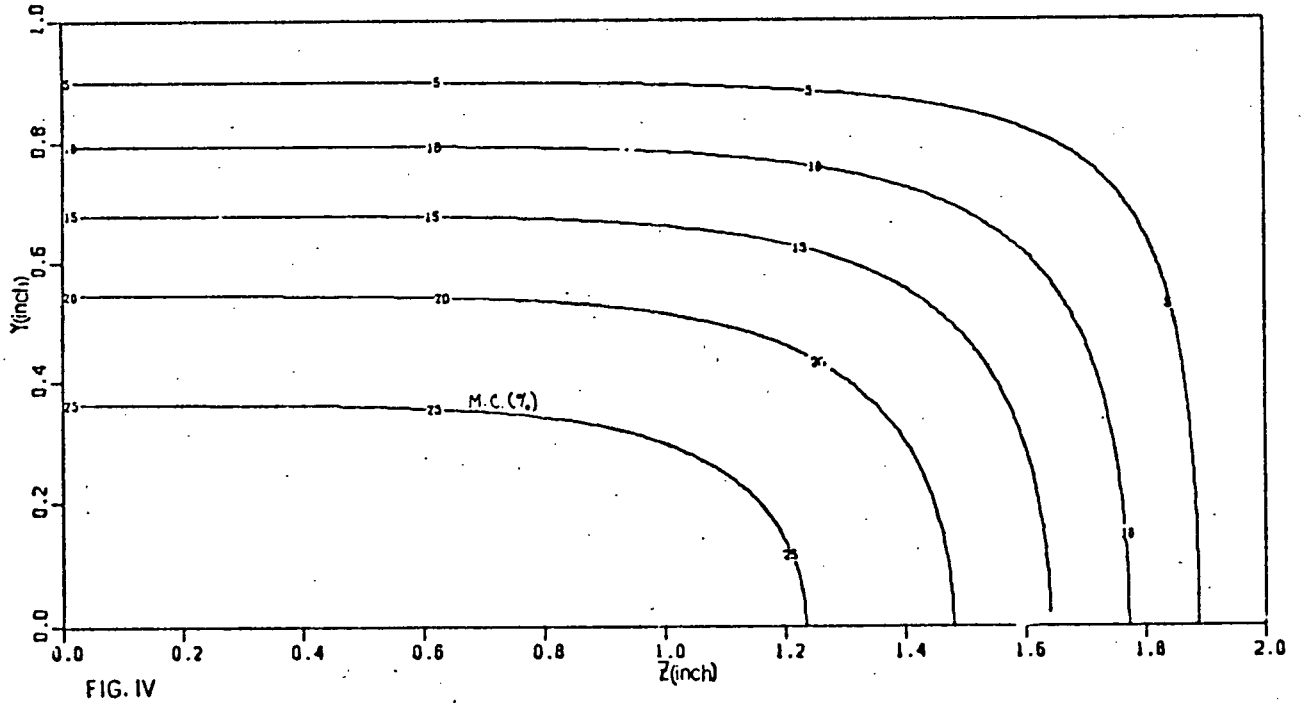

FIG. IV

θ, THETA = 7.0 HRS.

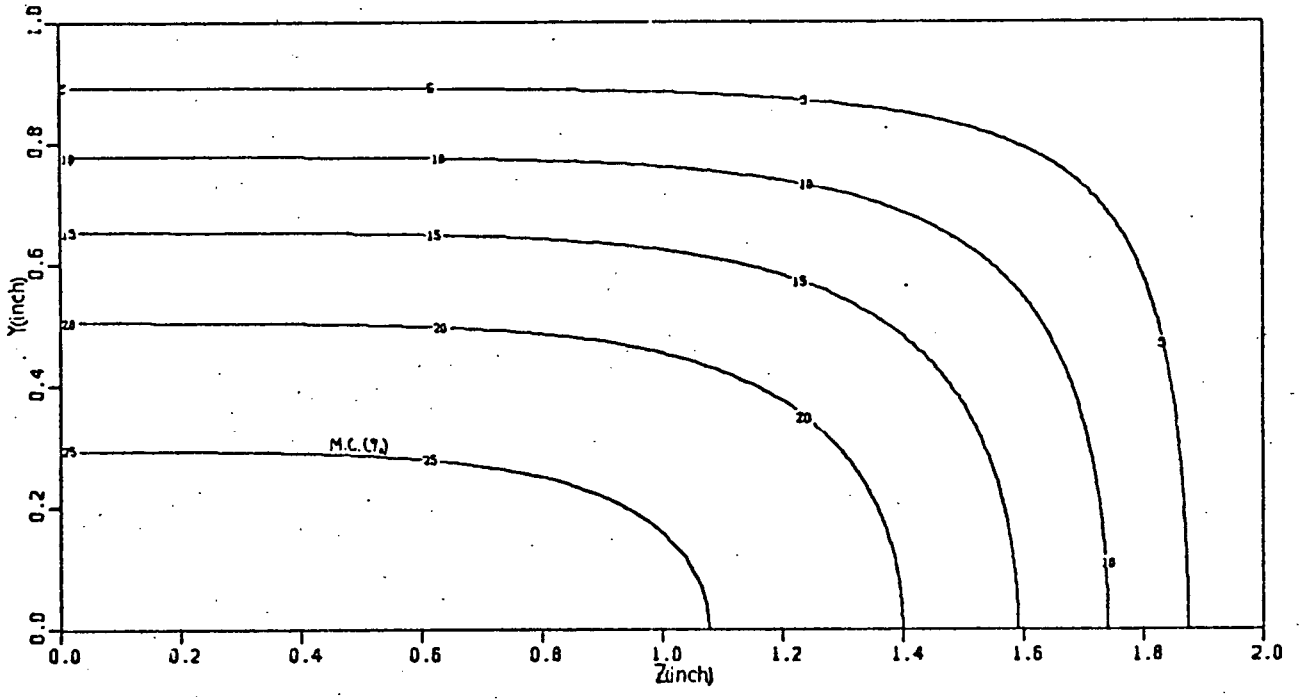

FIG. V

θ, THETA = 8.0 HRS.

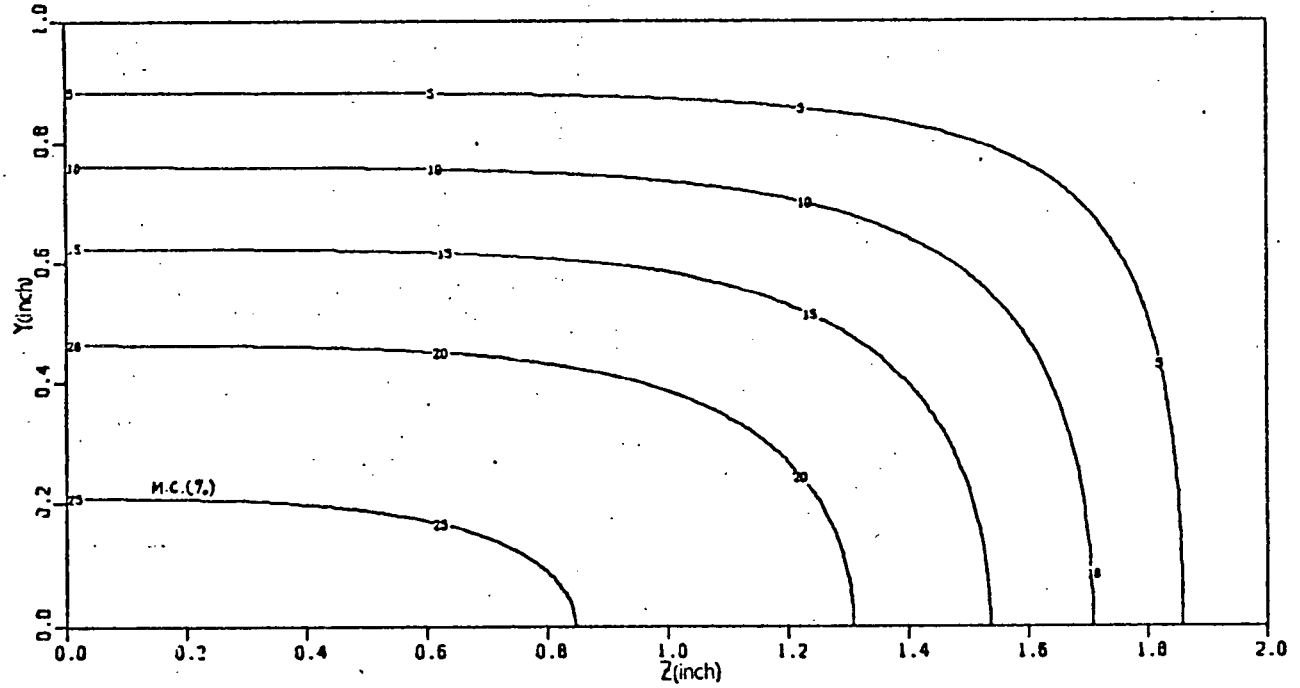

FIG. VI

No. 2 Computer Output - Average M.C. by Eq. (53)

RUN NO= 8
BED TEMP.= 217.
C=100000.00000

TST	ME	MT	D	SIG
0.0	0.330000	0.329123		
1.000000	0.240000	0.309154		
2.000000	0.215000	0.300682		
3.000000	0.195000	0.294248		
4.000000	0.186000	0.288872		
5.000000	0.175000	0.284172		
6.000000	0.170000	0.279951		
7.000000	0.165000	0.276094		
7.500000	0.150000	0.274276		
			0.00001	0.08435
0.0	0.330000	0.329123		
1.000000	0.240000	0.300682		
2.000000	0.215000	0.288872		
3.000000	0.195000	0.279951		
4.000000	0.186000	0.272524		
5.000000	0.175000	0.266053		
6.000000	0.170000	0.260260		
7.000000	0.165000	0.254982		
7.500000	0.150000	0.252501		
			0.00002	0.05888
0.0	0.330000	0.329123		
1.000000	0.240000	0.294248		
2.000000	0.215000	0.279951		
3.000000	0.195000	0.269189		
4.000000	0.186000	0.260260		
5.000000	0.175000	0.252501		
6.000000	0.170000	0.245573		
7.000000	0.165000	0.239275		
7.500000	0.150000	0.236319		
			0.00003	0.04287
0.0	0.330000	0.329123		
1.000000	0.240000	0.288872		
2.000000	0.215000	0.272524		
3.000000	0.195000	0.260260		
4.000000	0.186000	0.250111		
5.000000	0.175000	0.241313		
6.000000	0.170000	0.233475		
7.000000	0.165000	0.226365		
7.500000	0.150000	0.223034		
			0.00004	0.03159
0.0	0.330000	0.329123		
1.000000	0.240000	0.284172		
2.000000	0.215000	0.266053		
3.000000	0.195000	0.252501		
4.000000	0.186000	0.241313		
5.000000	0.175000	0.231537		
6.000000	0.170000	0.223034		
7.000000	0.165000	0.215244		
7.500000	0.150000	0.211599		
			0.00005	0.02326
0.0	0.330000	0.329123		
1.000000	0.240000	0.279951		
2.000000	0.215000	0.260260		

3.000000	0.195000	0.245573		
4.000000	0.186000	0.233475		
5.000000	0.175000	0.223034		
6.000000	0.170000	0.213768		
7.000000	0.165000	0.205392		
7.500000	0.150000	0.201478		
			0.00006	0.01696
0.0	0.330000	0.329123		
1.000000	0.240000	0.276094		
2.000000	0.215000	0.254982		
3.000000	0.195000	0.239275		
4.000000	0.186000	0.226365		
5.000000	0.175000	0.215244		
6.000000	0.170000	0.205392		
7.000000	0.165000	0.196503		
7.500000	0.150000	0.192354		
			0.00007	0.01215
0.0	0.330000	0.329123		
1.000000	0.240000	0.272524		
2.000000	0.215000	0.250111		
3.000000	0.195000	0.233475		
4.000000	0.186000	0.219831		
5.000000	0.175000	0.208098		
6.000000	0.170000	0.197723		
7.000000	0.165000	0.188376		
7.500000	0.150000	0.184019		
			0.00008	0.00848
0.0	0.330000	0.329123		
1.000000	0.240000	0.269189		
2.000000	0.215000	0.245573		
3.000000	0.195000	0.228084		
4.000000	0.186000	0.213768		
5.000000	0.175000	0.201478		
6.000000	0.170000	0.190629		
7.000000	0.165000	0.180872		
7.500000	0.150000	0.176328		
			0.00009	0.00572
0.0	0.330000	0.329123		
1.000000	0.240000	0.266053		
2.000000	0.215000	0.241313		
3.000000	0.195000	0.223034		
4.000000	0.186000	0.208098		
5.000000	0.175000	0.195299		
6.000000	0.170000	0.184019		
7.000000	0.165000	0.173889		
7.500000	0.150000	0.169177		
			0.00010	0.00370
0.0	0.330000	0.329123		
1.000000	0.240000	0.263083		
2.000000	0.215000	0.237292		
3.000000	0.195000	0.218274		
4.000000	0.186000	0.202765		
5.000000	0.175000	0.189496		
6.000000	0.170000	0.177820		
7.000000	0.165000	0.167351		
7.500000	0.150000	0.162488		
			0.00011	0.00229
0.0	0.330000	0.329123		
1.000000	0.240000	0.260260		
2.000000	0.215000	0.233475		

3.000000	0.195000	0.213768		
4.000000	0.186000	0.197723		
5.000000	0.175000	0.184019		
6.000000	0.170000	0.171978		
7.000000	0.165000	0.161199		
7.500000	0.150000	0.156198		
			0.00012	0.00138
0.0	0.330000	0.329123		
1.000000	0.240000	0.257565		
2.000000	0.215000	0.229840		
3.000000	0.195000	0.209482		
4.000000	0.186000	0.192936		
5.000000	0.175000	0.178827		
6.000000	0.170000	0.166450		
7.000000	0.165000	0.155387		
7.500000	0.150000	0.150261		
			0.00013	0.00091
0.0	0.330000	0.329123		
1.000000	0.240000	0.254982		
2.000000	0.215000	0.226365		
3.000000	0.195000	0.205392		
4.000000	0.186000	0.188376		
5.000000	0.175000	0.173889		
6.000000	0.170000	0.161199		
7.000000	0.165000	0.149877		
7.500000	0.150000	0.144638		
			0.00014	0.00080
0.0	0.330000	0.329123		
1.000000	0.240000	0.252501		
2.000000	0.215000	0.223034		
3.000000	0.195000	0.201478		
4.000000	0.186000	0.184019		
5.000000	0.175000	0.169177		
6.000000	0.170000	0.156198		
7.000000	0.165000	0.144638		
7.500000	0.150000	0.139296		
			0.00015	0.00102
0.0	0.330000	0.329123		
1.000000	0.240000	0.250111		
2.000000	0.215000	0.219831		
3.000000	0.195000	0.197723		
4.000000	0.186000	0.179844		
5.000000	0.175000	0.164670		
6.000000	0.170000	0.151422		
7.000000	0.165000	0.139644		
7.500000	0.150000	0.134210		
			0.00016	0.00152
0.0	0.330000	0.329123		
1.000000	0.240000	0.247804		
2.000000	0.215000	0.216746		
3.000000	0.195000	0.194110		
4.000000	0.186000	0.175835		
5.000000	0.175000	0.160349		
6.000000	0.170000	0.146852		
7.000000	0.165000	0.134875		
7.500000	0.150000	0.129359		
			0.00017	0.00225
0.0	0.330000	0.329123		
1.000000	0.240000	0.245573		
2.000000	0.215000	0.213768		

No. 3 Computer Output - Average Wood Temp. by Eq. (76)

RUN NO.= 6
BED TEMP.= 190.00000
D= 0.0001

TET	TE	TT	ALFA	SIG
1.000000	157.250000	157.250000		
2.000000	164.510000	157.580256		
3.000000	171.100000	159.112452		
4.000000	176.227000	160.958741		
5.000000	180.100000	162.895740		
6.000000	182.900000	164.829396		
7.000000	184.900000	166.712073		
8.000000	186.400000	168.517621		
			0.00051	697.95586
1.000000	157.250000	157.250000		
2.000000	164.510000	159.381426		
3.000000	171.100000	162.507368		
4.000000	176.227000	165.654374		
5.000000	180.100000	168.607436		
6.000000	182.900000	171.300127		
7.000000	184.900000	173.717433		
8.000000	186.400000	175.866001		
			0.0010	714.56704
1.000000	157.250000	157.250000		
2.000000	164.510000	160.744181		
3.000000	171.100000	164.946883		
4.000000	176.227000	168.853768		
5.000000	180.100000	172.294569		
6.000000	182.900000	175.255649		
7.000000	184.900000	177.771053		
8.000000	186.400000	179.889779		
			0.0015	318.97251
1.000000	157.250000	157.250000		
2.000000	164.510000	161.873411		
3.000000	171.100000	166.883845		
4.000000	176.227000	171.284543		
5.000000	180.100000	174.973385		
6.000000	182.900000	178.002662		
7.000000	184.900000	180.461220		
8.000000	186.400000	182.441033		
			0.0020	134.79773
1.000000	157.250000	157.250000		
2.000000	164.510000	162.851539		
3.000000	171.100000	168.499655		
4.000000	176.227000	173.234886		
5.000000	180.100000	177.039492		
6.000000	182.900000	180.038584		
7.000000	184.900000	182.376637		
8.000000	186.400000	184.185811		
			0.0025	47.28927
1.000000	157.250000	157.250000		
2.000000	164.510000	163.721760		
3.000000	171.100000	169.888532		
4.000000	176.227000	174.852855		
5.000000	180.100000	178.692836		
6.000000	182.900000	181.609600		
7.000000	184.900000	183.801568		
8.000000	186.400000	185.436957		
			0.0030	9.75650
1.000000	157.250000	157.250000		
2.000000	164.510000	164.509919		
3.000000	171.100000	171.106979		
4.000000	176.227000	176.226183		
5.000000	180.100000	180.049920		
6.000000	182.900000	182.856210		
7.000000	184.900000	184.894413		
8.000000	186.400000	186.364256		
			0.0035	0.00578
1.000000	157.250000	157.250000		
2.000000	164.510000	165.233129		
3.000000	171.100000	172.191858		
4.000000	176.227000	177.411479		
5.000000	180.100000	181.184743		
6.000000	182.900000	183.865915		
7.000000	184.900000	185.751606		
8.000000	186.400000	187.068512		
			0.0040	6.39986
1.000000	157.250000	157.250000		
2.000000	164.510000	165.903419		
3.000000	171.100000	173.168914		
4.000000	176.227000	178.447781		